FORSCHUNGSBERICHT AGRARTECHNIK
des Fachausschusses Forschung und Lehre der
Max-Eyth-Gesellschaft Agrartechnik im VDI (VDI-MEG) **492**

Anjum Munir

Design, development and modeling of a solar distillation system for the processing of medicinal and aromatic plants

Dissertation Witzenhausen 2010

Universität Kassel / Witzenhausen
Fachbereich Ökologische Agrarwissenschaften
Fachgebiet Agrartechnik
Prof. Dr. Oliver Hensel

Design, development and modeling of a solar distillation system for the processing of medicinal and aromatic plants

Dissertation zur Erlangung des akademischen Grades
Doktor der Agrarwissenschaften

von
M.Sc. Ing. Anjum Munir
aus Faisalabad, Pakistan

2010

Die vorliegende Arbeit wurde vom Fachbereich Ökologische Agrarwissenschaften der Universität Kassel als Dissertation zur Erlangung des akademischen Grades “Doktor der Agrarwissenschaften” angenommen.

Tag der mündlichen Prüfung: 22.07.2010

Erster Gutachter : Prof. Dr. Oliver Hensel
Zweiter Gutachter : Prof. Dr. Klaus Vajen

Mündlicher Prüfer: Prof. Dr. Jürgen Heß
PD Dr. Jens Gebauer

Im Selbstverlag: Anjum Munir

Bezugsquelle: Universität Kassel, FB Ökologische Agrarwissenschaften
Fachgebiet Agrartechnik
Nordbahnhofstr. 1a
37213 Witzenhausen

Acknowledgements

The work presented in this manuscript was accomplished under the inspiring guidance and dynamic supervision of Prof. Dr. Oliver Hensel, Institute of Agricultural Engineering, University of Kassel, Germany. His critical comments and useful suggestions during my Ph.D studies were very simulating to focus on my objectives. His constant help, keen interest and sympathetic attitude during the experiments and the preparation of this thesis are gratefully acknowledged.

The author takes an opportunity to express his heartiest thanks to Prof. Dr. Klaus Vajen, Institute of “Solar and system engineering” University of Kassel, Germany as a member of his supervisory committee for his sincere advice, valued criticism, and suggestions had been of much value during the preparation of this manuscript.

With the high emotion of benevolence and gratitude from the deepest core of my heart, I record my sincerest feelings of obligation to Mr. Wolfgang Scheffler and Mrs. Heike Hoedt “Solare Brücke Organization” who encouraged and provided me necessary facilities throughout the course of this investigation and writing of this manuscript. My sincere appreciations are also extended to Mr. Behringer, International Solar Food Processing Network, for his kind help during the development work of my project. I am deeply grateful to Higher Education Commission (HEC) of Pakistan, German Academic Exchange Service (DAAD) and University of Agriculture, Faisalabad, Pakistan for providing me an opportunity and finance for achieving quality education in Germany.

Deepest appreciations are due to all the team of Agricultural Engineering especially Christian Schellert, Heiko Tostmann, Uwe Richter, and Anne Noetzel for helping me and making available the research facilities and valuable advice. I would like to express my gratitude to Mrs. Monika Klaus to solve my academic and non-academic problems during my Ph.D studies. I cannot forget Florent Dupont and Salvatore Grigoli who worked in our project and helped me on many occasions. I would like to extend my special thanks to my friends, Farhan Saeed, Shafique Maqsood, M. Sohail, Sultan Mahmood, M. Qasim and Zaighum Zia for their moral support, inspiring guidance and encouragement during the course study.

I don’t have suitable words in my command to acknowledge my family members especially my mother, wife, brother, sisters and children for their patience and best wishes which boosted my moral high to accomplish my goals. I dedicate the dissertation to my Late father Ch. Munir Ahmad who left me on the way with a desire to see me a highly educated person.

Table of Contents

Table of Contents i
List of Figures iv
1 Introduction 1
Objectives of the studies 5
2 State of the art 7
2.1 Production of herbs and medicinal plants 7
2.1.1 Medicinal plants in Pakistan 7
2.1.2 Drying of medicinal and aromatic plants 9
2.1.3 Influence of drying temperature on active ingredients 10
2.2 Essential oils extraction from medicinal and aromatic plants 10
2.2.1 General 10
2.2.2 Essential oils extraction by distillation 11
2.2.3 Industrial utilization of essential oils 17
2.2.4 Economic importance of the industry 18
2.2.5 Essential oils in local and regional health care markets 19
2.2.6 Value addition in developing countries 20
2.2.7 Problems and prospective for aromatherapy in tropical counties 21
2.2.8 Different distillation plants for commercial applications 21
2.2.9 Guidelines during distillation 23
2.2.10 Distillation options 24
2.3 Solar energy utilization 25
2.3.1 Solar energy application in medium temperature range 25
2.3.2 Solar energy for industrial process heat demand 28
2.3.3 Evaluation of solar cookers 29
2.3.4 Use of high reflectivity material for the reflectors 30
2.3.5 Solar concentrators 30
2.3.6 Solar distillation of water 31
2.4 Auxiliary energy utilization in solar distillation system 32
3 Material and methods 33
3.1 Laboratory experiments 33
3.2 Selection of the solar collector 34
3.3 Development of Solar distillation system 35

3.3.1 Description of Scheffler reflector for solar distillation system 36
3.3.2 Use of secondary reflector for water and steam distillation 37
3.3.3 Fabrication of the still for solar distillation system 39
3.3.4 Fabrication of condenser 41
3.3.5 Florentine vessel or oil separator 41
3.4 Experimental set up and data acquisition 42
3.5 Operational procedure of the solar distillation system 44
3.6 Mathematical modeling of solar distillation system 45
3.7 Biomass energy utilization in solar distillation system 45
4 Results & discussions 47
4.1 Laboratory experiments 47
4.2 Design principle and mathematical calculations of Scheffler concentrator .. 50
4.2.1 Design of reflector parabola and reflector elliptical frame 50
4.2.2 Distribution of crossbars on the reflector frame 55
4.2.3 Calculation of equations for the crossbars ellipses 56
4.2.4 Calculation of depths and arc lengths for different crossbars 59
4.2.5 Installation of the Scheffler reflector on site 62
4.2.6 Daily tracking 63
4.2.7 Calculation of seasonal parabola equations 64
4.3 Calculation of the required size of the Scheffler reflector 72
4.4 Energy distribution in the solar distillation system 74
4.4.1 Available insolation from Primary reflector 75
4.4.2 Energy distribution at primary reflector 78
4.4.3 Energy distribution at secondary reflector 79
4.4.4 Energy losses from the distillation unit 80
4.5 Thermal losses calculation of the distillation still 81
4.5.1 Conduction and convection losses 81
4.5.2 Radiation losses 83
4.5.3 Determination of natural convection co-efficient 83
4.5.4 Parameters of the existing prototype of the distillation still 85
4.6 Mathematical model for the solar distillation system 86
4.7 Output of the mathematical model for the solar distillation system 93
Energy available for the solar distillation system 97
4.8 Performance evaluation of the solar distillation system 98
Determination of dryness fraction 98

4.9 Evaluation of Scheffler reflector by steam receiver 102
4.10 Essential oil extraction by solar distillation 104
4.10.1 Distillation experiments with Lemon Balm (*Melissa officinalis L*.) 108
4.10.2 Oregano (*Origanum vulgare SSP*.) 114
4.10.3 Cloves (*Eugenia caryophyllata*) 117
4.10.4 Cumin (*Cuminum cyminum*) 119
4.10.5 Rosemary (*Rosmarinus officinalis*) 120
4.10.6 Fennel (*Foeniculum valgure Mill.*) 122
4.11 Comparison of results-laboratory versus solar 124
4.12 Need of auxiliary energy for the solar distillation system 125
4.12.1 Distillation experiments with solar-biomass hybrid system 126
5 Overall discussion 132
6 Outlook 139
7 Recommendations and suggestions 140
8 Summary 141
Zusammenfassung 143
Literature Cited 145
Appendices 154

List of Figures

Figure 2.1 Flow diagram of water distillation process 14
Figure 2.2 Flow diagram of water and steam distillation process 15
Figure 2.3 Flow diagram of direct steam distillation process 17
Figure 3.1 Laboratory distillation apparatus ……..34
Figure 3.2 Secondary reflector for solar distillation system 38
Figure 3.3 Separator types 42
Figure 3.4 Schematic of solar distillation system..... 43
Figure 3.5 Solar-biomass hybrid system for distillation of essential oils..... 46
Figure 4.1 Process curves of different plant materials for laboratory experiments……. 47
Figure 4.2 Heat energy required (kW h) per 100 grams of different plant materials..... 49
Figure 4.3 Heat energy required per ml of essential oil for different plant materials..... 49
Figure 4.4 Section of the Scheffler reflector in a paraboloid..... 51
Figure 4.5 Description of parabola of the Scheffler reflector 52
Figure 4.6 Intersections points of seven crossbars (q_1 to q_7) 56
Figure 4.7 Description of the Scheffler reflector and the crossbars 57
Figure 4.8 Ellipse of the crossbar for the Scheffler reflector..... 60
Figure 4.9 Radius, depth and arc length details for nth crossbar 60
Figure 4.10 Installation and daily tracking details of the Scheffler reflector..... 63
Figure 4.11 Schematic of photovoltaic daily tracking system 64
Figure 4.12 Seasonal parabola equations for an 8 m^2 Scheffler reflector 67
Figure 4.13 Detail of pivot points and telescopic clamps of the Scheffler reflector..... 69
Figure 4.14 Effect of pivot points on reflector deformation 70
Figure 4.15 Functioning of pivot points and clamps to deform the reflector 71
Figure 4.16 Explanation of available energy and losses in a solar distillation system..... 75
Figure 4.17 Variation of solar declination and aperture area for standings reflectors..... 77
Figure 4.18 Variation of solar declination and aperture area for laying reflectors 78
Figure 4.19 Description of the solar distillation model 86
Figure 4.20 Predicted values of energy distribution in the northern hemisphere 93
Figure 4.21 Predicted values of energy distribution in the southern hemisphere 94
Figure 4.22 Predicted values of heat losses from the distillation still 95
Figure 4.23 Heat losses at different parts of the distillation still..... 96

Figure 4.24 Total energy available (modeled values) at the primary reflector and for the distillation process 97
Figure 4.25 Performance evaluation of solar distillation system (on Aug, 31 2008 with 20 liters of water, 30 readings averaged) 101
Figure 4.26 Infrared photos of the bottom and top part of the solar distillation still.... 102
Figure 4.27 Details of steam receiver installation 103
Figure 4.28 Experimental set up of the steam receiver 103
Figure 4.29 Detail of water and steam tests with and without secondary reflector 104
Figure 4.30 Experimental (dotted) and regression curves for percentage of essential oils extracted against different heat energy during solar distillation 106
Figure 4.31 Process curves for fresh, dry and chopped Lemon Balm 110
Figure 4.32 Comparison of fresh, chopped and dry Melissa 111
Figure 4.33 Process curved of Peppermint verities (Mentha piperita L, Mentha spec., and Mentha spicala) 113
Figure 4.34 Comparison of Peppermint varieties 114
Figure 4.35 Process comparison for chopped and un-chopped Oregano 115
Figure 4.36 Comparison for chopped and un-chopped Oregano 116
Figure 4.37 Experimental results for the essential oils extracted against different heat energy during solar distillation of Cloves 118
Figure 4.38 Experimental results for the essential oils extracted against different heat energy during solar distillation of Cumin 120
Figure 4.39 Experimental results for the essential oils extracted against different heat energy during solar distillation of Rosemary 122
Figure 4.40 Experimental results for the essential oils extracted against different heat energy during solar distillation of Fennel 123
Figure 4.41 Water temperature and beam radiations (max.) during distillation experimentse (Witzenhausen, Latitute:51.3°) 125
Figure 4.42 Distillation still with coils and steam connections 126
Figure 4.43 Process comparison for solar and solar-biomass hybrid system 128
Figure 4.44 Comparison of chopped and un-chopped European Silver Fir 129
Figure 4.45 Results of solar-biomass hybrid distillation system 130
Figure 4.46 Schematic diagram of solar-biomass hybrid system 131

1 Introduction

With the increasing population and industrialization, there is need to cut down the load of fossil fuels and to reduce environmental pollution. Unlike conventional energy utilization, solar energy is free of connections, unlimited supply of source and also decease gas emission. Solar energy investments in developing countries are imperative to avoid an energy crisis arising from over-dependence on fossil fuels. The situation is critical because fossil fuels are finite and fast depleting (Okoro, 2004). Various industrial surveys show that up to 24 percent of all industrial heat, directly used in the processes, is at temperatures from ambient to 180 °C. In several industries, 100 percent process heat requirement is below 180 °C which can be supplied economically by evacuated tube collectors and solar concentrators (Garg & Prakash, 2006). From a number of studies on industrial heat demand, several industrial sectors have been identified with favorable conditions for the application of solar energy. The most important industrial processes using heat at mean temperature level are: sterilizing, extraction, pasteurizing, drying, solar cooling and air conditioning, hydrolyzing, distillation and evaporation, washing and cleaning, and polymerization. The ranges of all these processes lie between 60-280 °C (Kalogirou, 2003). Most of the agro-based industries can be operated in this medium temperature range. The use of solar energy in agriculture sector can be used to process many perishable agricultural products at farm level. At present, various kinds of solar collectors are in use in the sector of agriculture and post harvest technology, yet their applications are restricted only to drying and warming water etc. Beyond this low temperature applications there are several potential fields of application of solar thermal energy at a medium and medium-high temperature level. Many important developments have occurred in solar concentrating systems for diverse applications in the last decades. In particular, an important research effort has been directed towards power generation applications, chemical systems, and process heat (Estrada, 2007). Tremendous efforts have been made in areas of application of solar energy in the agricultural sector. This can be seen in areas of solar water heating for dairy and micro irrigation (Oparaku 1991; Jenkins 1995; Essandu-Yeddu 1993). The promotion of small scale agro-based industries by using innovative solar collectors can open new landmarks in rural development especially in tropical countries.

Medicinal plants have been used for different purposes in many regions of the world since ancient times. After World Health Organizations (WHO), medicinal plants are commonly

used in preventing and treating specific ailments and diseases and are generally considered to play a beneficial role in health care. Some cultivars from medicinal plant families are also used as ingredients to season or to give a pleasant flavor or smell to foods. Therefore, the terms “medicinal” and “aromatic” are usually used in conjunction. Essential oils extraction from medicinal and aromatic plants is one of the medium temperature agro-based industries. These oils are used in medicinal and pharmaceutical purposes, food and food ingredients, herbal tea, cosmetics, perfumery, aromatherapy, pest, and disease control, dying in textiles, gelling agents, plant growth regulators, and paper making (Öztekin & Martinov, 2007). A single ounce of most of the oils is worth thousands of Dollars. In the last decade, these oils remedies have gained enormous popularity in industrialized countries as well particularly in the multi-million-dollar aromatherapy business. Out of all extraction methods, the distillation methods have advantages of extracting pure and refine essential oils by evaporating the volatile essence of the plant material **(**Malle & Schmickl, 2005). At present, there are large and centralized distillation units mostly located in city areas. Due to their high operating costs, these are sometimes unmanageable by farmers or even groups of farmers in most of the developing countries. Further, some essential oils come from extremely delicate flowers and leaves that must be processed soon after harvesting. Thus, for functional, economic and environmental reasons, there is need of a decentralized distillation system. Due to lack of adequate facilities for the decentralized distillation systems, farmers prefer to dry their product rather to sell it at very low price. Results show that conventional drying methods such as open sun drying and conventional-fuel dryers are not suitable which deteriorate the essential oils components in the herbs. Moreover, the drying process necessitates an enormous amount of thermal and electrical energy (Fargali, 2008). The on-farm solar distillation is a decentralized approach to reduce the post harvest losses and to prevent spoilage of essential oil components by processing the fresh herbs. Examples of the plants are Peppermint, Lemon Balm (Melissa), Lavender, Cumin, Cloves, Anise, Rosemarie, Patchouli, Caraway, Cassia, Oregano, European Silver Fir, and Fennel etc.

In order to run the distillation experiments, boiling, cooking and steam generation are the basic requirements. Increasing awareness of the growing global need for alternative cooking fuels has resulted in an expansion of solar cooker research and development (Funk, 2000). A system for solar process heat for decentralized applications in developing countries was presented by Spate et al. (1999). The system is suitable for community

kitchens, bakeries and post harvest treatment. The system employs a fix focused parabola collector, a high temperature flat plate collector and pebble-bed oil storage.

Decreasing the area from which the heat losses occur can increase energy delivery temperatures. With higher a concentration ratio, there is an increase in temperature at which heat is delivered due to an increase in flux intensity and a decrease in the receiver area. Modern parabola trough concentrators and central receiver towers are operated by high-tech computer programmed tracking system and are used only in large scale applications to justify the high investment costs and gross over design. The conventional paraboloidal concentrators converge all the beam radiations at the focus and are selected as the bottom part of a paraboloid parallel to the directrix. With such parabolic concentrators, not only the frequent tracking of two axes is required but also the receiver is fixed at the focal point as an integral part of the reflector. Moreover, focus lies in the path of incident beam radiations. Despite the high temperature output, such types of concentrators are rarely used for industrial applications due to frequent changes of the focus position and inadequacy of handling approach at the receiver. This limitation, however, is solved by the Scheffler fixed focus concentrator which not only provides simple and precise automatic tracking but also a fixed focus away from the path of incident beam radiations. This design also provides an opportunity to shift the receiver for indoor applications. The versatile reflector rotates along an axis parallel to polar axis with an angular velocity of one revolution per day from east to west to counterbalance the effect of earth rotation. Therefore, the relative position of the Scheffler reflector with respect to sun remains stationary and provides a fixed focus on the line of the axis of rotation (Scheffler, 2006). The reflector not only provides daily tracking but also a seasonal tracking device to ensure the focus remains at the same fixed point with changing solar declination. Nevertheless, there is a little compromise on the aperture area as compared with the conventional paraboloid concentrator but this drawback is compensated by precise automatic tracking and fixed focus with respect to earth. Scheffler reflector provides an extraordinary opportunity that can be used for domestic and industrial applications. The automatic tracking system with a stationary focus point has made it even more attractive for decentralized industrial applications in underdeveloped areas, where there is no electricity or fossils fuels availability. For small-scale applications, it can be used as a point source of heat, directly or indirectly by using a secondary reflector. On large scale applications and steam generation, a number of Scheffler reflectors are arranged in the form of tandems to get a common focus point in the center. It also provides an opportunity

to set the reflector in a standing position or in a laying position rotating along the same axis of rotation. In addition, the balanced structure of the Scheffler reflector requires only a nominal torque to track the sun. This is done with the help of a small PV tracking system or clock work driven by gravity. Different sizes of the Scheffler reflectors can be constructed ranging from 2 m^2 to 60 m^2.

In order to obtain direct absorption of solar energy, a parabolic dish with a receiver configuration is often used. These types of reflectors can be successfully used in distillation, baking, water distillation, solar community kitchen, etc. It is observed through comparison that the two axes tracking paraboloidal dish, which always faces the sun, is the most promising design for concentrating systems justifying the use of the Scheffler concentrator for industrial process heat applications (Bhirud & Tandale, 2006). These concentrators are capable of delivering temperatures in the range of 300 °C and are technically suitable for medium temperature applications (Delaney, 2003). Scheffler (2006) investigated that about half the power of sunlight which is collected by the reflector becomes finally available in the cooking vessel. The use of solar energy for the generation of steam is now an economically attractive possibility since the pay back period of such a system lies between 1.5 and 2 years. These cookers are economically viable if they are used regularly (Jayasimha, 2006). For small-scale applications in agriculture, post harvest technology and the food industry, this is a cheaper solution. A focal receiver absorbs the concentrated solar radiation and transforms it into thermal energy to be used in a subsequent process. The essential feature of a receiver is to absorb the maximum amount of reflected solar energy and transfer it to the working fluid as heat, with minimum losses (Kumar, 2007).

At present, solar energy is successfully utilized for cooking applications and steam generation. Processing of medicinal and aromatic plants by solar distillation system was a new research area of solar energy utilization in medium temperature range. By keeping all facts in view, the study has been initiated to develop a decentralized solar distillation system for essential oils extraction from medicinal and aromatic plants. The solar distillation system is installed at solar campus, University of Kassel, Witzenhausen, Germany. Beside the solar campus, a variety of fresh herbs and medicinal plants are available at the university farms and tropical greenhouse. The solar distillation system comprises of primary reflector equipped with daily and seasonal tracking devices, a secondary reflector, a distillation still with all mountings and fittings, a tubular condenser

and Florentine vessels. The system was designed to conduct distillation experiments for on-farm processing of medicinal and aromatic plants. Mathematical models were also developed to calculate different sizes of the solar concentrator according to the desired capacities of distillation system and to determine the heat losses and energy distribution at different components of the solar distillation system.

A solar distillation system will work effectively only during sunny days. The degree of reliability desired of a solar process to meet a particular load can be provided by a combination of properly sized collector and an auxiliary energy source. In the most climates, auxiliary energy is needed to provide high reliability and avoid gross over design of the solar system (Duffie & Beckman, 2006). In a solar process heat system, interfacing of the collectors with the conventional energy supplies must be done in a way compatible with the process (Kalogirou, 2003). For this purpose, solar distillation system was integrated with biomass energy to operate during adverse climatic conditions. The auxiliary biomass system comprises of a boiler, biomass furnace, and economizer and equipped with all safety mountings and fittings. The boiler operates under natural draught with the help of a chimney for efficient combustion process and can be operated with firewood, bagasse, spent and other biomass material etc. The main object of the work is to utilize solar energy as a primary heat source and the biomass energy as a secondary heat source to make up any steam deficiency for continuous distillation processes. For this purpose, steam connection from the biomass boiler is injected into the distillation still while the bottom of the still is always exposed to the beam radiations. The study presents the development, mathematical description and experimental results of solar distillation system integrated with biomass energy for the on-farm processing of medicinal and aromatic plants.

Objectives of the studies

The overall objective of the research is to develop a decentralized solar distillation system for the processing of medicinal and aromatic plants. The specific objectives include:

1. To design and develop solar distillation system for processing of medicinal and aromatic plants.
2. To evaluate the performance of the solar distillation system.

3. To develop mathematical models to design the required size of Scheffler concentrator and to predict the energy distribution at different parts of the solar distillation system.
4. To utilize biomass energy in solar distillation system to conduct the distillation experiments during bad weather conditions.

The work is presented in the form of state of the art, laboratory experiments, design and development of the solar distillation system. Up to now, no mathematical description of the design of Scheffler reflector has been done. Two mathematical models were developed to calculate the required size of the Scheffler reflector and to predict the energy losses from different components of the solar distillation system. The work also presents the evaluation of solar distillation system by using different medicinal and aromatic plants. The description of solar-biomass hybrid system is also explained to run the distillation experiments during adverse climatic conditions.

2 State of the art

The present study is conducted for the development of a solar distillation system; this chapter presents the review of literature related to the herbs and medicinal plants, details of distillation methods and techniques, and the application of solar energy in medium temperature range.

2.1 Production of herbs and medicinal plants

Currently, the worldwide interest in herbal or medicinal plant products has increased significantly. According to World Health Organization (WHO) survey, about 70-80 % of the world population relies on non-conventional medicines for their primary health-care. This strategy is mostly based on the medicinal plants products known as botanical, herbal, medicines or phetomedicines (Akerele, 1993; Calixto, 2000; Chan, 2003). Herbal medicines are composed of plant parts or plant materials in either the crude or processed state as active ingredients and may contain inert excipients (Busse, 2000). Herbal products are traded as fresh or dry products or as essential oils. These are in general used as raw materials for the extraction of active substances or chemical precursors and mainly for the production of teas, homemade-remedies, fluid extracts and also powders resulting from dried and comminuted plants or from the drying an extract (Runha et al., 2001; Daniel et al., 2005).

2.1.1 Medicinal plants in Pakistan

In Pakistan, almost 2000 medicinal plant species exist. About 50 % of the population in Pakistan is being cured using traditional medicines by more than 40,000 traditional herbal practitioners. There is burgeoning need for the promotion of medicinal herbs crop in Pakistan. Firstly, because these are re-emerging as a health aid due to the mounting costs of prescription drugs in the maintenance of personal health. Secondly, in the international market, the opportunities are emerging day by day for the trade of medicinal herbs, spices and essential oils to fetch foreign exchange for the country. Keeping in view, the government of Pakistan through ministry of Food, Agriculture and Livestock (MINFAL) has launched a project captioned as “Introduction of medicinal herbs and spices as crops” (IMHSC). The project will focus its activities on the cultivation, conservation and trade aspects of the medicinal herbs and spices in various agro-ecological zones of the country. The project has the collaboration of country’s apex institutes such as Hamdard University Karachi, Pakistan Forest Institute Peshawar, Pakistan Agricultural Research Council

including its centers i.e., PGRI, NARC Islamabad and Arid Zone Agricultural Research Centre, Quetta. In addition to these institutes, agricultural universities and colleges will be provided a grant up to 100 thousand Rupees for conducting research on medicinal herbs on topic of pragmatic nature.

Pakistan is blessed with an excellent climate and agriculture land quality. Both these factors contribute to the opportunity of production of highest-grade essential oils in Pakistan. The local climatic and soil conditions alter the chemo type (chemical composition) of essential oil in plants and make this essential oil most desirable. The domestic Pakistani market for essential oils is infinitesimal and represents less than 1 % of the world market. Therefore, the producers of essential oils in Pakistan would most likely be competing in the world market. As a relatively new entrant to world market, it is imperative that the essential oils from Pakistan should fetch lower price in world market at the beginning. But once a regular supply is established, and the quality standard is consistently high, price and demand start to rise at very handsome rates (Aslam, 2002).

Lawrence (1978) reported about the research work conducted for the cultivation and oil extraction from the medicinal herbs. He explained the possibilities of introducing Melissa as an essential oil crop in Pakistan where oil yield was obtained as 0.15 % on fresh weight basis.

Chemical constituents with antioxidant activity found high concentrations in herbs plants (Velioglu et al., 1998) determine their considerable role in the prevention of various degenerative diseases (Challa et al., 1997; Diplock et al., 1998; Hu & Willet, 2002). Besides the fruits and vegetables that are recommended at present as optimal source of such components, the supplementation of human diet with herbs, containing especially high amounts of compounds capable of deactivating free radicals may have beneficial effects (Madsen & Bertelsen, 1995). The benefits resulting from the use of natural products rich in bioactive substances has promoted the growing interest of pharmaceutical, food and cosmetic industries as well as of individual consumers in quality of herbal products (Kapecka et al., 2005).

The herb industry can be separated into three main categories, essential oils, medicinal crops and culinary herbs. The establishment of herb production venture involves relatively high capital investment, particularly for plant material, irrigation, machinery and distillation

or drying equipment. In addition, there is only limited information available. Therefore, there is high level risk involves in setting up a venture based herbal production. The level of risk declines as the industry develops, production technology increases, markets are defined and an industry infrastructure is established (Bruce, 2001).

2.1.2 Drying of medicinal and aromatic plants

Drying of medicinal herbs should take place as soon as possible after harvesting; otherwise insects and fungi, which thrive in most conditions, render them unusable. Conventional drying methods such as open sun drying and conventional-fuel dryers are not suitable; since they may yield a less quality product and may increase the drying cost or time. Moreover, they may not be reliable and environmentally safe. In most countries, enormous quantities of food losses have resulted from spoilage, contamination, attack by insects/rodents/birds and deterioration during the storage period. There are number of factors, which are responsible for the post harvest losses, such as system of harvesting, processing, storage, handling, and marketing. Drying of product is one of the important post harvest processes and it has enough potential to reduce the post harvest losses, and to prevent spoilage of the product in storage drastically. Moreover, good drying technique can enhance the quality of the product significantly (Garg et al., 2001). Therefore, the drying of medicinal herbs must be accomplished as soon as possible after harvesting, to increase the quality of the herb and to prevent the expected contamination and losses caused by the infestation of rodents, birds, insects, and fungi which thrive in moist conditions (Garg et al., 2001; Yahya et al., 2001).

The technical drying process necessitates an enormous amount of thermal and electrical energy. An improvement in the quality of the product to be dried and at the same time a decrease in the drying cost and time are achieved through the utilization of a controlled conventional drying method, which is based on a good utilization of the renewable energy sources. A complete dynamic modeling of the solar thermal subsystem, using the energy balance principle, is developed and the system results are indicated. The results illustrate that the designed control technique enables the developed herb dryer system to be in correct and continuous operation during the sunny/cloudy day and night hours (Fargali**,** 2008).

2.1.3 Influence of drying temperature on active ingredients

Generally, high temperature influence essential oil quality and quantity in medicinal and aromatic plants not only during drying; reduction in active ingredients continues during the storage period as well. Similar results are confirmed by different references (Koller, 1987; Shilcher, 1987). According to Jud (cited in Müller, 1992), the maximum drying temperature of Salvia Officinalis is declared as 30 °C. By increasing the drying temperature from 30 °C to 55 °C, essential oil losses increase by 15 % and the drug color changes from green to gray. Drying temperature usually has an influence on the temperature sensible components of essential oil.

Drying temperature has important effects on the color of medicinal and aromatic plants. The changes in color parameters of fresh and dried peppermint (Mentha piperita L.) as affected by drying air temperature were given in Soysal (2000). Statistical tests show that the color parameters of the fresh peppermint differed significantly from the dried products exposed at different drying air temperatures. Higher temperature could raise dramatic color deteriorations and burning of the product.

To withdraw the high amount of moisture from fresh crops, a large amount of energy is needed. The specific drying energy for drying depends on the material dried, material initial and final moisture content, drying process and the type of the dryer. According to the experiments conducted by Müller (1992) in a laboratory dryer, the results show a high influence of drying temperature on specific drying energy of S. officinalis. It was 13 MJ/kg at drying temperature 30 °C and increases to 42 MJ/kg at 40 °C. In the light of above discussion, the drying process is not only an energy intensive process but it deteriorates the quality of essential oil contents in the plant material. So, it is always preferable to process the fresh plant materials for good quantity and quality of the essential oils.

2.2 Essential oils extraction from medicinal and aromatic plants through distillation

2.2.1 General

Essential oils are the aromatic portions of the plant located within distinctive oil cells, glands, or internal sector canals. In some exceptional cases, essential oils are formed during the extraction of the source plant material. However, some essential oils are formed only as a result of enzymatic reaction. They originate from a single botanical source and can be described as highly concentrated, volatile, and aromatic essence of the plant. Each

essential oil contains hundreds of organic constituents that are responsible for their therapeutic actions and characteristic odor of the source plant material. These components are classified as monoterpenes, sesquiterpernes, aldehydes, esters, alcohols, phynols, ketones, oxides, and coumarins. Essential oils are extracted from various parts of the plant like leaves, roots, wood, bark, seeds/fruits, flowers, buds, branches, twigs, or whole plants (Öztekin & Martinov, 2007). About 65 % of the essential oils produced in the world are obtained from the woody plants that are trees and bushes (Baser, 1999).

According to Oyen & Dung (1999), an essential oil is a mixture of fragrant, volatile components, named after the aromatic plant material of a single type and identify from which it has been derived by a physical process and whose odor it has. The definition indicates that a given essential oil is derived from a single specie or variety. The definition given above states that an essential oil is derived by a physical process, i.e., it has not purposely changed chemically. The physical process by which the essential oils are obtained may also influence the chemical composition of an essential oil.

Essential oils and other flavoring products are isolated from plant material by various extraction techniques such as cold pressing or expression, distillation, solvent extraction, vacuum microwave distillation, maceration, and enfleurage. The products of extraction are usually termed as concretes, absolutes, pomades, and resinoids, which are not regarded as essential oils. Although the extraction and distillation refer to different isolating techniques, in this text, we use the extractable compounds like essential oils and other flavoring products from the plant materials (medicinal and aromatic plants), mixtures and compounds by chemical, physical, or mechanical ways. Essential oils are generally obtained by various distillation techniques such as water distillation, water and steam distillation, steam distillation, and expression or cold pressing. Among them steam distillation or hydro distillation is the most widely accepted method for the production of essential oils on a commercial scale. Approximately 90 % of the essential oils are produced in this way (Öztekin & Martinov, 2007).

2.2.2 Essential oils extraction by distillation

The oldest distillation equipment known dates from the 4th Century AD. It used the familiar process of condensation of vapors on the lid of a cooking pot; the main modification was a rim around the inside of the lid to collect and remove the condensate. A mixture of water and the material to be distilled was heated to the pot or vat by direct fire, charring

occurred, causing some of the compound to decompose. In the 11th century, the Iranian physician, Abu Cina (known in Europe as Avicenna) added a frame to the vat fixed above the level of water, on which the material is to be distilled was placed. In this way, the material came into contact with steam only, and fewer degradation products were formed. This improvement later led to the development of steam distillation. A final major improvement made in the 12th century was the addition of condenser in which the water could be cooled and condensed rapidly. This greatly improved the efficiency of the distillation process (Oyen & Dung, 1999).

The process of essential oil extraction is an old age essential oil extraction whereby a liquid is separated into components that differ in their boiling points. The distillation technology is relatively simple and adoptable in rural areas. Basically, a simple distillation unit consists of four parts: furnace (heat source), distillation still, condenser, and oil separator. Although the principle of distillation is the same, practical application of this technique differs depending on the type and physical form of the plant material. Three types of distillation are in practice. These are water distillation (distillation with water), water and steam distillation, and steam distillation (distillation with steam). The yield, composition, quality, and commercial value of the essential oils are generally affected by the type and efficiency of the distillation unit, as well as the age of the harvested plant material and the ecological conditions where the plant material is cultivated or wild harvested (Öztekin & Martinov, 2007).

2.2.2.1 Water distillation

Water distillation is the oldest and cheapest distillation method, which is simple in design and easy to construct. It is generally used to extract the essential oils of the dried or powdered plant materials, that is, spice powders, ground woody plants like cinnamon bark as well as some flowers such as rose and orange and very tough material such as roots, woods, or nuts. During the boiling process, the volatile component, essential oils from special structures inside or at the surface of the plant material, is mostly extracted at temperature just below 100 °C by diffusion mechanism. The extracted volatile constituent is transported along with the steam to the condenser where the mixture of the vapor is cooled and transferred to the liquid phase. This liquid is then taken to the oil separator called the Florentine vessel. Due to density difference, the essential oil is decanted from the water. The remaining distillate, which is the by product of the distillation called floral

water or hydrosol, can be added to another distillate and redistilled together with it (Öztekin & Martinov, 2007).

The principle of water distillation is to boil and vaporize a suspension of aromatic plant material and water in a vat so that its vapors can be condensed and collected. The essential oil which is immiscible with water is them separated by gravity in a “Florentine flask”. The water in the still must be kept in motion to prevent the plant material from clogging together and settling at the bottom of the still. This would result low yield of essential oil, charring of the material and degradation of thermo-instable compounds, resulting in “still odors”. Water distillation is still used in traditional field stills, but is mainly used for the distillation of floral material such as flowers and citrus that clog together in other distillation procedures. The main drawback of water distillation system is that large amounts of water have to be heated and the plant material should always be in contact of water which will be used to create steam for distillation (Oyen & Dung, 1999).

To prevent agglomeration of dense plant material and to insure that the plant material is always in contact with the boiling water, the plant material should be stirred throughout the distillation process. As the agglomerated material will settle down, at the bottom of the still, these material will be overheated and thermally degraded, which leads to the formation of off-notes. As the distillation still is directly heated by a furnace, water in this still must always be more than enough to last throughout the distillation process to prevent the overheating and charring of the plant material which leads also to the formation of the off-notes (Lawrence, 1995). The disadvantages of water distillation system are energy becomes expensive due to slower process, produces lower quality oil, incomplete release of the essential oil, and skilled labor and large numbers of stills are required as charge has to be less dense (Lawrence, 1995; Vukic et al., 1995). The flow diagram of water distillation process is shown in Fig. 2.1

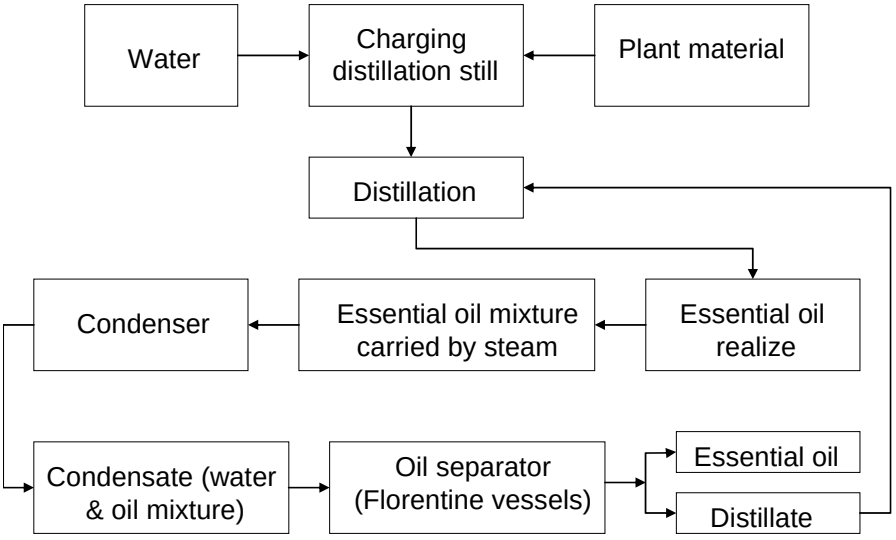

Figure 2.1 Flow diagram of water distillation process (Source: Adapted from Lawrence, 1995; Öztekin & Martinov, 2007)

2.2.2.2 Water and steam distillation

Water and steam distillation (also named wet steam distillation) is a method that has characteristics of both water distillation and steam distillation. With this method, a metal grid is placed in the still above the level of water and the plant material is thus avoided. As only the water is heated, the risk of charring and the formation of “still odors” is reduced but the hot walls of the still may cause some damage. Water and steam distillation are used for many kinds of plant material, e.g., lavender, thyme, and peppermint (Oyen & Dung, 1999).

The design of the equipment used is generally very similar to that used in water distillation (Lawrence, 1995). The wet steam can be supplied from the boiling water below the perforated grid at the bottom of the distillation still to provide a uniform steam passage (Vukic et al., 1995). Otherwise, the steam will pass through dominant channels and will be in contact with just some parts of the material. Even if the plant material can not be in direct contact with the fire source beneath the still, as the walls of the stills are good conductors of heat, unwanted still notes can also be obtained by over heating the plant material. The wet steam can make the lower plant material resting on the grid quite wet, and slow down the distillation process. It provides time and fuel economy as compared with water distillation system. Higher yields of essential oils with minimum chemical changes are obtained (Öztekin & Martinov, 2007). The flow diagram of water and steam distillation is shown in Fig. 2.2.

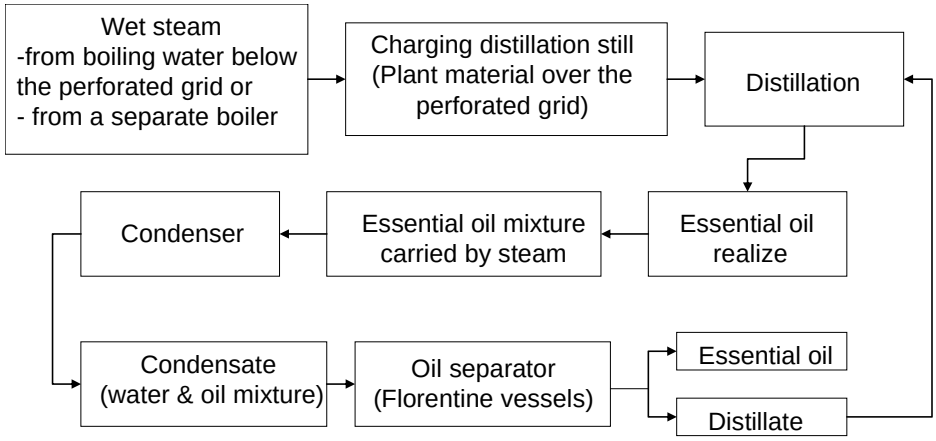

Figure 2.2 Flow diagram of water and steam distillation process (Source: Adapted from Lawrence, 1995; Öztekin & Martinov, 2007)

2.2.2.3 Direct steam distillation

In steam distillation (sometimes called “dry steam” distillation), a separate steam generator is attached to the still. As in steam and water distillation, plant material is placed on a grid in the distillation vat, but no water is added. Steam produced in the generator is forced through the material to be distilled. High pressure steam is often used, e.g., steam of 5-10 bars pressure at 150-200 °C. The duration of the distillation process depends on the steam temperature and the ease with which the essential oil can be removed from the plant material. Plants in which oil is stored in hair glands can be distillated very easily; those in which oil is stored in or below the epidermis require more intensive distillation. The main advantage of steam distillation is that the amount of steam used and its temperature can be readily controlled. As the vat walls do not become hotter than the temperature of the steam, the risk of charring is minimal. Steam distillation is used for most of the essential oils, except those from delicate flowers. The only precaution necessary when distilling leafy material it is ensured that it is cut not too fine, since this may cause `channeling` resulting in poor distillation yields. Channeling occurs when the plant material becomes too compact. The steam then forces its way through via a few large channels, instead of moving through the entire mass of plant material. Steam distillation is sometimes conducted under reduced pressure, to lower the distillation temperature (Lawrence, 1995).

Steam distillation is the most common method of extracting essential oils on a commercial scale. Approximately 80 to 90 percent of the essential oils are produced in this way. This method is used for the fresh plant material that has high boiling point like seeds, roots and woods. It is also used for fresh plant such as peppermint and spearmint, oil roses, and

chamomile. This type of distillation plant is similar to other types of distillation plants. The only difference is that there is no water inside the still body during distillation. After the plant material is loaded into the perforated grid, or in a basket or cartridge in side the still body, the saturated or sometimes, overheated, pressurized dry steam that is generated in a separate boiler or a steam generator is injected below the plant material as the steam will flow in the direction of less resistance, the plant material should be uniformly distributed in the still body. The essential oil of the plant material is separated by the process of diffusion while steam passes through the plant material. The steam with a certain contents of essential oil vapors moves through the condenser, usually cooled by running fresh water, where the mixture is condensed. The mixture of condensed water and essential oil is then collected and separated by decantation in Florentine vessel (Öztekin & Martinov, 2007). The process of steam distillation is more suitable for commercial scale operations. However, steam distillation has several advantages over the previously described variants (Lawrence, 1995; FAO, 1992). It is more energy efficient, cost effective and is the cheapest method of essential oils extraction. It provides better control of the distillation rate. Quality of essential oils produced by this type of distillation units is more consistent and repeatable. There is the possibility of changing working pressure that enables the use of low pressure for high volatile oils and high pressures for low volatiles ones. The rapid distillation is less likely to damage those oils containing reactive compounds like esters. The obstacle for wider use of this type of distillation plant in developing countries and its biggest disadvantage is the high capital expenditure for the equipment.

Many of the demands of the process of steam distillation are often contradictory. According to the existing knowledge the most important demands are to obtain all, or most of the available essential oil from the raw material. To economically justify the process, approximately 85 % of the essential oil in the plant must be obtained. The “dominant channels” can be formed in the still during water and steam, and steam distillation processes. This happens because the plant material gets denser by absorbing water and fresh steam is now not able to move it, and pores in the randomly placed material in the beginning get larger. In this way, only some part of the material is in touch with the steam and obtaining essential oil is far from complete. This can be prevented by using mixers such as auger inside the still body or chopping of the plant material before processing. The risk of losing considerable amount of essential oil exists while chopping the plant material.

As the most efficient of all distillation processes, steam distillation is a very wasteful process. It is always necessary to evaporate relatively high amounts of water to obtain a small quantity of essential oil. Water is never saturated with essential oils vapors. On the other hand, cooling water consumption is high. Cooling water temperature is usually 20 °C at the input and is about 70 °C at the exit from the condenser. The flow rate of this water is, for example, for processing of 300 kg of fresh plant material, up to 2000 kg per hour. The problem is not just finding the enough rich sources, but affording the price and also the possible micro pollution with water at that temperature. Further more, water from the commercial pipe lines, for instance, has to be de-mineralized, prepared for the use in steam generators and for some spiral type condensers (Dachler & Pelzman, 1989). For the improvement of steam distillation system, the techniques like mobile distillation units, turbo distillation, hydro diffusion, continuous steam distillation systems are used (Lawrence, 1995). The flow diagram of direct steam distillation is shown in Fig. 2.3.

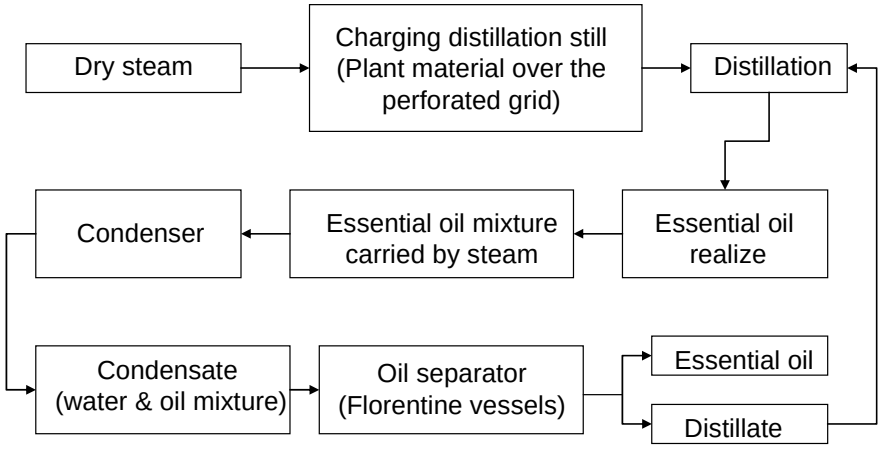

Figure 2.3 Flow diagram of direct steam distillation process (Source: Adapted from Lawrence, 1995; Öztekin & Martinov, 2007)

2.2.3 Industrial utilization of essential oils

A broad range of plants are used for medicinal and aromatic purposes, namely herbs, spices, vegetables, trees, natural gums and resins, algae, flowering plants, gymnosperms, ferns, bryophytes, mushrooms, and the like. In general, the whole plant or various plant parts are used for medicinal and aromatic raw material. Medicinal and aromatic plant (MAP) materials are used by a large number of industries such as pharmaceutical, food and spices, cosmetic, dental hygiene, paints, adhesives, beverage, herbal tea, agriculture, textile, paper and printing, motor, petroleum, plastic, tobacco, animal feed, dairy and the like (Öztekin & Martinov, 2007).

Essential oils find a use in variety of industries as flavoring and fragrances materials. Generally they are processed further to generate their major constituents in a pure form or as “isolates" by which term is meant a group of constituents with similar properties and boiling point range. The ranges of industries that utilize essential oils or their down-stream products are many and varied. Major Industrial products in which essential oils are utilized as given is Table 2.1

Table 2.1: Major industrial products of essential oils utilization

Catagory	Industrial products
Adhesives	Gums, pastes, glues, scotch Tapes, Surgical bandages etc
Motor Industry	Polishes, Cleaners, Paints, Furnishings
Pharmaceuticals	Toothpastes, Dental preparations, patent medicines, Toiletries, Medicated hair preparations, body applications, etc., Herbal products range
Polymers and paints	Household paints, Distempers, Varnishes, Plastic goods, and toys, Household utilities
Insecticidal and Repellants	Sprays, Odor eliminators, Disinfectant coils, Repellant preparations
Leather	Deodorants and fragrances
Paper, printing, and packing	Special stationary, Inks, Wrapping materials, Packing materials, Adhesive taps etc,
Petroleum	Cream deodorants, Naphtha solvents, Lubricating oils, Petroleum special distillates, waxes.
Beverages	Bitters, Cordials, carbonated drinks, Liqueurs, concentrates, Essences
Veterinary	Animal feeds, Sprays and deodorants, medicaments and anti-parasitic preparations
Home goods	Kitchen utensils, detergents, soaps, cleansing preparations
Rubber	Gloves, surgical goods, Toys, Water proofing compounds, rubber, utility goods
Textiles	Deodorants, Upholstery materials, Dyes and pigments preparations
Toiletries	Perfumes, Fragrances, Shampoos, Colognes, oils, creams, General toilet utilities, Powders etc

(Source: Dürbeck, 1997. The distillation of essential oils, manufacturing and plant construction handbook)

2.2.4 Economic importance of the industry

The essential oil industry may not be regarded as a major contributor to the national economy of many a producer country but it is evident that the number of consumer goods that are processed which require a small quantum of a product derived from essential oil, is considerable. However, given adequate incentive and good management this industry, with essential oils produced to quality specifications, would enable even a small

developing country to enhance its economic gains to a sustainable degree. The technology involved is relatively simple and the variations possible enable innovations to be made to accommodate a diverse range of conditions.

Agronomic expertise is available or can be produced. The industry itself is not always capital intensive and the local design and fabrication of distillation equipment can cut capital costs down to the absolute minimum. The labor intensive nature of the industry is an advantage where labor availability is a factor. Price fluctuations so common to the industry can also be circumvented if economic cultivation and harvesting techniques are adopted, field distillations are carried out wherever feasible and quality ensured for the products. The development of downstream processing of products such as isolates and aroma chemicals from essential oils is an exercise that would also be profitable in the correct circumstances, for even a developing country producer (Öztekin & Martinov, 2007).

2.2.5 Essential oils in local and regional health care markets

The health systems are presently in a crisis. In the western world medicine is suffering from the delusion of offering better and better individual services, most of them not actually required or not adjusted to breaking diseases. Therefore, the medicines are no longer in the position to fulfill its duty of health care. This is the present in the present scenario for the application of aromatherapy for its use of local and regional traded essential oils. Due to the emergency and emergence of the tropical diseases and the missing interests and responsibilities of western pharmaceutical companies, the applications of genuine and authentic essential oils for the primary health service of tropical countries offers local and regional market incentives to essential oil producers out side the established markets overseas. Figures of World Health Organization (WHO) show that, by western standards, rather manageable diseases are the efficient killers on a global scale, or for that matter in developing countries. For an appreciation of the potential of essential oil based health care in developing nations, it is useful to take a look at the disease causing, in absolute numbers, the most deaths globally.

Table 2.2: Description of different infectious diseases

Infectious diseases	Cause	Annual deaths
Acute respiratory infections	Bacterial, viral	4,300,000
Diarrhoeal diseases	Bacterial, viral	3, 200, 000
Tuberculosis	Bacterial	3,000,000
Hepatitis B	Viral	1-2,000,000
Malaria	Protozoan	1.000.000
Measles	Viral	880,000
Neonatal tetanus	Bacterial	600,000
AIDS	Viral	550,000
Pertussis (whooping cough)	Bacterial	360, 000

(Source: World Health Organization, Harvard school of public health, 1990 figures)

Between 50-90 % of the population in developing countries depend on traditional healing systems, rather than “modern” western medicines, to treat these diseases. It is the aim of development policies of organizations like Protrade to strengthen primary health care provided by traditional healing systems. This is achieved through scientific and technological support provided to the traditional healing systems and consequently, through increased availability of local produced essential oils. Infectious diseases in these countries are often a result of poor hygienic conditions and low nutritional standards and are of a nature often easily controlled with medical aromatherapy. Essential oils can be used in multiple ways; by improving hygiene, as a preventative measure and as intervention when disease needs to be treated. As a result, demand for genuine essential oils for primary health care in developing nations may ultimately eclipse that of the more industrialized countries (Dürbeck, 1997).

2.2.6 Value addition in developing countries

The Protrade activities are designed to aid developing countries by improving their ability to cultivate medicinal plants and benefit, by value addition, though the additional processing step of essential oil production by local industries. These measures are taken to benefit local economies by improving trade through exports of essential oils processed from cultivated plants rather than by exporting wild-harvested raw material to foreign processors and secondly, by providing essential oils for local markets from primary health care. It is not possible to establish a small and medium scale industry based on wild flora without assessing the quality and quantity of the raw materials available and without taking into account the protection of the environment. If no incentives are given to the private sector, the present development will go on with the final aim of extinction of plant species. If the extinction of plant species is going on in this manner, the 50-80 % of the people in

developing countries will suffer in their primary health care from two very dominant developments. Firstly, modern medicines from the developing countries are not accessible and secondly the medicinal plant species for their traditional preparations are extinguished. One commercial approach to ameliorate the scientific developments of the past is to make information and technology available to the decision makers of government and private sector natural product industries in developing countries. In some countries of medicinal plant industry is heavy under pressure from the scientists educated in developed countries because they are afraid of commercial competition with traditional healers and associated industries and on this new view of the ability of the essential oils to be useful, holistic pharmaceuticals, novel approaches to support primary health care in developing nations have been adopted. As a result of Protrade activities, genuine oils from countries like Nepal, Madagascar, Tanzania and EI Salvador are beginning to gain a share in the aromatherapy markets of industrialized nations, mainly France, Germany and US. Essential oils from these countries, having found their way into aromatherapy commerce, include: Nardostachys jatamansi, Palmarosa, Vetiver, Niaouli, Cinnamon and Cardamom. It appears that essential oils manufacturers in developing nations are comfortable in satisfying the requirements for genuine oils by the customers interested in medical aromatherapy (Dürbeck, 1997).

2.2.7 Problems and prospective for aromatherapy in tropical counties

Beside commercial plantations the industrial production of genuine and authentic essential oils faces serious threats to a secured and sustainable supply of raw material due to extinction of plant species from the wild caused by over consumption and endangered habitats. Domestication, cultivation, forestry of essential oil plants in many developing countries is limited due to the problems of technology transfer (pilot plants, distillation unit, cold pressed essential oil), information transfer (market, IPR, EINECS), no standardization (big quantity standard oils in demand) and local and regional marketing. The intellectual property rights (IPR) and traditional knowledge of essential oil plants enclose the enormous potential for biodiversity prospecting and for new regional and local markets in Aromatherapy. The commercialization of new oils from tropical forests offers a treasure house for a new horizon of applications out of The Hot Zone.

2.2.8 Different distillation plants for commercial applications

As a sample, Dürbeck (1997) explained different distillation plants for commercial applications. LT plant comprises a still mounted over a brickwork fireplace, a flue gas

stack, a condenser, a separator, and a lifting aid for the still cover. The fuel to be used for firing the still is intended to be the spent plant material, but firewood is an acceptable alternative. The type RT distillation plants are the improved version of the type LT and are designed for continuous distillation on a commercial scale. The plant comprises two stills heated by steam supplied from an external source, two shell and tube type condensers, each with its own separator, and a load handling system. In most duplex plants, the two stills are served by one condenser. The production capacity of RT plant is therefore much higher than that of the type LT, and for this reason it is best suited at some central location where it can serve a wide plantation area, therefore most likely to be in a town.

The type RT plant is offered in two versions, the type RTA and the type RTB. The only difference between the two is that the type RTA uses a steam heating coil immersed in the water in the still and therefore requires a still feed water system, where as the type RTB uses a steam sparker at the bottom of the still which admits steam into it (steam injection type). In RTA, the coil has been designed to provide the heating rate required to achieve the rated distillation rate of the still when supplied with steam at 10 bars. The water in the still boils, becomes steam at 100 °C and rises up through the charge of the plant material, contacting it at this temperature. In RTB type distillation plants, plant material with high boiling point oils, the higher temperature steam can be used by adjusting the supply of pressure accordingly, for instance, steam at 3 bars would be at 141 °C. In most cases, however the requirement would be for steam as close to 100 °C as is practical, that is, steam at atmospheric pressure. The pressure reducing valve at the sparker inlet would therefore be adjusted say, 0.25 bar. The condenser from the type RTB is therefore contaminated and must be discarded, whereas that from the type RTA is recovered and returned to the boiler. RTB is well suited for the distillation of high boiling point oils, and the desired temperature can be obtained by setting the boiler operating pressure accordingly. For most plant materials, however, the supply steam pressure RTB should be as close as is practical possible to atmosphere. The heating coils of type RTA operates at 10 bars and this must be in fabricated from seamless pipe to a high standard of workmanship. Meanwhile a spare cartridge which has been loaded with plant material is picked up and loaded in the still and the second distilling cycles commences.

The type BT distillation unit consists of a simple still made of two standard 200 liters oils drums placed one above the other, a small shell and tube condenser, and a type LT separator. It is fired by a gas burner using cooking gas in standard cylinders. In remote

locations, firewood can be used in which case, the still must be mounted outdoors and a suitable brickwork fireplace with a steel grating provided. Provision has been made to remove the upper section of the still. The cover can then be transferred to the lower section and the still, in its reduced state, can be used for distilling from very small amounts of plant materials. The plant can easily set up and dismantled. The separator and the support legs assembly can be placed within the still body for transport. It requires no foundation.

The type QT distillation plant is designed as a research still for low volume of distillation of high value oils. Its condenser is of shell and tube type and is mounted integral with the still to provide a single unit plant. The top of the cover is in the shape of an inverted cone which enables any vapors that condense on its surface to run down and drip into the condenser vapor inlet. Heating is by a steam coil supplied from an external source at a supply pressure of 3 bars or alternately it can be electrically heated by an industrial type heating element fitted in place of steam coil. The heat input is limited by the capacity of heating device (be it steam or electric) and there is no need for low-water protection. The plant is made of stainless steel through out, except for the condenser shell which is of mild steel. This gives the plant a long service life and facilitates cleaning of its internals (Dürbeck, 1997).

2.2.9 Guidelines during distillation

In the case of stills, of the type LT, where the steam is generated in situ, the wetness of the steam is fixed and the rate of flow is determined by the rate at which heat is applied to the water containing reservoir at the base of the still itself. The time of completion the distillation has to be determined by plotting the graph for total volume of oil condensed versus time. The distillation is complete when the curve is flattens off indicating that almost a hundred per cent of the oil has come over. Studies in order to determine optimum time of distillation may be carried out using the pilot plant scale stills such as type BT. However such results should be extrapolated to the field situation with care, as things could be different. It is best to use the pilot scale results as a guide and to determine the operating conditions in the field for use thereafter (Dürbeck, 1997).

In the RT-type stills, there is very facile control of the variables possible and hence the steam related parameters could be determined with accuracy and applied with a degree of consistency. When the batch size and the steam pressure is maintained constant and the

rate of injection of steam is varied with several conditions, a plot of the percentage recovery of oil versus time will indicate the optimum steam injection rate. The optimum distillation is again when near complete recovery of the oil is achieved, as recovery of the final traces of the oil may not be economical in comparison to the expense of distilling for several hours longer. The ultimate judgment on those parameters must be made by the technologist after consideration of both the economic as well as scientific and technological factors. The analysis of the oil in the prolong distillations must be compared with that of a sample distilled where economical considerations have curtailed the time of distillation and the analytical picture must warrant the economic trade off else the oil may fall short of market stipulations.

The efficiency of steam heating is not much affected by the steam supply pressure. The higher the pressure, the hotter the steam and this can be detrimental to the product quality. The most convenient operating pressure is, of course, atmospheric. All the stills presented here operate normally at atmospheric pressure, but it must be appreciated that there will be a small back pressure on the still which is needed to push the distillate through the condenser. This varies from 25 mm to 500 mm of water depending on the condenser type and the operating conditions.

The types BT and LT stills contain a small amount of water at the bottom which is boiled by lighting a fire under base of the still. These stills are intended for field use where firewood or spent plant material is plentiful, and where electricity may not be available. Also these stills are intended for local manufacture at low cost. Direct firing is the best available option in these circumstances but it must be appreciated that the base of the still will deteriorate from repeated firing and that there is an inherent “low water-overpressure “danger potential. The steam contacting the plant material is at 100 °C which is acceptable for most plant material. This temperature remain constant for the duration of the distillation without any action from the operator, but the rate of distillation will depend on the rate of firing and much depends on the skill and experience of the operator to achieve the exact firing rate and to maintain throughout the distillation run (Dürbeck, 1997).

2.2.10 Distillation options

The distillation options are often dictated by the nature of the raw material and the equipment available. Bulky materials call for the use of field stills. They can be either the LT-type with built-in fire places or the RT-type which use a satellite steam source.

Although the former is less costly, the latter affords better control of the distillation and, as discussed earlier, is in the longer term more cost effective. These stills and their respective features have been discussed before from the view point of their utility. The pre-preparation of the raw material is an important consideration in the production of quality essential oils. The pre-preparation varies from material to material due to differences in the manner the essential oils containing cellular vessels are located within the plant (Dürbeck, 1997).

Distillation is a heat dependent separation and purification process of a liquid mixture based on the vapor pressure difference. It can be defined as a method of extracting an essential oil from the plant material by evaporating and subsequent condensation of the liquid. Similarly, the cost of production depends highly on the scale of the production small, medium or industrial scale production, raw materials, processing equipment, energy, and labor requirement (Öztekin & Martinov, 2007).

For the distillation of moderately volatile oils under atmospheric pressure, the rate of steam flow is a greater factor in the speed of oil recovery than the steam's density. The volume of steam generation is then more important than the operating pressure (Denny, 1991).

2.3 Solar energy utilization

2.3.1 Solar energy application in medium temperature range

A large number of industrial processes demand thermal energy in the temperature range of 80–240 °C (Proctor & Morse, 1977; Kalogirou, 2003). Solar thermal flat plate collectors are not suitable for very high temperature applications. For high temperature applications, different solar concentrators may be employed. A number of solar industrial process heat systems are installed and operated on experimental basis have reported the status of the development of medium temperature solar collectors for industrial applications. In this temperature range, solar thermal systems have a great scope of application (ESTIF, 2004; Weiss & Rommel, 2005). However, the challenge lies in the integration of a periodic, dilute and variable solar input into a wide variety of industrial processes. Issues in the integration are selection of collectors, working fluid and sizing of components. Application specific configurations are required to be adopted and designed. The specific configuration consists of concentrating collectors, pressurized hot water storage and a load heat exchanger. The solar systems are in a developmental stage for medium temperature industrial applications and yet to achieve a full commercialization (ESTIF, 2004).

Application-specific configurations are required to be adopted and designed. Design issues in solar industrial process heat systems involve the selection of appropriate type of collector and the working fluid, and optimal system sizing i.e., to determine the appropriate collector area, required storage volume and the size of the heat exchanger.

Kulkarni et al. (2008) described that as far as selection of appropriate type of collector is concerned, thermal efficiency at the desired temperature, energy yield, cost and space occupied are the deciding factors. Water, as a working fluid, is the preferred choice for low temperature applications on the basis of thermal capacity, availability, storage convenience and cost. However, for process heat applications above 100 °C, water must be pressurized. Storage cost rises sharply with increasing system pressure. Commercially available mineral oils are also used for medium temperature (above 100 °C) applications. However, applicability of these oils is restricted due to cost, tendency of cracking and oxidation.

An important design issue in solar thermal system for industrial applications is the optimal sizing of the system i.e., appropriate sizing of the collectors, storage and heat exchanger. Different guidelines and methodologies are available to design solar thermal systems operating up to 100 °C (Klein et al., 1976; Klein & Beckman, 1979; Pareira et al., 1984; Abdel-Dayem & Mohamad, 2001; Kalogirou, 2004). For systems operating above 100 °C, detailed simulation programs such as TRNSYS and SOLIPH have been applied (Kutscher et al., 1982). However, there is a scope for developing general design guidelines for solar industrial process heat systems for medium temperature applications (Clark, 1982; Eskin, 2000; Weiss, 2003).

Goswami (1999) described that for temperatures of up to 100 °C required for many process heat applications; forced circulation water-heating systems can be used requiring a large collector area, storage and pumps etc. For higher temperatures, evacuated tube collectors or concentrating collectors must be used.

Proper design of solar water heating system is important to assure maximum benefit to the user, especially for a large system. Designing a solar hot water system involves appropriate sizing of different components based on predicted solar insolation and hot water demand (Kulkarni et al., 2007).

Beyond the low temperature applications there are several fields of application of solar thermal energy at a medium and medium-high temperature level (80-240 °C). The most important of them are: heat production for industrial processes, solar cooling and air conditioning, solar drying and sea water de-salination. The industrial-heat demand contributes about 15 % of overall demand of final energy requirements in the southern European countries. The present energy demand in the EU is estimated to be 300 TWh/year (Kalogirou, 2003).

Norton (1999) presented the most common applications of industrial process heat. In particular, the history of solar industrial and agricultural processes applications was presented and practical examples were described.

Around 105 GWth correspond to 150 million square meters of solar thermal collectors were installed by the year 2004 worldwide. Until now, the wide spread use of solar thermal plants has focused almost exclusively on swimming pools, domestic hot water preparation and space heating in the residential sector. The use of solar energy in commercial and industrial companies is currently insignificant compared to the sectors mentioned above. Most solar applications for industrial processes have been on a relatively small scale and are mostly experimentally in nature. The major share of energy, which is needed in commercial and industrial companies for production, processes and for heating production halls, is below 250 °C. The low temperature level (80 °C) complies with the temperature level, which can easily be reached with solar thermal collectors already on the markets. For applications where temperatures up to 250 °C are needed, the experiences are rather limited and also suitable collectors are missing. Therefore, for these applications, the development of high performance solar collectors and system components are needed. One of the objectives of Task 33/IV is to develop, improve and optimize solar thermal collectors for the temperature level from 80 °C to 250 °C (medium temperature collectors). The collectors investigated in cooperation with the industry are double glazed flat plate collectors with anti-reflection coated glazing, stationary CPC collectors, MAReCos (maximum reflector collectors), Parabola trough collectors as well as linear parabola Fresnel collectors. This report gives an overview and some background information about the present state of the art of the medium temperature collector developments carried out in the frame work of the EIA Task 33/IV on Solar Heat for Industrial processes (Weiss, 2005).

Various high-temperature solar thermal power systems have been suggested and developed, such as parabolic trough, compact linear Fresnel reflector in single axis tracking technology area and paraboloidal dishes, single tower-central generation, distributed tower systems in two axis tracking technology area (Mills, 2004). But owing to the complex technologies and high costs, the high-temperature, solar thermal systems are still non-competitive, especially in developing countries (Wang et al, 2010).

2.3.2 Solar energy for industrial process heat demand

Most of the process heat is used in food and textile industries for such diverse applications as drying, cooking, cleaning, extraction and many others. Favorable conditions exist in food industry, because food treatments are storage and processes with high energy consumption and high running time. Solar thermal energy can be used for low-pressure steam generation at 100-110 °C and for refrigeration which can be accomplished with absorption cooling.

Dairies are very interesting applications for solar energy, because they often work seven days a week, thus fully utilize the solar system compared to other industries, which allow the system to be idle for 2 days per week. In the milk industry, thermal energy is used for pasteurization (60–85 °C) and for sterilization (130–150 °C) processes. Drying of milk powder, due to the high constant energy demand, is another important consumer. In the production, milk and whey are spray-dried in huge towers with air, which is heated from 120 °C to 180 °C. The drying process can have a running time up to about 8000 h per annum (Benz et al., 1998). In food preservation industries, several processes were identified, where solar thermal energy could be used: scalding of vegetables, sterilization (vegetables, fish and meat) with hot water or direct steam, scalding, cleaning and pre-cooking of fish, sealing and cleaning of cans, cooking. In addition, cold demand can be covered by solar absorption cooling and refrigeration. In the textile industry, energy is mainly consumed for heating of liquid baths close to 100 °C for washing, bleaching and dyeing. Drying processes usually use hot air or gases from 140 to 220 °C (Kalogirou, 2003). It is concluded from the results that it is more advantageous to apply solar energy to higher temperature processes than to lower temperature ones as the saving incurred are much higher. High technology collector like PTC cannot be used effectively for low temperature applications (Kalogirou, 2003). It is also concluded that as the fuel price increases, the more expensive collectors become viable and give much higher LCDs (Life cycle savings) that flat-plate collector. The solar contribution drops at higher operating

temperatures and vice versa. This is because at higher load temperature more energy from the auxiliary is required to cover the load. At low temperature, the best contribution is from FPC whereas at higher temperature PTCs give the best contribution (Kalogirou, 2003).

Many important developments have occurred in solar concentrating systems for diverse applications in the last decades. In particular, an important research effort has been directed towards power generation applications, chemical systems, and process heat (Estrada, 2007)**.** High temperature heat production for electricity generation often requires direct absorption of solar energy. To obtain direct absorption of solar energy, a parabolic dish with receiver configuration is often used. A focal receiver absorbs the concentrated solar radiation and transforms it into thermal energy to be used in a subsequent process. The essential feature of a receiver is to absorb the maximum amount of reflected solar energy and transfer it to the working fluid as heat, with minimum losses. Generally, a conventional receiver is used to accomplish this purpose (Kumar, 2007). These parabolic dishes with receiver configuration are often used for cooking applications and are termed as solar cookers.

2.3.3 Evaluation of solar cookers

The performance of solar cookers is evaluated by considering the controlled and uncontrolled variables. The uncontrolled variables are wind, ambient temperature, pot content temperature, insolation and solar altitude and azimuth. While controlled variable includes loading, tracking and temperature sensing. Solar cooker tests should be conducted when wind is less than 1.0 m/s at the elevation of the cooker being tested. If the wind is over 2.5 m/s for more than 10 minutes, the test data should be discarded. The reason is that the heat loss is strongly influenced by wind velocity. Wind velocities less than 1.0 m/s help to maintain a heat loss coefficient close to the natural convection loss coefficient. If wind shelter is required, it must be designed so as to not interfere with incoming total radiation. Solar cooker tests should be conducted when ambient temperatures are between 20 and 35 °C. The ambient temperature extremes experienced in one location may be difficult to replicate at another location. Cooking power is influenced by temperature difference. Available solar energy is to be measured in the plane perpendicular to direct beam radiation (the maximum reading) using a radiation Pyranometer. Variation in measured insolation greater than 100 W m^{-2} during a 10 minutes interval or readings below 450 W m^{-2} or above 1100 W m^{-2} during the test render the test

invalid. The reason is that by maintaining moderate fluctuations in insolation levels reduces the variability caused by thermal inertia effects. It is expected that most locations will meet these criteria. If not, exceptions need to be specially noted. It is also strongly recommended that tests be conducted between 10:00 and 14:00 solar time. Because the solar zenith angle is somewhat constant at midday, and the difference between insolation measured in the plane of the cooker aperture and the plane perpendicular to direct beam radiation will vary least. Exceptions necessitated by solar variability (presence of clouds) or ambient temperature (midday is too hot) must be specially noted. Parabolic-type units may require more frequent adjustment to keep the solar image focused on the pot or absorber. Thermocouples are recommended for their low cost, accuracy and rapid response. Thermocouple junctions should be immersed in the water in the pots and secured 10 mm above the pot bottom. The average water temperature (°C) of all the pots in one cooker is to be recorded every 10 minutes, to one tenth of a degree if possible. Solar insolation (W m^{-2}) and ambient temperature are recorded at least as frequently (Funk, 2000).

2.3.4 Use of high reflectivity material for the reflectors

Until a few years ago highly reflective aluminium sheet materials were predominantly used as reflectors for lamps in office and industrial buildings. Because of their mechanical properties and low cost compared to silvered glass mirrors, aluminized reflectors are finding applicability to high temperature solar concentrating technologies. Furthermore high reflectance aluminized sheet is already being successfully applied in low concentrating technologies like compound parabolic concentrator (CPC) troughs and day lightening. Of the material investigated, highly secular aluminium has an excellent chance to meet the requirements for medium concentrating technologies like parabolic troughs. For applications in humid climates, an additional polymer coating is necessary for durability. Standard anodized materials show satisfactory hemispherical reflectance properties after outdoor and accelerated exposure. Because of their manufacturing flexibility and their low costs, mirrors based on anodized or coated sheet aluminium are a promising alternative as primary or secondary concentrators in a number of solar energy applications. They offer solar weighted reflectances of 88-91 %, good mechanical properties and are easy to recycle (Fend, 2000).

2.3.5 Solar concentrators

Solar thermal power plants generally concentrate the direct beam radiation, incidentally rejecting a majority of diffuse radiations. Concentration by a factor C increases the incident

flux density at the solar receiver to the extent that radiation and convection losses are acceptable even at elevated receiver temperatures. Even photovoltaic power systems may use concentration, but here the objective is to reduce the required area of expensive photovoltaic element by a factor of C. In any case, there are several points which must be made about the optical systems employed so the design elements involved can be appreciated.

- All the basic laws of optics apply without modification.
- The objectives are commonly different to concentrate energy cheaply rather than to form a precise image, consequently different approximations are valid resulting in sometimes surprising configurations.
- Collectors must be very large (compared to a camera lens) in order to intercept significant power of order 2 m^2 per thermal kilowatts or 2 km^2 per thermal giga watt (Winter et al., 1991).

Since 1990, solar community kitchens of the Scheffler cooker type have been manufactured and installed at different places in Gujrat, India. The technical concept of the Scheffler cooker is very appropriate to local infrastructure. This is because the tools needed for constructions as well as the handling device are simple. This is fundamental for a local production and for the acceptance of the kitchen staff. Two major problems were found in the field of technical production, a rather complex construction and the needed precision demand a sound training and careful workers and the mechanism for the daily tracking of the reflector is obviously the week point of the whole system. Here every effort should be made to find a less temperamental design. Scheffler cookers have an excellent energetic efficiency with an estimated energetic payback of about half a year. Scheffler cookers are economically viable if they are used regularly (Sutter, 1996).

2.3.6 Solar distillation of water

Solar energy represents a vast energy resource which is most available in many areas where population density may be low and where conventional energy resources may be expensive. Its use for operation of desalination processes for production of fresh water is technologically feasible. The principles basic to solar distillation had been known for many years before the first significant installation was made in Chile in 1872. Located at Las Salinas in a desert area, this solar still was a glass-covered installation which covered a

ground area of 50,000 sq. ft. and produced a maximum of some 5000 gallons per day (gpd) of distillate for watering mules (Anonymous, 1970).

The double glazed AR-collector from ESE is applied in a solar driven, energy self sufficient, stand-alone system for sea water desalination. It produces about 100-150 liters of distilled water per day. The system was installed in December 2004 on the test site of ITC in Gran Canaria. The typical operating collector temperatures are between 50 and 95 °C. The system uses 3 modules with an aperture area of 2.325 m^2 each. The distillation unit is developed by Fraunhofer ISE. The distillation technology is based on the membrane distillation process (Weiss & Rommel, 2005).

2.4 Auxiliary energy utilization in solar distillation system

The degree of reliability desired of a solar process to meet a particular load can be provided by a combination of properly sized collector and an auxiliary energy source. In the most climates, auxiliary energy is needed to provide high reliability and avoid gross over design of the solar system (Duffie & Beckman, 2006). In a solar process heat system, interfacing of the collectors with the conventional energy supplies must be done in a way compatible with the process (Kalogirou, 2003). Several experiments were carried out during adverse climatic conditions using solar energy integrated with biomass energy. During hybrid solar distillation experiments, the distillation still was filled with water to produce steam by reflected beam radiations on the still bottom and the extra energy was taken from the biomass boiler. The experiments were conducted with different plant material like Melissa, Peppermint, Lavender etc. (Munir & Hensel, 2009).

3 Material and methods

The research work comprised of two phases, laboratory experiments with small scale distillation system followed by field experiments using solar energy.

3.1 Laboratory experiments

Laboratory experiments were conducted using small scale distillation units. The apparatus comprises of insulated electric heaters (0 - 500 W), round glass boilers each having 2 liters capacity, glass still tube, counter current flow glass condensers and Florentine flasks. In each experiment, 100 grams of the herbs were used. The electric connections to the heaters were provided through energy meters. The experiments were conducted for both “water distillation”, and “water and steam distillation” systems. In the process, the water vapors along with volatile essence of the plant material flow through the still vessel and then condense. The condensate is then collected in a Florentine flask where oil is separated from hydrosol due to specific weight difference. The power was maintained 500 W at the start of the experiments and 250 W when the steam generation started in order to maintain steady state condition during processing. The experiments were conducted when there were no more contents of essential oils in the plant material. The conversion factor of electric heater (from electrical energy to heat energy) was also calculated by water boiling test in the laboratory distillation apparatus. This factor is obtained by dividing the sensible heat calculated for water in the boiler with the electrical energy noted from the energy meter simultaneously and found to be 0.667 for the laboratory distillation apparatus. Identical conditions were maintained during experiments for different herbs. Energy meters and thermometers (Error < ± 0.2 K) were used to record real time data to investigate the optimal thermal and physical parameters during the distillation of essential oils. The laboratory data lead in design and development for solar distillation unit. The laboratory distillation apparatus is shown in Figure 3.1.

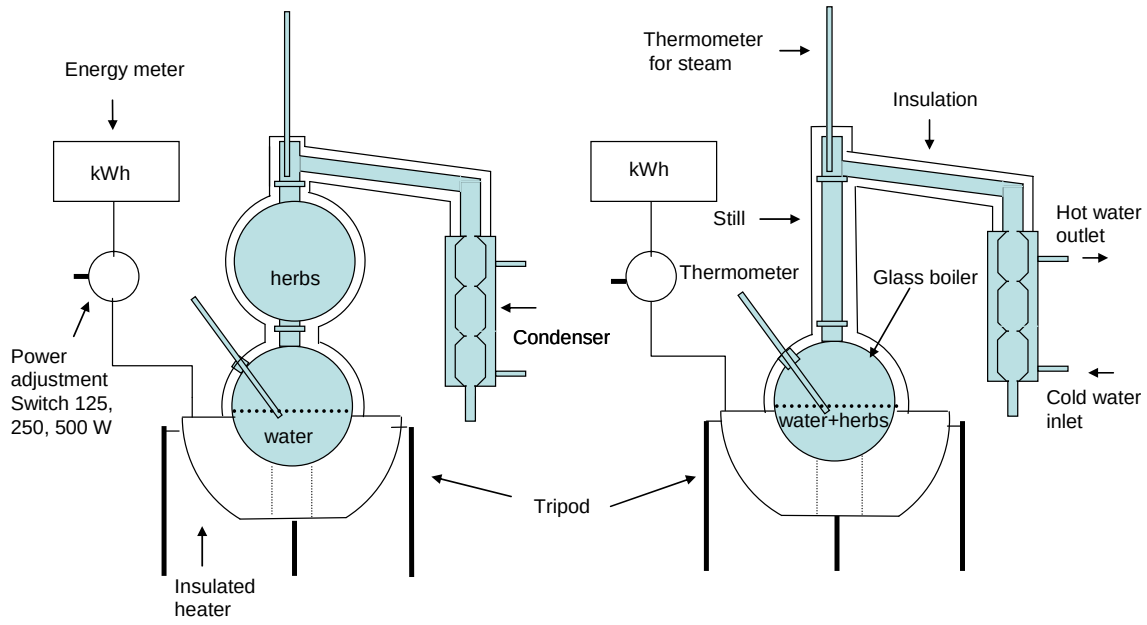

Steam distillation unit

Hydro distillation unit

Figure 3.1: Laboratory distillation apparatus

3.2 Selection of the solar collector

The main object of the research is to develop an on-farm solar distillation system. The basic criterion of solar collector selection was to conduct different types of distillation experiments successfully without changing the basic design principle of different distillation systems. From a number of studies on industrial heat demand, several industrial sectors have been identified with favorable conditions for the application of solar energy. Several experiments were carried out to utilize the solar energy in medium temperature range using vacuum tube collectors to increase the temperature in medium-high temperature range (Sharma et al., 2005; Stumpf & Balzar, 2001; Morrison, 1993; Esen, 2004; Balzar et al, 1996). These vacuum tube collectors are efficient in low temperature range but not suitable for continuous processing in medium-high temperature range due to higher heat losses by increase in the amount of exposed area. Decreasing the area from which the heat losses occur can increase energy delivery temperatures. With higher a concentration ratio, there is increase in temperature at which heat is delivered due to an increase in flux intensity and a decrease in the receiver area. For high temperature applications, different solar concentrators may be employed. A number of solar industrial process heat systems are installed and operated on experimental basis have reported the status of the development of medium temperature solar collectors for industrial applications. In this temperature range, solar thermal systems have a great scope of application (ESTIF, 2004;

Weiss & Rommel, 2005). Modern parabola trough concentrators and central receiver towers are operated by high-tech computer programmed tracking system and are used only in large-scale applications to justify the high investment costs and gross over design. In conventional paraboloid concentrators, not only frequent tracking about two axes is required but also receiver has to fix at the focal point as an integral part of the reflector. Moreover, focus lies in the path of incident beam radiations. Despite of the high temperature output, such types of concentrators are not suitable for distillation and cooking purpose due to frequent changes of the focus position and inadequacy of handling approach at the receiver. This limitation, however, is solved by the Scheffler fixed focus concentrator which not only provides simple and precise automatic tracking but also a fixed focus away from the path of incident beam radiations. For small scale applications in agriculture, post harvest technology and food industry, this is a cheaper solution. Moreover, this type of concentrator can be completely fabricated in an ordinary workshop. In order to operate an on-farm distillery for the processing of different kinds of medicinal and aromatic plants, Scheffler concentrator was selected because of fixed focus and can be used for different types of distillation system and easy to fabricate. The present work also describes the complete design details to construct a Scheffler fixed focus concentrator which is one of the major components of the solar distillation system.

3.3 Development of Solar distillation system

The main object of the research is to develop an on-farm solar distillation system to process the fresh supply of different medicinal and aromatic plants with solar energy. The distillation technology is relatively simple and adoptable in rural areas. Basically, a simple distillation unit consists of four parts: furnace (heat source), distillation still, condenser, and oil separator. Although the principle of distillation is the same, practical application of this technique differs depending on the type and physical form of the plant material. Three types of distillation are in practice. These are “water distillation” (distillation with water), “water and steam distillation”, and “steam distillation” (distillation with steam). The yield, composition, quality, and commercial value of the essential oils are generally affected by the type and efficiency of the distillation unit, as well as the age of the harvested plant material and the ecological conditions where the plant material is cultivated or wild harvested (Öztekin & Martinov, 2007). The present study is focused to develop a solar distillation system where all these three types of the distillation can be run successfully. The system comprised of a paraboloidal type primary reflector (8 m^2 surface area),

secondary reflector (0.343 m^2), distillation still, condenser and Florentine flasks to separate the essential oils from hydrosol.

3.3.1 Description of Scheffler reflector for solar distillation system

The prototype of solar distillation for the processing of medicinal and aromatic plants was designed and developed using an 8 m^2 surface area of Scheffler fixed focus concentrator. The complete construction of Scheffler fixed focus concentrator was carried out in the Agricultural Engineering workshop, University of Kassel, Witzenhausen, Germany to develop the solar distillation prototype. The solar system comprised of a primary reflector having 8 m^2 surface area and secondary reflector. The main components of the primary reflector are elliptical reflector frame, a rotating support, tracking channel, reflector stand, and daily and seasonal tracking devices. The primary reflector is designed by considering the lateral part of a specific paraboloid. The semi-major axis and semi-minor axis of elliptical reflector frame were taken as 1.88 and 1.37 m respectively. Seven crossbars were designed and used in the elliptical frame to form the required section of the paraboloid. These crossbars were equally distributed along minor axis with one crossbar at the center and others were located at a distance of 0.48 m from the preceding on both sides. These crossbars were checked with the help of a jig specially designed for the profiles checking of the Scheffler reflector. The design and construction of the elliptical reflector frame and the crossbar curves are detailed in section 4.2. Aluminium profiles were fixed on the crossbars and aluminium sheets were pasted on aluminium profiles to give the required shape of the lateral part of the paraboloid. The rotating support was fabricated as an integral part of the primary reflector comprising of an axis of rotation (constructed of a steel pipe), a tracking channel (channel bent in semi-circular form and welded around the axis of rotation with supports). The reflector stand was grouted vertically on the site with its foundation firmly bolted with the steel plates and reinforced by welding. The solar distillation system was installed at solar campus, University of Kassel, Witzenhausen, Germany (latitude, 51.3°). The journal bearings assembly was welded with the reflector frame along the line parallel to the polar axis by setting it in north-south direction and inclination angle (51.3°) with the horizontal. At the end, the axis of rotation (steel pipe) of the reflector assembly was inserted into the journals bearings to complete the reflector.

Photovoltaic (PV) tracking device was used to rotate the primary reflector by chain sprocket mechanism for daily tracking. This PV tracking system composed of two PV

plates, a geared motor, and cables and was attached on the center bar of the primary reflector to operate with solar energy. Daily tracking device rotates the reflector along an axis parallel to the polar axis of earth with an angular velocity of one revolution per day to counter balance the effect of earth rotation. The seasonal tracking device is made of telescopic clamps mechanism and is rotated manually at half the angle of solar declination. It also induces the desired shape of the reflector paraboloid in order to get the fixed focus through out the year. The principle of operation for daily and seasonal tracking is detailed in sections 4.2.6 and 4.2.7. In order to run the distillation experiments according to the standards indicated in different literature (Dürbeck, 1997; Öztekin & Martinov, 2007; Denny, 1991), a secondary reflector was constructed to further reflect the beam radiations on the circular bottom of the distillation still. The secondary reflector comprised of seven aluminium strips which are arranged in a circular form on a fixed bricks foundation to run the distillation experiments throughout the year. The secondary reflector has provision to accommodate 400 mm diameter and 120 mm lateral part of the distillation still inside the secondary reflector.

3.3.2 Use of secondary reflector for water and steam distillation

In order to fulfill the standards of distillation stills designed for “water” and “water and steam” a secondary reflector has been used to further reflect the beam radiations onto the bottom of distillation still as shown in Fig. 3.2.

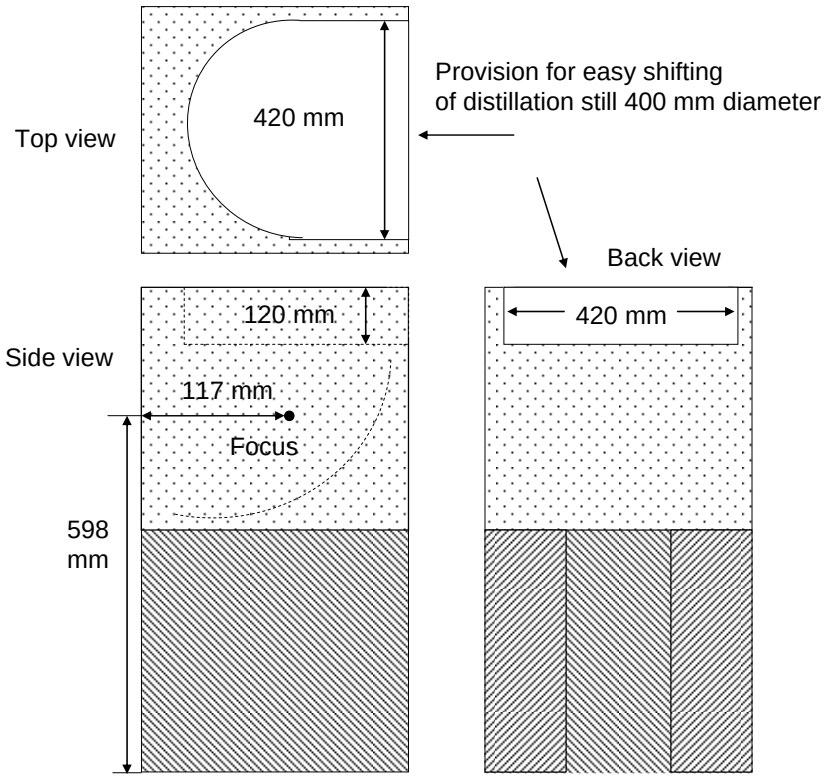

Figure 3.2: Secondary reflector for solar distillation system for an 8 m^2 Scheffler reflector

In this way, the heat energy is supplied from the bottom side of the still as in case of conventional distillation unit. This design is easy to operate and handle. The beam radiations are equally scattered onto the bottom of the distillation still and solar thermal energy is best utilized like a conventional furnace under the still. The geometric concentration ratio of Scheffler reflector is 100. The secondary reflector is designed to converge all the radiations onto the bottom of distillation tank (400 mm diameter) for distillation experiments. The bottom surface area (400 mm diameter) and 120 mm of bottom lateral part of the still is exposed to solar radiations as shown in Figure 3.2. So, this area (equivalent to 15 kg of water) must remain filled with water to save it from overheating. Nevertheless, a significant amount of energy (about 10-15 %) is lost due to the addition of secondary reflector. But the distillation experiments need heat at the bottom side to facilitate conventional processing (Dürbeck, 1997; Öztekin & Martinov, 2007; Denny, 1991). For an 8 m^2 reflector design, seven pieces of aluminium profiles are prepared to the specific radius and are fixed on the secondary reflector frame. The length of each aluminium piece is 700 mm and width is 100 mm. These aluminium sheets are attached on the curved steel bars to attain the required curve. These plates have the same material as used in primary reflector. These pieces are easy to take out and refit after cleaning. The secondary reflector is designed to receive all the solar radiations reflected

from the primary reflector and then further reflect it to the bottom of the distillation still. The secondary reflector is placed on a fixed concrete foundation bed which facilitates the accurate position of the secondary reflector. The focal point lies at a height of 598 mm from the base level of the foundation and 117 mm away from the inner surface central point as shown in Fig. 3.2.

Before starting experiment, the aluminium profiles of secondary reflector should be washed with water by adding 2-3 drops of washing solution. These strips are placed in some shady place for drying and then replaced. The primary reflector should also be washed in the same way twice in a month to improve the reflectivity of the aluminium profiles. The frequency of washing depends on the presence of dust particles on the site etc.

3.3.3 Fabrication of the still for solar distillation system

The still body is the container for the charge of plant material which is to be distilled. The capacity of distillation still is variable and dependent on the scale of the envisaged operation. The cylindrical still body that is mounted vertically has more practical usage than any other and is suited to a variety of needs prevalent in the producer countries. The judgment of the appropriate size is related to the quantity of the plant material available for distillation per harvest, availability of water and steam, energy sources and availability, labor availability, transport and storage facilities for the raw material and oil (Dürbeck, 1997). The still body is also equipped with a perforated grid near the bottom of the body itself. The charge is loaded so as to rest on this grid while performing water and steam distillation. In the experiments where water-cum-steam distillation method is used, the compartment below the grid serves as the reservoir for the boiling which generates the steam. In a cylindrical still, the space between the water and the herb supporting grid should have a depth to one-fifth of the still's diameter. This leaves room for an efficient scheme of baffles (Denny, 1991). In the present model designed for water cum steam distillation, the still body rests on secondary reflector which heats the bottom of the still indirectly by secondary reflected beam radiations containing the reservoir of water. The perforated grid comprises of two semi-circular pieces and is removable to conduct water distillation experiments. Various protective coatings are available on mild steel but these do not stand up to operation at 100 °C, in the long term, and when they eventually begins to part from the parent surface, this actually accelerate corrosion (Dürbeck, 1997). The

distillation still was fabricated of a food grade stainless steel vessel having 1210 mm column height, 400 mm diameter and 2 mm as shown in the Figure 1-A (Appendix A).

The diameter of distillation still is taken as 400 mm to reflect all the radiations on the bottom of the distillation still. The still vessel is fabricated as pressure tight and all welds relevant to this requirement are made continuous and of the required quality. Weld surfaces are prepared in accordance with good welding standards. The still is also provided with safety mountings and fittings like safety valve, pressure gauge, water level indicator etc. The drain line connection was provided at the bottom to drain the water of used charge. The still was pressure tested to check against any leakage by installing a vertical pipe element to the vapor outlet connection plugging the drain line and filling with water to the top of vertical pipe element. The top cover is of conical shape and is made of 2 mm stainless plate and its lateral part is 4 mm thick so that it may not distort during welding and must seat flat on the rim packing to provide a pressure tight seal as shown in the Fig. 2-A (Appendix A). Three I-bolts are used for quick opening and closing of the conical top cover during distillation experiments. The clamps were accurately positioned and those parts of it mounted on the cover are registered exactly with those on the still body as shown in Fig. 3-A (Appendix A).

3.3.3.1 Thermal insulations

Loss of heat from the still is accompanied by a corresponding condensation within the still, which later re-boils. This could have detrimental effect on product quality (Dürbeck, 1997). Thermal insulation is therefore an important requirement quite apart from energy usage considerations. Rockwool was used to insulate the distillation still and the insulation was held with a wire or strap binding. The galvanized sheet cladding was then placed in position, the battens pushed in on the bolts, and their nuts tightened. The entire still body was adequately insulated with 60 mm thickness rockwool insulation to minimize the losses of heat. The galvanized sheet cladding (1 mm thickness) is then placed in position, the battens pushed in on the bolts, and their nuts tightened. The insulation was held with a wire or strap binding. The distillation still comprised of vertical shell (900 mm height) and top cover. Upper 780 mm of the vertical shell of the distillation still was insulated while bottom and 120 mm bottom lateral part was not insulated as this portion of the still exposed to the solar radiations and painted black with solar mat.

3.3.4 Fabrication of condenser

The main function of the condensing system is to convert the vapor mixture of the steam and essential oil which emerges from the still body outlet, swiftly into liquid phase. This function involves the removal of the heat from the vapor phase to render it into the liquid phase and to bring the resultant mixture of aqueous and oil phases to near ambient temperature, about 35-45 °C.

In general practice within the essential oil industry, there is variety of different types of condensers in common use. The most two popular designs are known as the coil-in-water type and shell-and tube type. In the developing country situations in the field, the coil type is more prevalent. The reason is based both on economy as well as on grounds of ease of fabrication in circumstances where good workshop facilities are not available.

The condenser is provided with steel coil, a cold water inlet connection and warm water outlet connection and acts as a counter current flow heat exchanger. The whole coil is immersed in static water tank. The upper part of the water is maintained boiling whilst the lower part of the tank in which rest of the coil is immersed, completes the cooling process. The complete condenser unit is also made of stainless steel material along with the vapor outlet pipe from still to condenser. The shell and core of the condenser are fabricated for water tight. The shell was leak tested by filling with water and core by immersing in water and checking for air bubbles. The coil is a stainless steel tube bent on a tube bending machine of the correct diameter to produce a coil of the specified diameter and pitch. The diameter of coil is 10 mm and pitch is 25 mm. The diameter, height and wall thickness of the shell are 250, 350 and 3 mm respectively as shown in Figure 4-A (Appendix A). The coil unit is placed loose inside the shell. Cooling water inlet and outlet connections are provided from the bottom and top sides of the condenser shell respectively for efficient condensation of the steam inside the coil.

3.3.5 Florentine vessel or oil separator

The condensate that emerges from steam distillation (that is the distillate), is a mixture of essential oil and water. The essential oil may eventually settles as an upper layer (lighter than water) or as a lower layer (heavier than water). Sometimes, it settles as both an upper layer and lower layer due to the fact that lighter fractions which come over first form a single upper layer while the heavier fractions agglomerate at the bottom as a lower layer. The function of oil separator or Florentine vessel is to separate the oil from the water

phase and is designed to accommodate all of the situations above. The essential oils are sparingly soluble in water and this is the property that makes it possible to affect the separation from the aqueous phase. The Florentine vessels were designed to enable the continuous removal of the water phase during distillation. In some cases, water-soluble oil contents are economically significant and are recycled.

When the specific gravity of the oil is only marginally less than that of water, it is preferable if the condensate flows into the separator at about 40-45 °C. This is because the specific gravity (SG) of the oil decreases relatively more than water in increased temperature. The greater the differential between respective specific gravities, the better the separation of the two phases into layers. Where the specific gravity of the oil is marginally greater than water, the distillate should run as cold as possible (Dürbeck, 1997). All three types of Florentine flasks were used to separate the oil from the water depending upon the experiments performed as shown in the Fig. 3.3. Different volumes of glass Florentines were fabricated for the distillation system from the Glasswerk, University of Kassel, Germany.

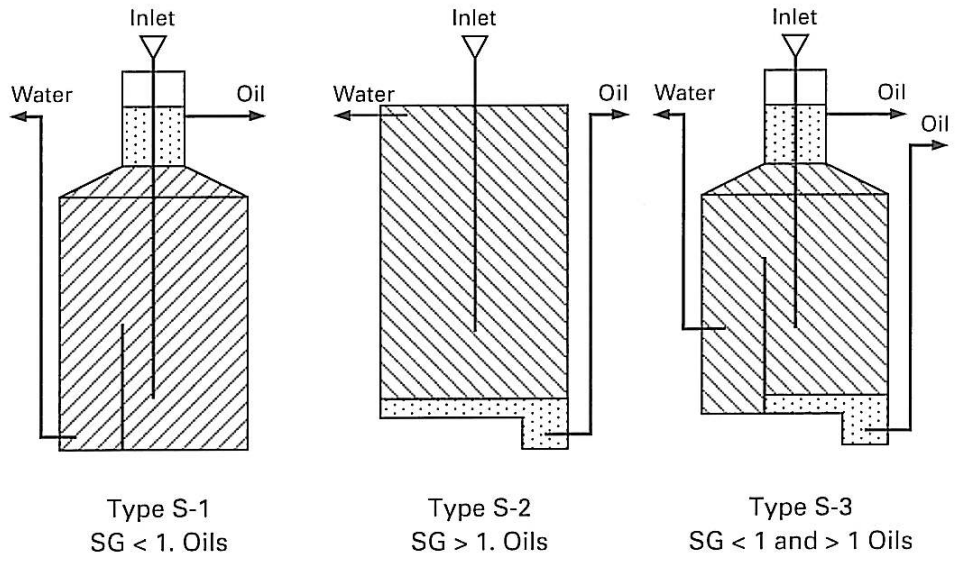

Figure 3.3: Separator types (Source: Dürbeck, 1997; Öztekin & Martinov, 2007)

3.4 Experimental set up and data acquisition

The distillation unit has provision to operate for “water” and “water and steam” distillation. A stainless steel pipe connects the top end of the distillation still to the steel condenser. In order to record the power during distillation process, a barrel calorimeter is connected at

the outlet connection of the steam to record dryness fraction during different intervals. The schematic of solar distillation system is shown in Fig. 3.4.

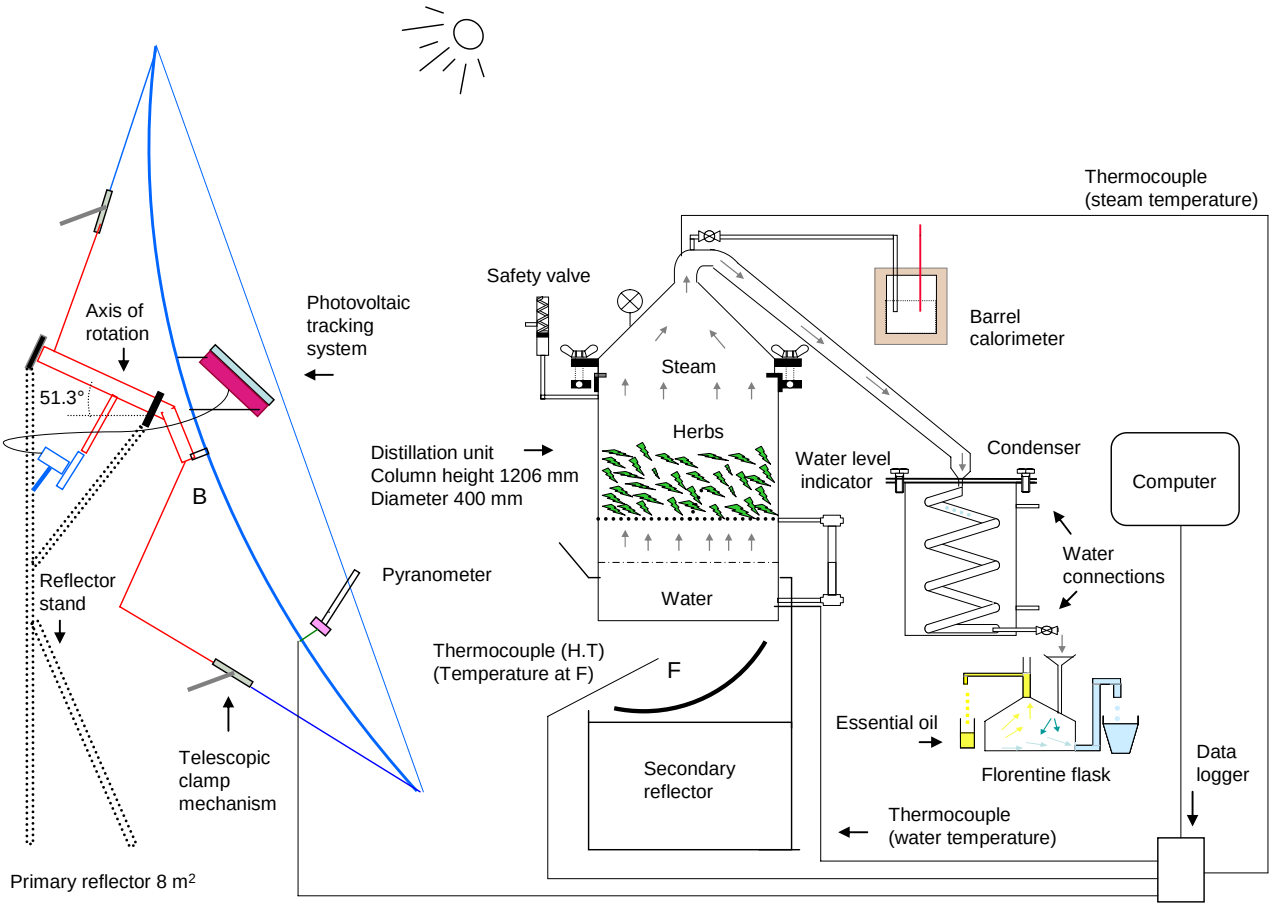

Figure 3.4: Schematic of solar distillation system

In order to evaluate and control the solar distillation system continuously during the experiments, the system is equipped with pyranometer and thermocouples (K-type and T-type with standard errors ±1.5 K and ±0.5 K respectively). The intensity of solar radiation is recorded by the pyranometer (SP Lite: response time < 1 s). The pyranometer is fixed at major axis of the primary reflector with the help of adjustable lever and a black pipe (0.020 m long) is mounted on it to record beam radiations only. Thermocouple connections are provided to record focal point, water, and steam temperatures during the distillation process. All thermocouples and pyranometer connections are attached to a computer via data logger as shown in Fig. 3.4. Secondary reflector is placed in the optimum position with respect to focus and distillation still is placed on it. The experiments were conducted and the regression analysis was performed to find out the appropriate model of the process curves. Different parameters like fresh versus dry herbs and chopped versus un-chopped herbs were also compared at 5 % level of significance using Tukey test.

3.5 Operational procedure of the solar distillation system

Operation commences with the opening of the still cover prior to loading it with the plant material. The cover weighs about 5 kg and can be handled manually. The cover I-bolts are loosened and swung out of the way. The still is charged with the plant material manually and the cover replaced after checking the cover seal. For “water distillation”, the plant material is placed in water and for “water & steam” and “steam distillation”, the plant material is placed on the perforated grid. The water level in the distillation still is maintained minimum 120 mm in the distillation still and this is equivalent to 15 liters (kg) of water level under the available size of the distillation prototype. This water level corresponds to the surface area of the still exposed to the solar radiations. While setting the focus before starting an experiment, both the bolts of telescopic clamps are opened to make the reflector free along seasonal tracking axis. The rotation along daily tracking axis is always flexible due to the presence of clutch plate. In this way, the reflector can also be rotated along both axis of tracking by holding telescopic clamps either from top side or bottom side to set the focus accurately. The optimum focus is set by visualizing the illuminated beam of solar radiation at the focus. If the focus is a little bit higher than the designed focus point, then the top side of the reflector is tightened by fixing the downward side and vice versa. The position of Pyranometer is adjusted to record the maximum beam radiations. After the setting the reflector and position of Pyranometer, the data logger and computer are taken in circuit to record the real time data. The data is automatically recorded after 10 second intervals for the temperatures and beam radiations with the help of thermocouples and pyranometer respectively.

All the running distillation parameters are observed during processing of plant materials. Condenser flow rate is established in the condenser when the steam generation is started. When the process is over, the reflector is rotated out of the focus to stop the distillation process; the spent charge material is removed manually using a hay hook. The still is drained out and washed. If there is much residual plant material remaining in the still, it may be necessary to lift out the charge tray and hose the strainer clear of the material. The still is filled with water again to set the level. The distillation cycle is now complete and the still is ready for the next distillation cycle.

Two dangerous conditions can arise in the still during distilling; these are “over pressure” and “low water”. Over pressure can cause the vessel to fail by stressing it beyond the design limits. This is dangerous because the vessel contains vapor which is compressible

and will release energy if it fails. Low water is also dangerous as the vessel is being fired and if there is no water; its base will become red hot and fail, with the same release of energy. Overpressure can arise if there is some obstruction downstream of the vessel's vapor outlet. In the event of overpressure, the safety valve will blow off its steam. In order to avoid low water level, ensure that the water level in the still should always be above the safe minimum level of 180 mm for the existing design.

3.6 Mathematical modeling of solar distillation system

The present study is conducted for a specific size of a solar distillation prototype. Two mathematical models were developed in Matlab 7 and Microsoft Excel spreadsheet. First model was developed to design the required size of Scheffler reflector which is one of the major components of solar distillation system. Second model was developed to predict the energy distribution and heat losses from different components of the solar distillation system. These models can be used to optimize the existing solar distillation system as well as to predict useful information for any required size and location of the solar distillation system.

3.7 Biomass energy utilization in solar distillation system

The degree of reliability desired of a solar process to meet a particular load can be provided by a combination of properly sized collector and an auxiliary energy source. In the most climates, auxiliary energy is needed to provide high reliability and avoid gross over design of the solar system (Duffie & Beckman, 2006). For this purpose, a small scale biomass boiler was developed as an auxiliary heat source to compensate for distillation process during adverse climatic conditions at the site. The boiler is a vertical boiler type and is designed only to hybrid the solar distillation system. The boiler comprises of a vertical shell (360 mm diameter and 400 mm height), biomass furnace, and economizer (360 mm diameter and 1 m height) and is equipped with all safety mountings like safety valve, water level indicator, and blow off valve. The furnace has an arch with gradual increasing area on top which opens in combustion chamber. A chimney passes though the center of the boiler and economizer and then is exhausted to the atmosphere. Firewood, bagasse, chaff husk or other spent biomass materials can be used as fuels in the furnace. As a result of combustion, the heat energy is transferred to the bottom of the shell and the burnt biomass is dropped down at the ash pit in the form of ash for continuous boiler operation.

In order to equally distribute the steam in the distillation still, two steam coils (250 mm diameter) are provided in the distillation still. Small holes are drilled on the top and sides of the coils. The upper coil is used for steam distillation and the lower coil is used for water distillation in the absence of solar energy. Both coils are connected to the boiler via a wire-braided high pressure hose. The main object of the work is to utilize solar energy as a primary heat source and the rest by the biomass boiler. The bottom of the distillation still is always exposed to beam radiations reflected from secondary reflector of Scheffler fixed-focus concentrator while the biomass system provides steam through stop valve to make up any deficiency of steam. The required steam flow rate is maintained by monitoring the condensate flow rate. The detail of the whole system is shown in Figure 3.5. The boiler was hydraulically tested at 5 bar pressure before the steam trials. The system was design to run maximum 0.5 bar pressure but most of the distillation experiments are carried out under atmospheric pressure.

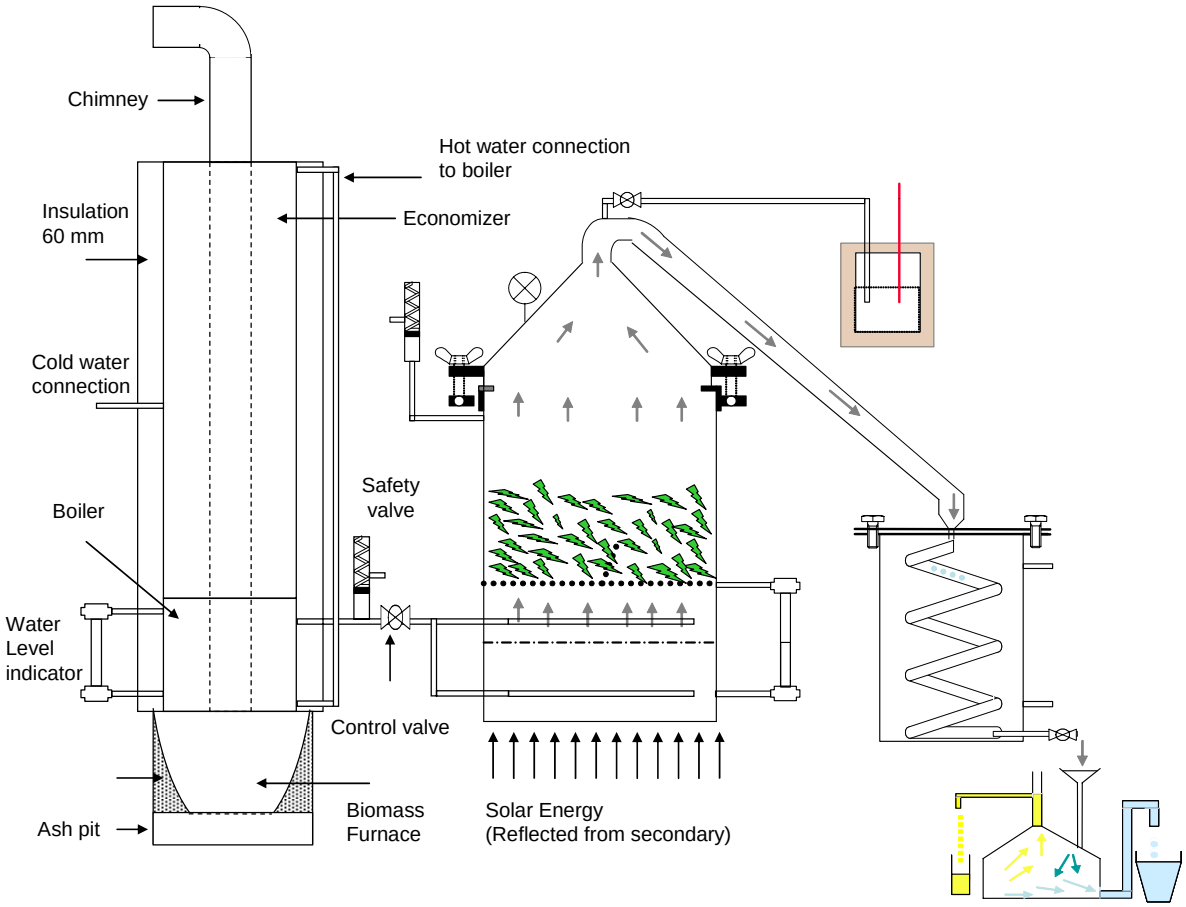

Figure 3.5: Solar-biomass hybrid system for distillation of essential oils

4 Results & discussions

The main objective of the research is to develop a solar based distillation system for the processing of medicinal and aromatic plants using solar energy. This section includes the results of laboratory experiments, design, development, performance evaluation and modeling of the solar distillation system. The results of solar-biomass hybrid system are also explained in this chapter.

4.1 Laboratory experiments

Distillation experiments for essential oils extraction from medicinal and aromatic plants are energy and temperature sensitive due to presence of volatile component in the plant material. During the first phase of the research, laboratory experiments were carried out to estimate the optimal thermal and physical parameters for different herbs and medicinal plants. Data were collected for essential oils extraction (ml) versus heat energy consumed for different medicinal and aromatic plants. Process lines for different plant materials were also drawn for percentage of essential oils extracted against total heat energy required and are shown in Fig. 4.1

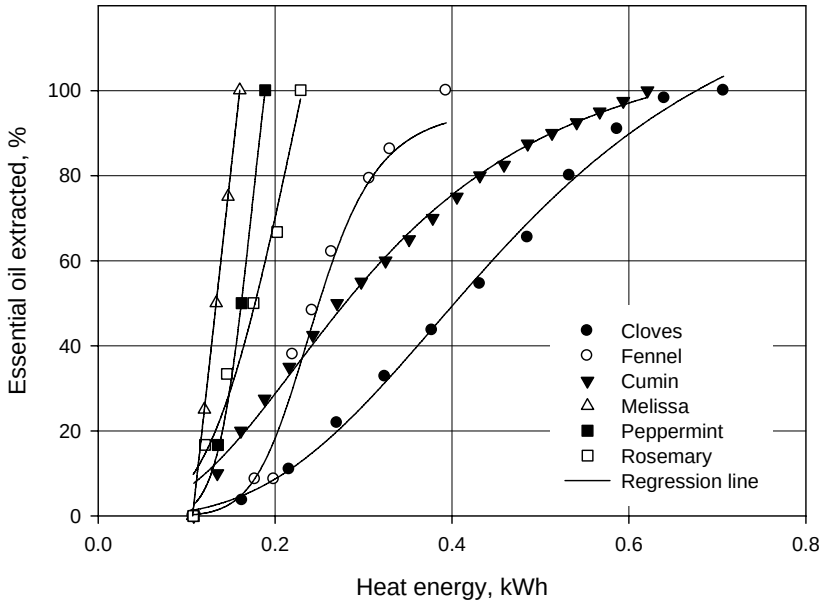

Figure 4.1: Process curves of different plant materials for laboratory experiments

Regression analysis was performed to fit the appropriate model for the percentage of oil extracted against heat energy required for the distillation process. The best fitted regression model for all the plant materials was found to be the sigmoid/logistic curve as given below:

$$y = \frac{k}{1+\left(\frac{z}{z_o}\right)^l}$$

where y and z are the variables of the regression model, k, l, z_o are the coefficients of regression model. The coefficients of the regression equation for different herbs are given in Table 4.1.

Table 4.1: Coefficient of determination (R^2) and coefficient of regression model of different plant materials for laboratory experiments

Plant material	Coefficient of determination (R^2)	Coefficients of regression model		
		k	l	z_o
Peppermint	0.9984	168.3553	-8.0688	0.1801
Melissa	0.9881	118.1655	-10.8419	0.1379
Rosemary	0.9731	273.2452	-3.5889	0.2690
Cumin	0.9945	116.0756	-2.4974	0.3121
Cloves	0.9962	134.3749	-3.0692	0.4776

The reliability of the developed model was evaluated by comparing the experimental and predicted curves. The model fitted the results well as indicated by high values of coefficient of determination (R^2). These results show that the higher oil extraction rates at the start of the distillation process and lower extraction rates towards the end of the process. It is also evident from Fig. 4.1 that the fresh plant materials (Melissa, Peppermint, Rosemary) are less energy consuming to complete the distillation process as compared to dry herbs (Cloves, Cumin). Since different plant materials have different contents of oils and require different quantities of heat energy consumptions during distillation of essential oils. It depends on the oil contents, time of harvesting, moisture contents and part of the plant used etc. It is also evident from Fig. 4.1 that there is gradual increase in oil extraction in latent heat phase. At a specific energy level, there is no further increase in essential oil contents and the line becomes parallel to abscissa. The experiments were carried out for longer range of energy to see further effect (not shown in the graph). For each plant material, there is a specific energy level at which 100 % of essential oil is extracted. Similarly, the optimum energy levels for different plant materials were recorded. The energy consumptions to extract the full contents per 100 grams of Cloves buds, Fennel, Cumin, Melissa, Patchouli, Cassia, Orange barks, Lavender, Peppermint were found to be

0.718, 0.399, 0.576, 0.163, 0.440, 0.446, 0.379, 0.419 and 0.366 kWh respectively as shown in Figure 4.2

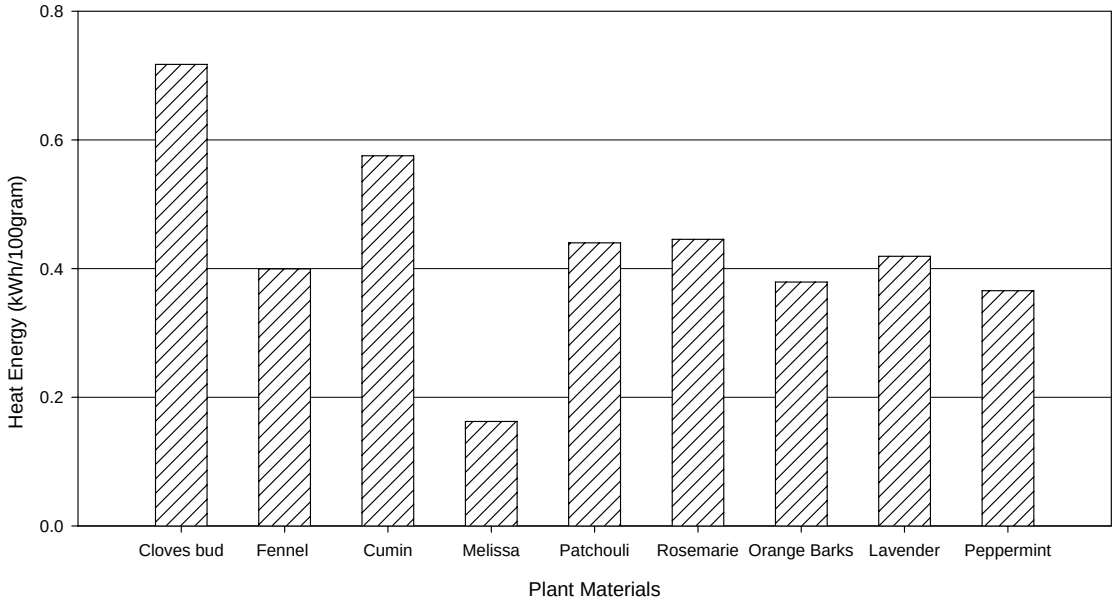

Figure 4.2: Heat energy required (kW h) per 100 grams of different plant materials

From the recorded data, energy consumptions per ml of essential oils were also calculated. The heat energy consumed per ml of Cloves buds, Fennel, Cumin, Melissa, Patchouli, Cassia, Orange barks, Lavender, Peppermint were found to be 0.133, 0.503, 0.574, 2.667, 2.716, 1.000, 2.807, 1.995, 0.500 kWh respectively as shown in Fig. 4.3

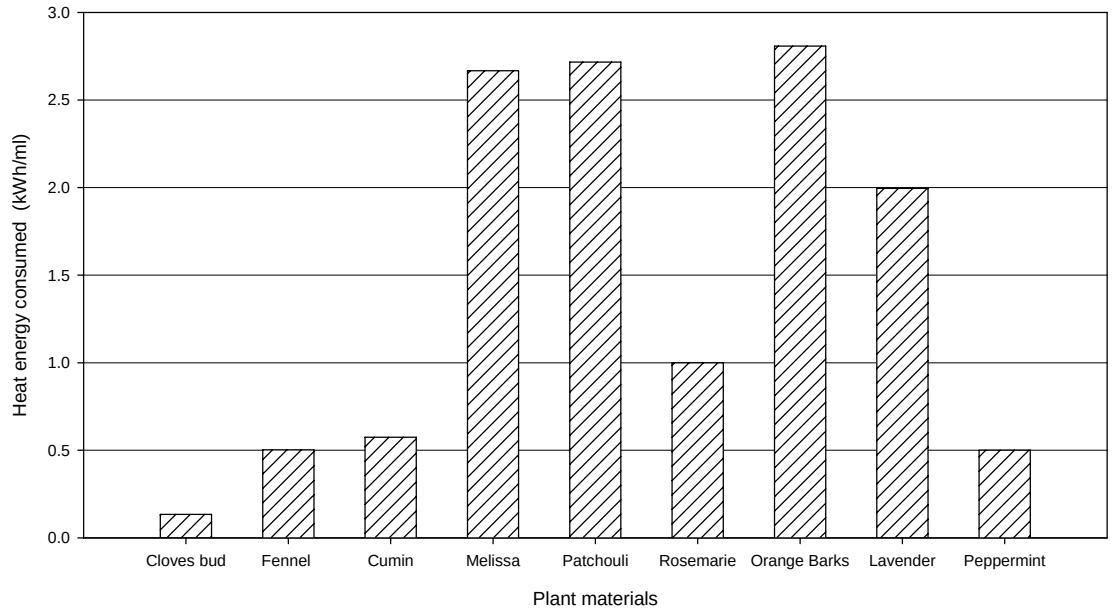

Figure 4.3: Heat energy required per ml of essential oil for different plant materials

These results show that 1.63 to 7.18 kWh heat energy is required per kg of the plant material for the experiments using laboratory apparatus. It is also concluded that the fresh herbs consume less energy comparatively. As the study is focused for the on-farm installation of solar distillation system of the fresh medicinal and aromatic plants, about 16 kWh heat energy is required to process 10 kg of plant material which can be utilized by using an 8 m^2 Scheffler reflector at 50 % efficiency during sunny days. These results provide useful information in adopting appropriate distillation parameters to process the herbs at farm. These results also lead to the development of solar distillation system. From the laboratory experiments, it was found that successful distillation experiments can be carried out by using a still, condenser, Florentine flask and a heat source. In order to apply this technology for field experiments, the solar energy was selected as a heat source for the distillation experiments. The main object of the study is to use the solar energy in a simple and easy way that it can be used like a conventional heat source for the distillation system. For this purpose, Scheffler fixed focus concentrator was used to adopt this technology at farm level by using solar energy. The design and development details of this solar based distillation system have been explained.

4.2 Design principle and mathematical calculations of Scheffler fixed focus concentrator

The solar distillation prototype for the processing of medicinal and aromatic plants was designed and developed by using an 8 m^2 surface area of Scheffler fixed focus concentrator. The complete solar unit was constructed in the Agricultural Engineering workshop, university of Kassel, Deula, Witzenhausen, Germany. Being a lateral part of a paraboloid, the design of Scheffler fixed focus concentrator is the most complicated and sophisticated component of the complete solar distillation system. Up to now, no mathematical description of the design of Scheffler reflector has been done. The manuscript explains the complete principle and mathematical calculations to design an 8 m^2 Scheffler concentrator for the development of a solar distillation system.

4.2.1 Design of reflector parabola and reflector elliptical frame

Unlike conventional paraboloid concentrator, Scheffler fixed focus concentrator is a lateral part of a paraboloid as shown in Fig. 4.4.

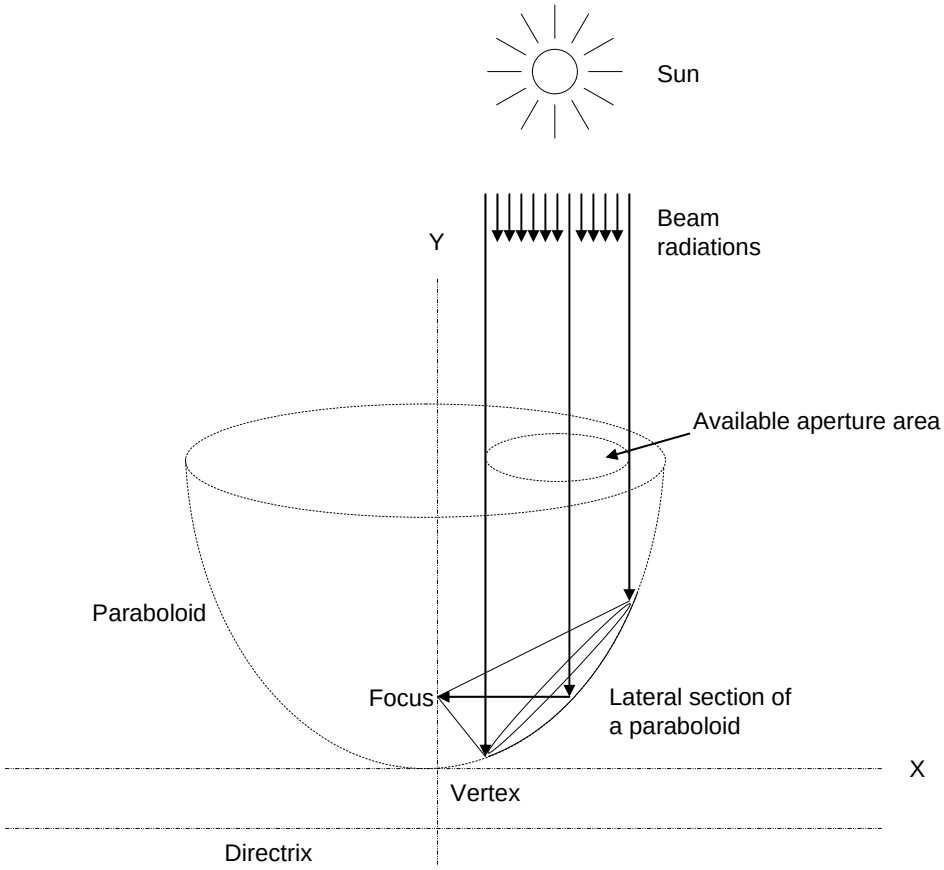

Figure 4.4: Section of the Scheffler reflector in a paraboloid

While designing a parabola curve for the Scheffler reflector, all calculations are made with respect to equinox with zero solar declination. In order to calculate the equation of the parabola curve, the calculations are made by considering the side view of the paraboloid. In this way, paraboloid and reflector frame are drawn in the form of a parabola curve and straight line respectively. The general equation of a parabola in *xy*-plane with its axis passing through y-axis can be written in the following form:

$$P(x) = m_p x^2 + C_p \tag{4.1}$$

Where m_p is the slope of parabola and C_p is the y-intercept of the parabola
Taking first derivative of Eq. (4.1) for the slope of parabola

$$P'(x) = 2m_p x \tag{4.2}$$

Commencing from a point P_n of the parabola curve in the positive coordinate axes where solar radiation is reflected at 90° as shown in Fig. 4.5.

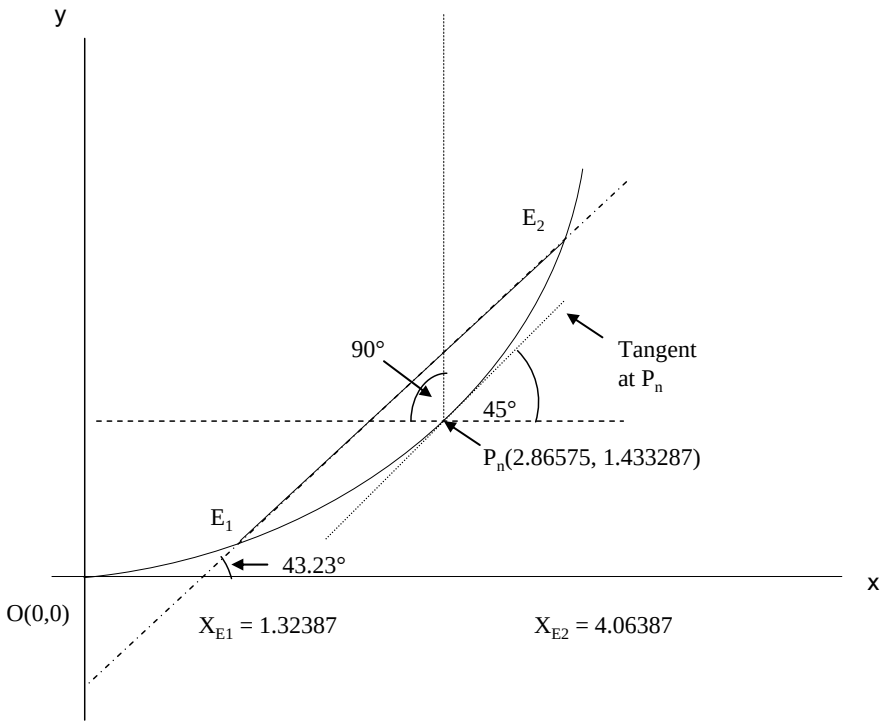

Figure 4.5: Description of parabola of the Scheffler reflector

At this point of the parabola curve, the tangent is cut at 45° angle and the value of the y-coordinate is half that of the x coordinate. In order to design the reflector parabola, the study based on the following two aims:

1. To construct an 8 m^2 Scheffler reflector
2. The reflector frame should be balanced with respect to central pivot point

In order to meet these two aims, the following procedure is considered

1. Selection of x-coordinate of point P_n (x_P) in order to get a reasonable distance to the focal point; calculation of y-coordinate of point P_n (y_P) and slope m_P with the help of Eq. (4.1) and Eq. (4.2)
2. Selection of x_{E1} and x_{E2} in order to get a surface of approximately 8 m² and a balanced collector; calculation of y_{E1}, y_{E2} and angle of the line joining the points E_1 and E_2

3. Check if the two aims are roughly reached (calculation of surface area right and left of P_m and check their difference for balancing and their sum for collector surface); otherwise adapt a new set of P_n, E_1 and E_2
4. Calculation of semi-major and semi-minor axis of the reflector frame

For a surface area of 8 m^2, this point is taken as P (2.86575). This point varies with different sizes of surface areas of Scheffler reflector. For a parabola of a 3.93 m^2, this point, where the reflection is 90°, is (2,1). The first derivative of Eq. (4.1) at this point is equal to slope at the point. The tangent cuts this point P_n at an angle of 45° with x-axis (directrix), so we can write:

$$P'(2.86575) = tan\,45°$$

$$P'(2.86575) = 1$$

According to definition of parabola, the coordinates at point P_n are given as

$$P(2.86575) = (1/2)(2.86575)$$

$$P(2.86575) = 1.43287$$

By using Eq. (4.1) and Eq. (4.2), the values of m_p and C_p are calculated as 0.17447 and 0 respectively. The parabola equation for the equinox is given as:

$$P(x) = 0.17447x^2 \tag{4.3}$$

In order to approximately construct a balanced reflector (8 m^2 surface area), two points x_{E1} and x_{E2} are chosen on a graph paper as 1.32387 and 4.06387. The reason of selecting these points is to construct a balanced parabola in order to rotate the reflector with a nominal force. In this way, the line joining these two points E_1 and E_2 of the parabola curve represents the cutting section of the elliptical frame of the Scheffler reflector. This line E_1E_2 is not parallel to the tangent at point P_n (which makes 45° angle with x-axis) but makes a 43.23° angle as shown in Fig. 4.5. The structure is equilibrated and needs a little force to move the reflector. The general equation of this straight line is given by:

$$G(x) = m_g x + C_g \tag{4.4}$$

Differentiating Eq. (4.4) with respect to x

$$G'(x) = m_g$$

$$m_g = \tan 43.23°$$

$$G'(x) = \tan 43.23°$$

$$m_g = 0.94$$

The coordinate x of point E_1 (x_{E1}) is selected to be 1.32387 and the coordinate y is calculated to be 0.31 by using Eq. (4.4). By substituting the values of x, y and m_g in Eq. (4.4), the y-intercept (C_g) is calculated to be −0.94 and the equation of the straight line becomes:

$$G(x) = 0.94x - 0.93866 \tag{4.5}$$

The coordinate x of point E_2 (x_{E2}) is calculated by comparing and solving Eq. (4.1) and (4.4), the general form of a quadratic equation is as follows:

$$x^2 - \left(\frac{m_g}{m_p}\right)x + \frac{C_p - C_g}{m_p} \tag{4.6}$$

Through solving Eq. (4.6) with the help of a quadratic formula to get two points of intersection (x_{E1} and x_{E2}) of the parabola curve and straight line, we get:

$$x_{E1} = \frac{m_g}{2m_p} + \sqrt{\left(\frac{m_g}{2m_p}\right)^2 - \frac{C_p - C_g}{m_p}} \tag{4.7}$$

$$x_{E2} = \frac{m_g}{2m_p} - \sqrt{\left(\frac{m_g}{2m_p}\right)^2 - \frac{C_p - C_g}{m_p}} \tag{4.8}$$

The straight line cutting the curve represents a cutting plane of an ellipse with axes ratio $a/b = \cos \alpha$, where "a" and "b" are the semi-minor axis and semi-major axis respectively. For a given paraboloid, the cutting section of the lateral part will make an ellipse and its projection on the ground (horizontal plane) will make a circle. So, the semi-minor axis of the ellipse and radius of projection on the ground will become the same. The projection of this ellipse on the horizontal plane (xz-plane) is a circle with a diameter of $2a$. The general equation for the diameter of circle ($2a$) is calculated for a Scheffler reflector by subtracting Eq. (4.8) from Eq. (4.7) and is given by:

$$2a = (2).\sqrt{\left(\frac{m_g}{2m_p}\right)^2 - \frac{C_p - C_g}{m_p}} \tag{4.9}$$

The semi-minor axis of the ellipse is 1.37000 m and semi-major axis of the reflector is calculated to be 1.88029 m by dividing with axes ratio (cos 43.23).

4.2.2 Distribution of crossbars on the reflector frame

For the construction of a Scheffler reflector, it is necessary to know the exact position of the crossbars on the reflector frame. The frame of Scheffler reflector is elliptical in shape and this can easily be calculated by using the equation of ellipse which is given below:

$$\left(\frac{x}{b}\right)^2 + \left(\frac{y}{a}\right)^2 = 1 \tag{4.10}$$

where a is the semi-minor axis of the ellipse, b is the semi-major axis of the ellipse. In order to locate any point "y_n" with respect to "x_n" on the elliptical frame, Eq. (4.10) can be written as:

$$y_n = \cos\alpha \sqrt{b^2 - x_n^2} \tag{4.11}$$

Eq. (4.11) is used to calculate the position of the crossbars on the elliptical frame of the Scheffler reflector. A number of points can be taken but seven crossbars are sufficient to make the required section of the paraboloid for an 8 m^2 Scheffler reflector. Taking the centre of ellipse as origin and major axis along x-axis, the middle crossbar passes through

the origin. The other crossbars are located at a distance of ±0.48 m, ±0.96 m, ±1.44 m from the origin along major axis and the corresponding points on minor axis are calculated as ±1.37000, ±1.3246, and ±1.17798 m respectively as shown in Fig. 4.6.

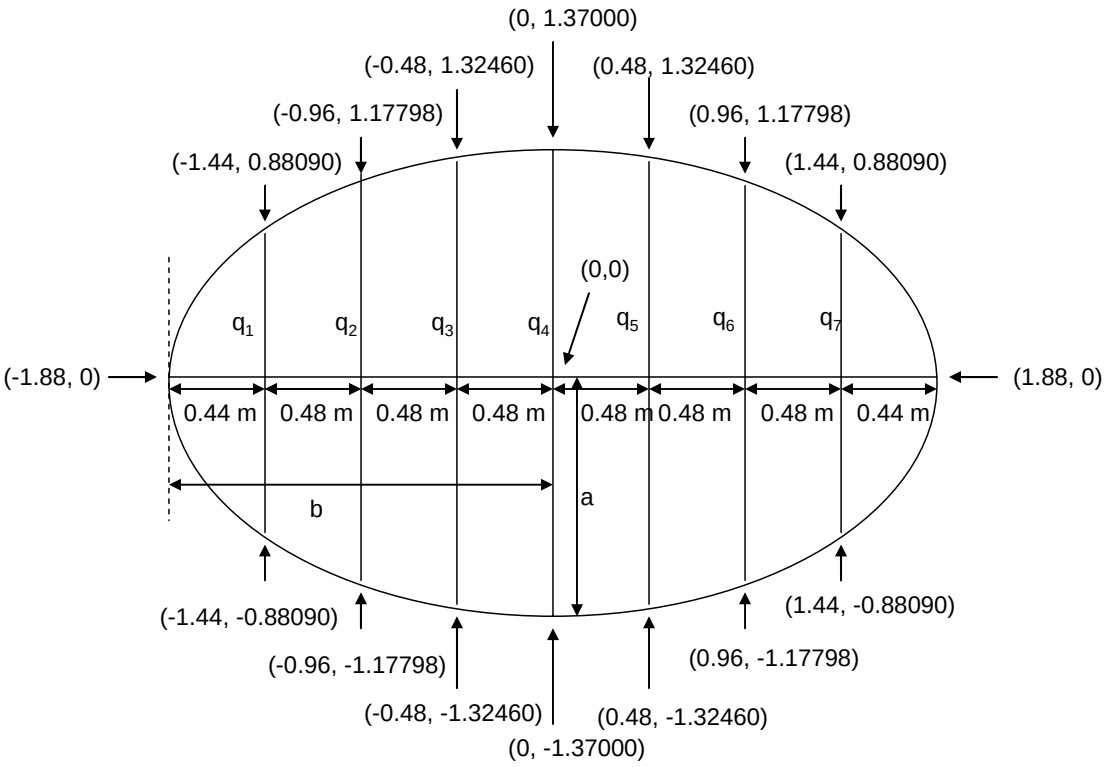

Figure 4.6: Intersections points of seven crossbars (q_1 to q_7) on an elliptical reflector frame

After the construction work of reflector frame, intersections points of crossbars are marked on the elliptical reflector frame.

4.2.3 Calculation of equations for the crossbars ellipses

The cutting planes of the crossbars are perpendicular to the cutting plane of the reflector frame and are shown in the form of seven straight lines (q_1 to q_7) in Fig. 4.7

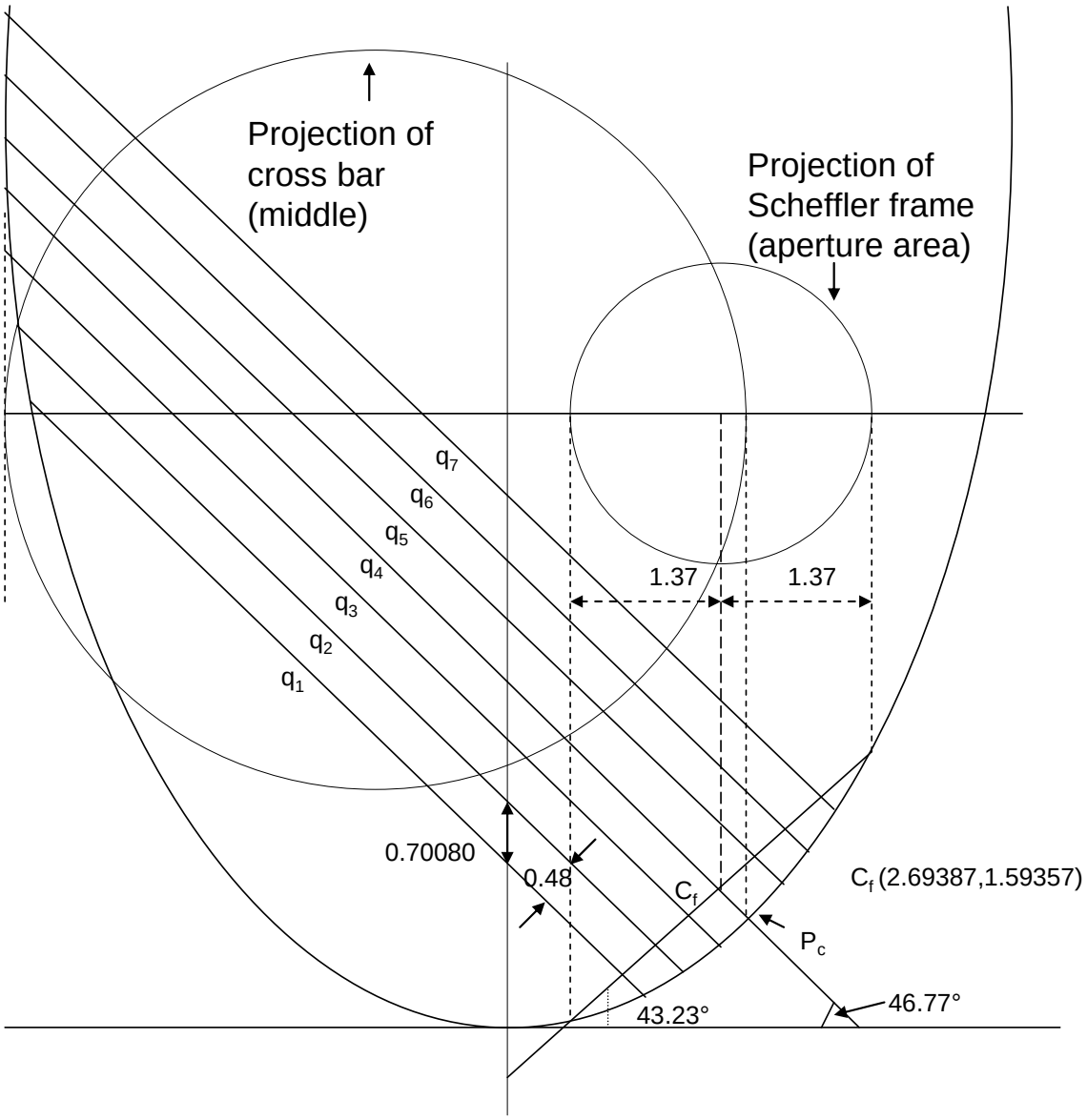

Figure 4.7: Description of the Scheffler reflector and the crossbars on a parabola curve

The inclination angle of cutting plane of crossbars is found to be -46.77° by subtracting the angle of cutting plane of the reflector frame from 90°. These cutting lines are also ellipses with axes ratio (a_q/b_q) = cos 46.77°. Starting from the middle crossbar (q_4, passing through P_c), we take from the basic equation of the line and is given as:

$$q_4(x) = m_{q4}x + C_{q4} \tag{4.12}$$

Slope of middle crossbar is calculated as:

$$m_{q4} = tan(-46.77) = -1.06377$$

The *x*-coordinate of the point of intersection (C_f) of the middle crossbar and the reflector frame is the central point of x_{E1} and x_{E2} and y-coordinate is calculated by substituting this value of *x* in Eq. (4.5) and is given as follows:

$$q_4(2.69387) = 1.59357$$

Substituting the values of m_{q4}, $q_4(x)$ and *x* in Eq. (4.12), the y-intercept (C_{q4}) for the middle crossbar is calculated and the equation of the middle crossbar (q_4) for 8 m^2 surface area of Scheffler reflector is given as:

$$q_4(x) = -1.06377\ x + 4.45923 \tag{4.13}$$

It is evident from Fig. 4.7 that the slopes for all the cutting crossbars are the same as these are perpendicular on the same cutting plane of the Scheffler frame. As the crossbars are equally distributed (from center of the reflector frame), so the difference between two successive *y*-intercepts is calculated to be 0.70080 by dividing 0.48 with cos 46.77.

The equations for the 4th, 5th and 6th crossbars are calculated by adding 0.70080, 2(0.70080) and 3(0.70080) in the y-intercepts values of Eq. (4.13) respectively. Similarly, the equations for 3rd, 2nd and 1st crossbars are calculated by subtracting 0.70080, 2(0.70080) and 3(0.70080) from the *y*-intercepts values of Eq. (4.13) respectively.

The equations for all crossbars can be generalized as $q_n(x) = m_q x + C_{qn}$. Similarly, for semi-minor axis (a_{qn}) of any ellipse of a crossbar, Eq. (4.9) can be modified for crossbars and reflector frame and is generalized as:

$$a_{qn} = \sqrt{\left(\frac{m_{qn}}{2m_p}\right)^2 - \frac{C_p - C_{qn}}{m_p}} \tag{4.14}$$

where subscript "*n*" represents the number of crossbar
Similarly, *y*-intercepts, equations of the cutting sections on *xy*-plane, semi-minor axis and semi-major axis for all the seven crossbars are calculated and are given in Table 4.2

Table 4.2: Equations, semi-minor axis and semi- major axis of different crossbars

Crossbar "n"	Y-intercept "C_{qn}" (m)	Equation of cutting section of crossbars on xy-plane	Semi-minor axis "a_{qn}" (m)	Semi-major axis "b_{qn}" (m)
1	2.35683	$q_4(x) = -1.06377\ x + 2.35683$	4.77516	6.97176
2	3.05763	$q_4(x) = -1.06377\ x + 3.05763$	5.17870	7.56093
3	3.75843	$q_4(x) = -1.06377\ x + 3.75843$	5.55299	8.10740
4	4.45923	$q_4(x) = -1.06377\ x + 4.45923$	5.90360	8.61929
5	5.16003	$q_4(x) = -1.06377\ x + 5.16003$	6.23452	9.10244
6	5.86083	$q_4(x) = -1.06377\ x + 5.86083$	6.54874	9.56120
7	6.56163	$q_4(x) = -1.06377\ x + 6.56163$	6.84855	9.99892

4.2.4 Calculation of depths and arc lengths for different crossbars

After the calculation of equations for different crossbars, the depths and lengths of arcs for different crossbars are calculated for the construction of Scheffler reflector. The depth of reflector for nth crossbar (Δn) is calculated from the following formula and is explained in Fig. 4.8

$$\Delta_n = \frac{a_{qn}}{\cos 46.77} - Z \tag{4.15}$$

where $Z = \frac{\sqrt{a_{qn}^2 - Y_n^2}}{\cos 46.77}$ (by using the basic formula of ellipse)

By substituting the values of "*Z*" in Eq. (4.15)

$$\Delta_n = \frac{a_{qn} - \sqrt{a_{qn}^2 - Y_n^2}}{\cos 46.77} \tag{4.16}$$

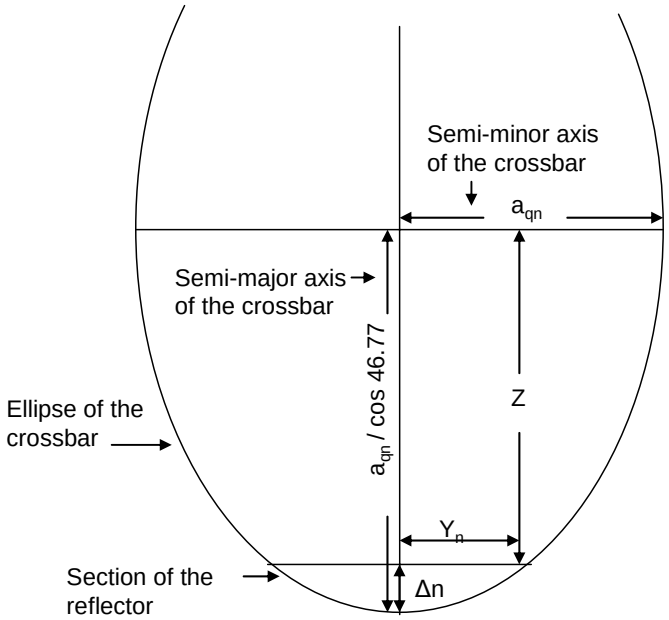

Figure 4.8: Ellipse of the crossbar for the Scheffler reflector

We can see that all the crossbars are the parts of the ellipses that differ slightly from the circle segment. For the solar concentrator optics, different approximations are valid to concentrate energy cheaply rather than to form a precise image (Winter et al., 1991). As the small segments are used of large ellipses, these small elliptical segments are taken as the parts of circle segments. In this case, since it is along the crossbar, a small placement deviation means also a small angle deviation. For nth crossbar, radius (R_n), depth (Δ_n), arc length (b_n) and angle made with half arc length ($ß_n$) are shown in Fig. 4.9.

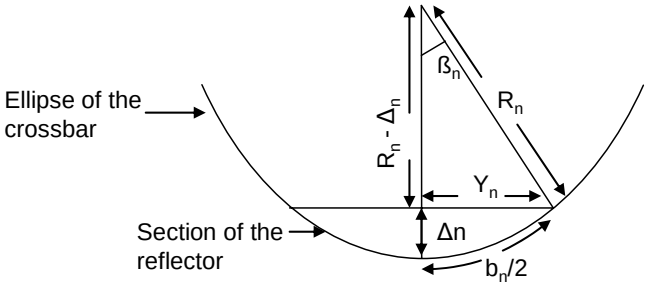

Figure 4.9: Radius, depth and arc length details for nth crossbar

It is evident from Fig. 4.9

$$R_n^2 = \left(R_n - \Delta_n\right)^2 + Y_n^2$$

By simplifying the above equation

$$R_n = \frac{\sqrt{\Delta_n^2 + Y_n^2}}{2\Delta_n} \tag{4.17}$$

It is also clear from Fig. 4.9

$$\beta_n = sin^{-1}\left(\frac{Y_n}{R_n}\right) \tag{4.18}$$

and

$$\frac{b_n}{2} = R_n\left(\frac{2\pi\beta_n}{360}\right) \tag{4.19}$$

The depth (Δ_n), radius (R_n) and arc length (b_n) of nth crossbar are calculated by using Eqs. (4.17) - (4.19) and are given in Table 4.3.

Table 4.3: Depths and lengths of different arcs of the crossbars for 8 m^2 Scheffler reflector

Crossbar "*n*"	Y_n (m)	Depth "Δ_n" (m)	Radius "R_n" (m)	Angle "$ß_n$" (degree)	Half arc length "$b_n/2$"(m)	Arc length "b_n"(m)
1	0.88090	0.11965	3.30255	15.46997	0.89169	1.78338
2	1.17798	0.19820	3.59969	19.10163	1.20008	2.40016
3	1.32460	0.23403	3.86552	20.03966	1.35199	2.70398
4	1.37000	0.23529	4.10612	19.49036	1.39678	2.79356
5	1.32460	0.20781	4.32536	17.83280	1.34623	2.69246
6	1.17798	0.15595	4.52695	15.08281	1.19169	2.38338
7	0.88090	0.08305	4.71331	10.77170	0.88611	1.77222

After calculating the required parameters, a brief description of the construction work (Scheffler reflector) is presented to give value to the theoretical results. The arcs of different radii are marked on the bending templates as given in Table 4.3. Mild steel round bars (10 mm thickness) are used for the crossbars and are cut according to the required arc lengths as detailed in Table 4.3. These lengths are then bent with respect to marked circular curves on the templates. After going through the straightness tests, these curves are then welded on the marked positions of the reflector frame as shown in Fig. 4.6. These welded curves are then thoroughly examined for precision and evenness with the help of a jig. The reflector frame is painted with primer and suitable paint to avoid corrosion.

Thereafter, aluminum profiles are fixed on the reflector frame to shape the base for the aluminium reflectors. These aluminium profiles are tied with crossbars with the help of steel wires. Aluminium reflecting sheets are pasted on these profiles with silicon glue to shape the required lateral part of the paraboloid. Of the material investigated, highly secular aluminium has an excellent chance to meet the requirements for medium concentrating technologies like parabolic troughs for example. They offer a solar weighted reflectance of 88–91 %, good mechanical properties and are easy to recycle (Fend et al., 2000). Aluminium profiles from Alcan Company, Germany are normally used with reflectivity at more than 87 %.

4.2.5 Installation of the Scheffler reflector on site

The above calculations are made with respect to equinox with zero solar declination. While installing a Scheffler reflector at any site, the axis of rotation is fixed very precisely at an angle equal to “the latitude of the site” with horizontal in north-south direction. For daily tracking, these reflectors rotate along an axis parallel to polar axis with an angular velocity of one revolution per day to counterbalance the effect of daily earth rotation. The daily tracking is accomplished with the help of a small self-tracking PV system or clock-work operated by gravity which provide angular velocity at one revolution per day. Up until now, the manuscript has only discussed reflector design with respect to zero solar declination. The detail for the other days of the year is explained in the next article.

Scheffler reflectors are classified as standing reflectors and laying reflectors depending upon the direction of the reflector face. All standing reflectors face towards south in the northern hemisphere, and north in the southern hemisphere, as well as providing focus at ground level. The installation detail for standing reflectors in the northern hemisphere (at Ø° latitude angle) is shown in Fig. 4.10. The laying reflectors face towards north in the northern hemisphere and south in the southern hemisphere, as well as providing an elevated focus.

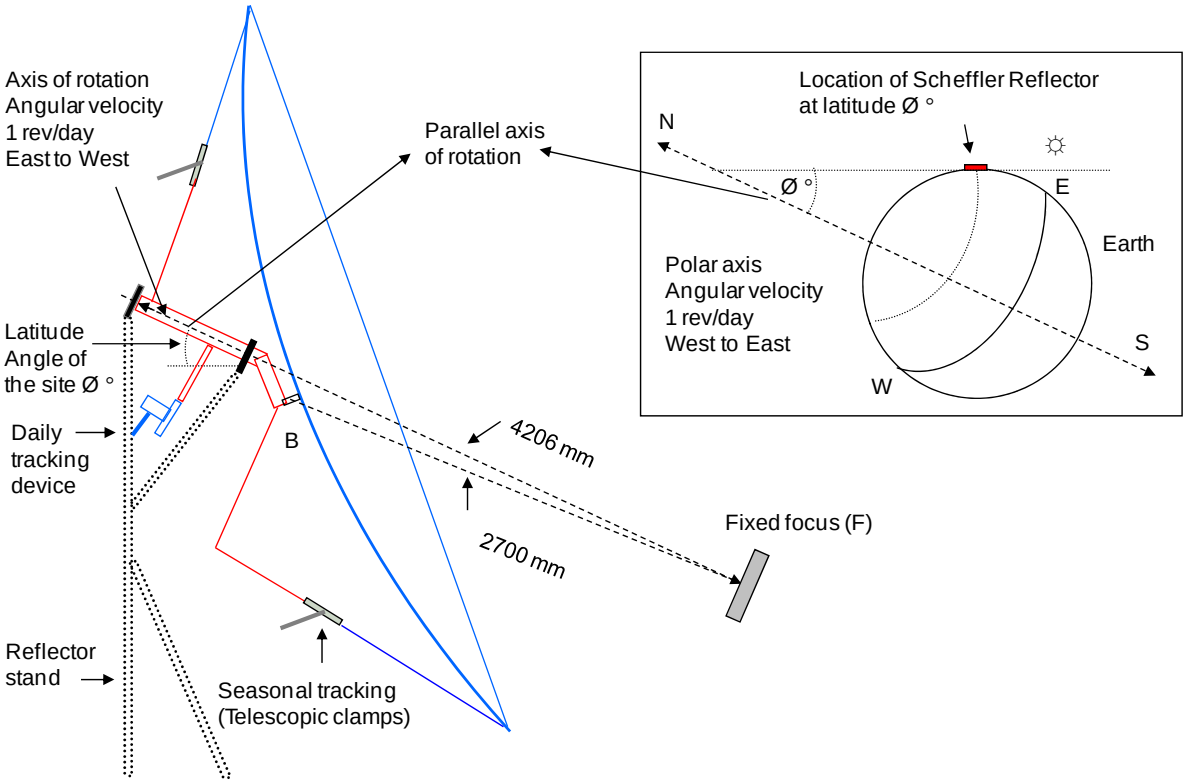

Figure 4.10: Installation and daily tracking details of the Scheffler reflector (valid for standing reflectors in the northern hemisphere)

4.2.6 Daily tracking

Both standing and laying reflectors rotate along their axis of rotation with an angular velocity of one revolution per day to counterbalance the effect of daily earth rotation. The tracking mechanism normally comprises of small self-tracking PV system or clock-work operated by gravity. In clock-work system, a weight pulled the reflector with the help of a string due to force of gravity through tracking channel. The pendulum of clock mechanism maintains the angular velocity of one revolution per day to counter balance the effect of earth rotation. Performance evaluation and distillation experiments were carried out by both clock-work tracking system and PV tracking system. Out of the two methods, exact results were obtained by PV tracking system. In fact, this system is based on the actual sensing of the sun position and more realistic tracking approach. It comprises of two aluminum plates to form a v-shape angle (51°). Four small photovoltaic panels (each having 0.5 volts, 300 mA) are pasted on aluminum plates (two on either side) and covered by cylindrical glass. This glass behaves like a lens and produces concentrated line image for precise tracking. The changing position of the sun causes a current difference in two PV plated which actuates the DC geared motor. The structure of primary reflector is completely balanced and need very low power to track the sun. In this way, the primary

reflector rotates with the help of this motor by chain-sprocket mechanism to track the sun very precisely as shown in Fig. 4.11

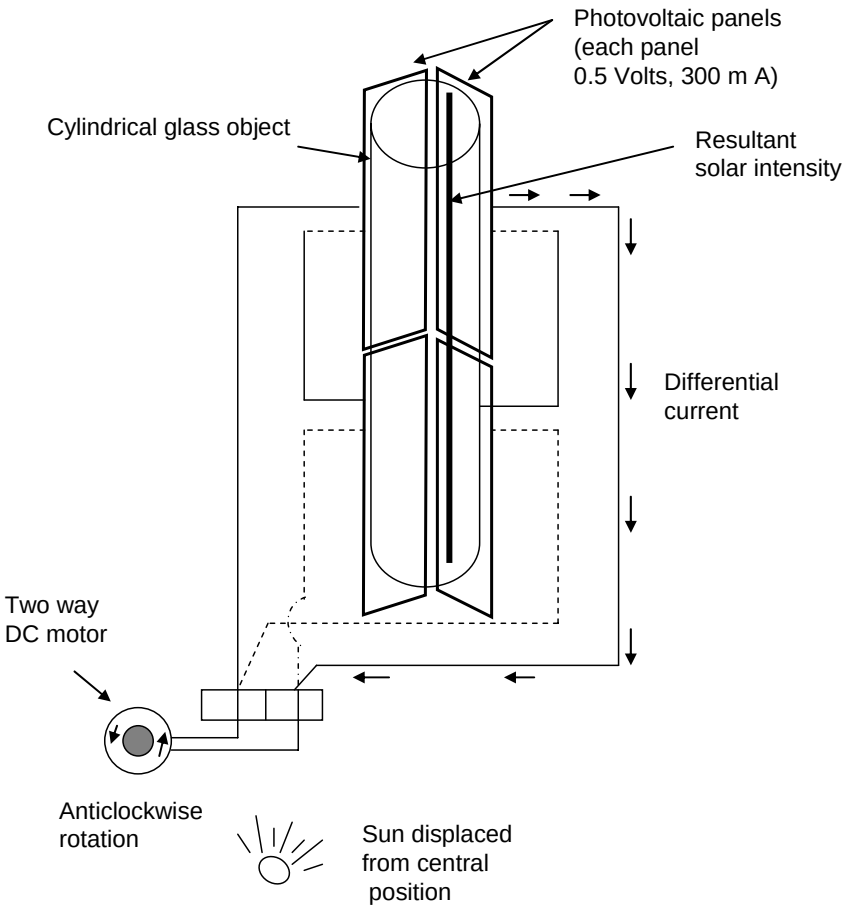

Figure 4.11: Schematic of photovoltaic daily tracking system

4.2.7 Calculation of seasonal parabola equations

In order to adjust the reflector with respect to the changing solar declination, the reflector has been provided with a telescopic clamp mechanism to adjust the inclination of the reflector by half of the change of the solar declination angle and to attain the required shape of the parabola for any day of the year. In order to attain the required parabola equation, a fixed point B with x-coordinate 2.69338 on the parabola curve is selected which is the common point for all seasonal parabolas and at the same time acts as the central pivot point for the required shape change of the crossbars. As the point B lies on the same parabola, the y-coordinate is calculated to be 1.26469 by substituting the value of the x-coordinate (2.69338) in Eq. (4.3). The general form of a parabola equation for any day of the year is given below

$$D(x) = m_d x^2 + C_d \tag{4.20}$$

Taking first derivative of Eq. (20)

$$D'(x) = 2m_d x$$

but

$$D'(x) = tan\left(43.224 + \frac{\alpha}{2}\right)$$

$$m_d x = tan\left(43.224 + \frac{\alpha}{2}\right) \tag{4.21}$$

where "α" is solar declination. Duffie & Beckman (2006) quoted the equation with the least error (Error < 0.035°) for the determination of solar declination for any day of the year

$$\alpha = (180/\pi)[0.006918 - 0.399912\cos(n-1)2\pi/365 + 0.070257\sin(n-1)]2\pi/365 - 0.006758\cos 2(n-1)2\pi/365 + 0.000907\sin 2(n-1)2\pi/365 - 0.002679\cos 3(n-1)2\pi/365 \; 0.00148\sin 3(n-1)2\pi/365 \tag{4.22}$$

where "n" is the day of the year and "α" is solar declination varies from -23.5° to + 23.5° from December 21 to June 21 respectively (Goswami, 1999)

First of all, the general equation of seasonal parabola equations for standing Scheffler reflectors (8 m^2) in the northern hemisphere is calculated. The coordinates of new set of points at any day of the year are calculated by using the "Rotation Matrix" to rotate the point B(2.69338, 1.26569) about focus F(0,1.43287) and are given in Eq. (4.23).

$$(x_d, y_d) = (x, y).\begin{bmatrix} +\cos\alpha & +\sin\alpha \\ -\sin\alpha & +\cos\alpha \end{bmatrix} \tag{4.23}$$

This equation shows that the coordinates x_d and y_d depend only on the fix pivot points "B(x,y)" selected on the Scheffler reflector and the solar declination. For a selected reflector, the coordinates depend only on the solar declination and are calculated by

expanding the rotation matrix given in Eq. (4.23). By substituting the values of x_d, y_d and α in Eq. (4.20) and Eq. (4.21), the equation of parabola in terms of slopes and *y*-intercepts can be calculated for any day of the year.

In order to see the variation of parabola equations for two extreme seasonal positions on June 21 and December 21, the reflector has to rotate at half the solar declination angle. The angles at point B for summer (June 21) and winter (December 21) are +11.75 (+23.5/2) and -11.75 (-23.5/2) respectively with reference to equinox position. For summer, the Eq. (4.20) can be re-written as:

$$S(x_s) = m_s x^2 + C_s \tag{4.24}$$

Differentiating with respect to *x*

$$S'(x_s) = 2m_s x$$

This rate of change is equal to the slope

$$S'(x) = tan\left(43.223 + \frac{23.5}{2}\right)$$

$$2m_s x_s = 1.42676 \tag{4.25}$$

For summer, substitute the value of α = 23.5°, *x* = 2.69338 and *y* = 1.26569 in Eq. (4.23). The value of *y*-coordinate of focus i.e., 1.43287 is subtracted first from the y-coordinate of the point B i.e., 1.26569 before solving the matrix and is then added this value to the *y*-coordinate obtained from the specific day (in this case, y_s) after the solution as a rule of the rotation matrix.

$$(x_s, y_s) = (2.69338, 1.26569 - 1.43287).\begin{bmatrix} +cos\,23.5 & +sin\,23.5 \\ -sin\,23.5 & +cos\,23.5 \end{bmatrix}$$

$$(x_s, y_s) = (2.53665,\ 0.92068 + 1.143287)$$

$$(x_s, y_s) = (2.53665,\ 2.35355)$$

Substituting the values of x_s, y_s in Eq. (4.24) and Eq. (4.25), the equation for the summer parabola is found out and is given below:

$$y = 0.28123\,x^2 + 0.54394 \tag{4.26}$$

For winter, substitute the value of α = -23.5°, x = 2.69338 and y = 1.26569 in Eq. (4.23). The same procedure is repeated as done for the determination of the equation of the summer parabola; the equation for winter parabola is calculated and is given below:

$$y = 0.12736\ x^2 + 0.53004 \tag{4.27}$$

The inclination of the fixed point B of parabolas on June 21 and December 21 are found to be 54.974° and 31.474° by adding and subtracting 11.75° to the inclination angle of fixed point B at equinox (43.224°). The detail of parabola equations for equinox, summer and winter for the northern hemisphere (standing reflectors) is shown in Fig. 4.12.

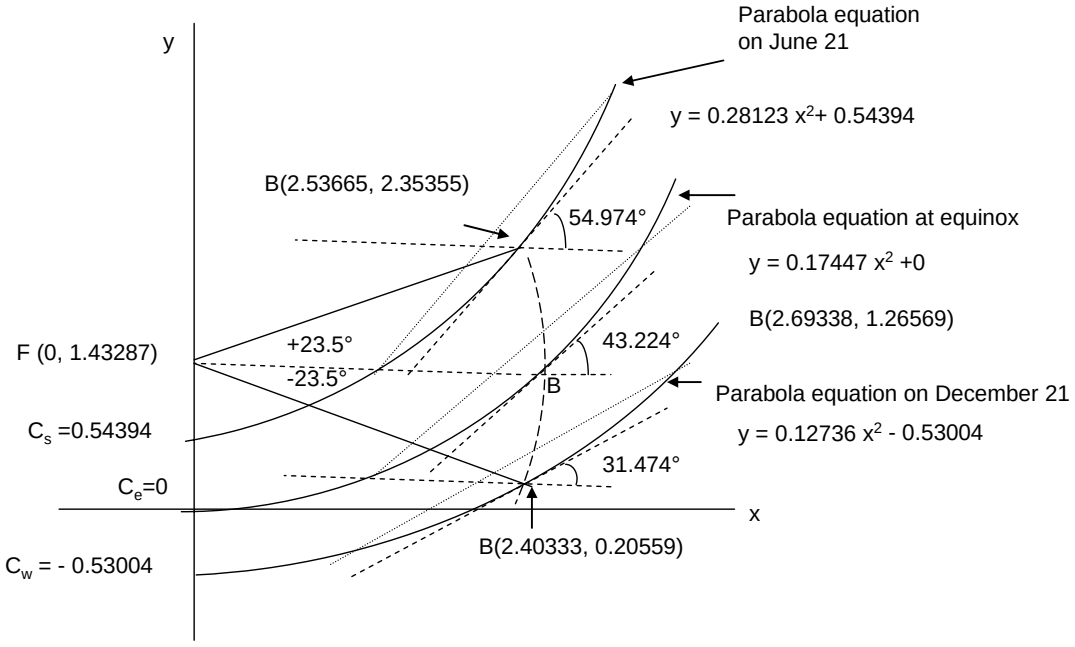

Figure 4.12: Seasonal parabola equations for an 8 m^2 Scheffler reflector (valid for standing reflectors in the northern hemisphere) at equinox, summer (June 21) and winter (December 21)

By comparing Eq. (4.3), Eq. (4.26), and Eq. (4.27) and from Fig. 4.12, it is evident that the shapes of parabolas are different in summer and winter. The slopes of parabola curves with respect to equinox (solar declination =0), summer (solar declination = +23.5) and winter (solar declination = -23.5) for the Scheffler reflector (8 m^2 surface area) are calculated to be 0.17447, 0.28123, and 0.12736 respectively. The y-intercepts of the parabola curves for equinox, summer and winter are found to be 0, 0.54394, and -0.53004 respectively. Through comparison with the equinox parabola curve, that of the summer parabola is found to be smaller in size and uses the top part of a parabola curve, while the winter parabola is bigger in size and using the lower part of a parabola curve to provide the fixed focus.

For the calculations of seasonal parabola equations in the southern hemisphere, the above procedure is repeated by replacing angle α by ($-\alpha$) in Eq. (4.23). In this way, the parabola equations on June 21 and December 21 in the southern hemisphere are found to be the same as parabola equations on December 21 and June 21 in northern hemisphere respectively. In laying reflectors, the parabola equations for the northern hemisphere will be the same as the parabola equations for the southern hemisphere (standing reflectors). Similarly, the parabola equations for laying reflectors in southern hemisphere will be the same as the parabola equations in the northern hemisphere for standing reflectors.

4.2.7.1 Use of pivot points for the required profiles of the Scheffler reflector

Scheffler reflector is a lateral part of a paraboloid and is designed with respect to equinox (solar declination = 0). In order to achieve the same fixed focus for all days of the year, different paraboloidal surfaces are needed depending on the solar declination. For this purpose, the Scheffler reflector is provided by three points, two pivot points “A” are attached with a reflector frame while the third point B is attached on a parabola curve (center bar). Pivot points “A” are fixed at the line joining the minor axis of the reflector frame in such a way that these two points and the point P_n pass through the same line (when the reflector is set at equinox position). Third pivot point “B” is taken a little bit down slightly from point P_n lying on the parabola curve (center bar). When the reflector is seasonally adjusted with the help of telescopic clamp mechanism from points C and D by rotating at half the solar declination angle, these pivots (two on the reflector frame “A” and one on the parabola shaped center bar “B”) induce the required change in the shapes of the crossbars. For this reason, the complete structure of the Scheffler reflector is constructed as a flexible assembly to attain the desired shape. The details of pivot points

and the telescopic clamps by marking the exact positions of fix and non-fix points of the Scheffler reflector as well as articulations and forces that lead to a deformation of the collector in the desired direction in 3-D perspective is shown in Fig. 4.13.

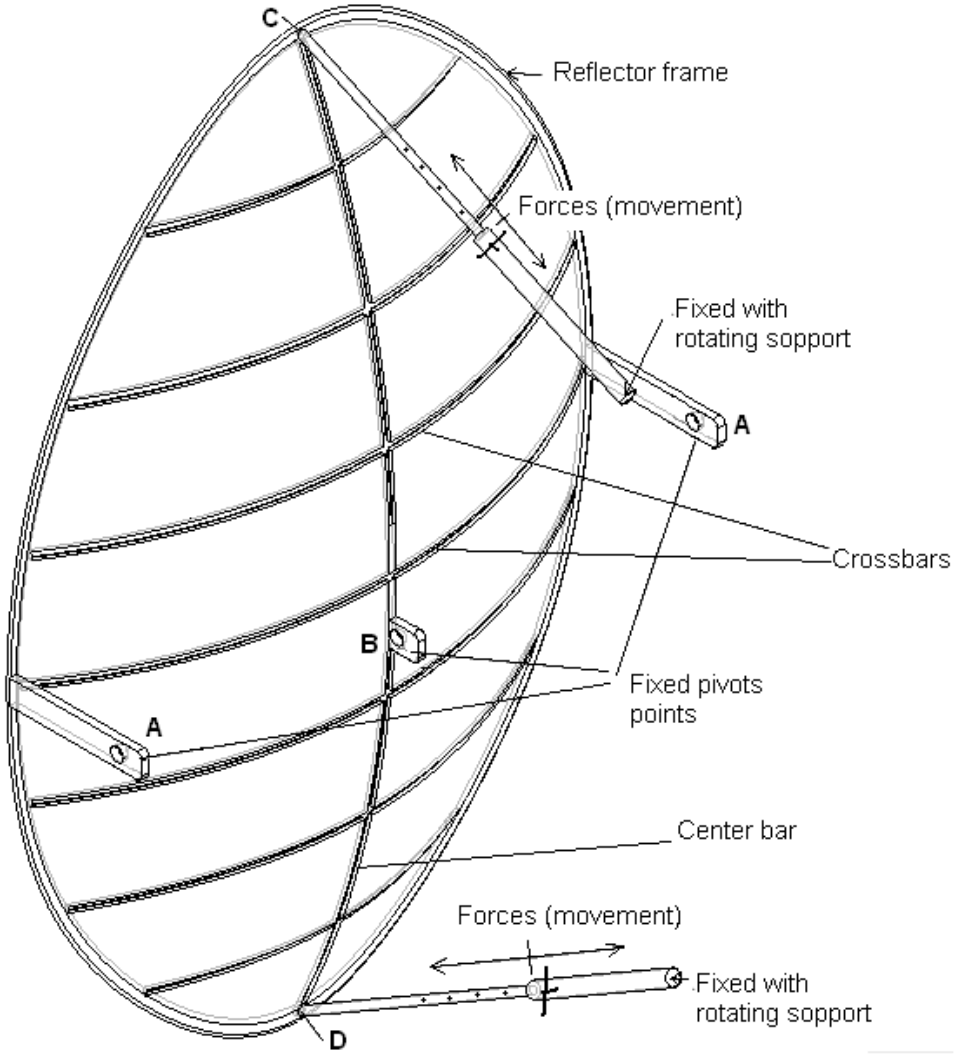

Figure 4.13: Detail of pivot points and telescopic clamps of the Scheffler reflector (3 D perspective)

When the reflector is seasonally adjusted by the application of forces at point C and D, the effect of pivot points on the reflector deformation for equinox, summer and winter positions is shown in Fig. 4.14.

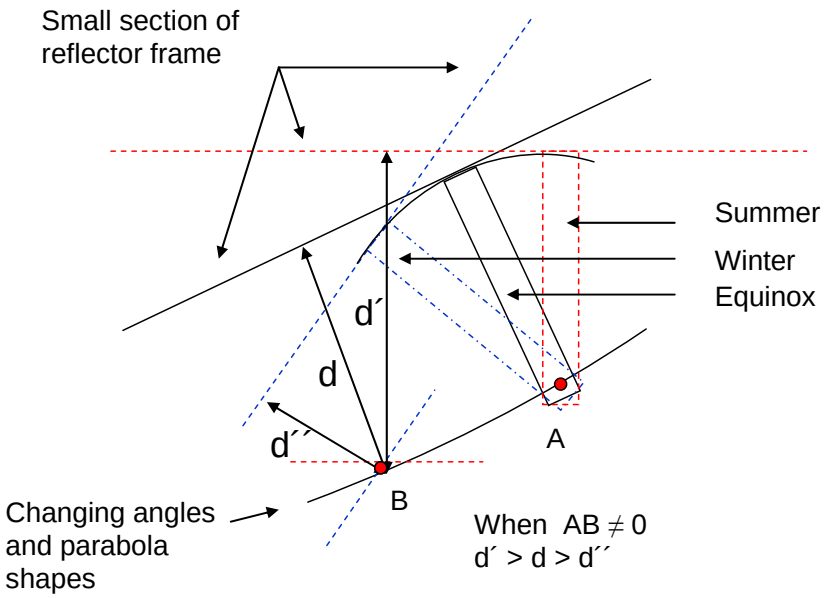

Figure 4.14: Effect of pivot points on reflector deformation (valid for the standing reflectors in the northern hemisphere)

Point B is the common point for all the parabolas of the year. Fig. 4.14 shows that the shortest distance between point B and the reflector frame increases for summer parabola and decreases for the winter parabola for the standing reflector in the northern hemisphere (where d, d´ and d´´ are the distances from point B to the reflector frame at equinox, summer and winter respectively). The deformation of the complete reflector on June 21 and December 21 for the standing reflector in the northern hemisphere is also shown in Fig. 4.15.

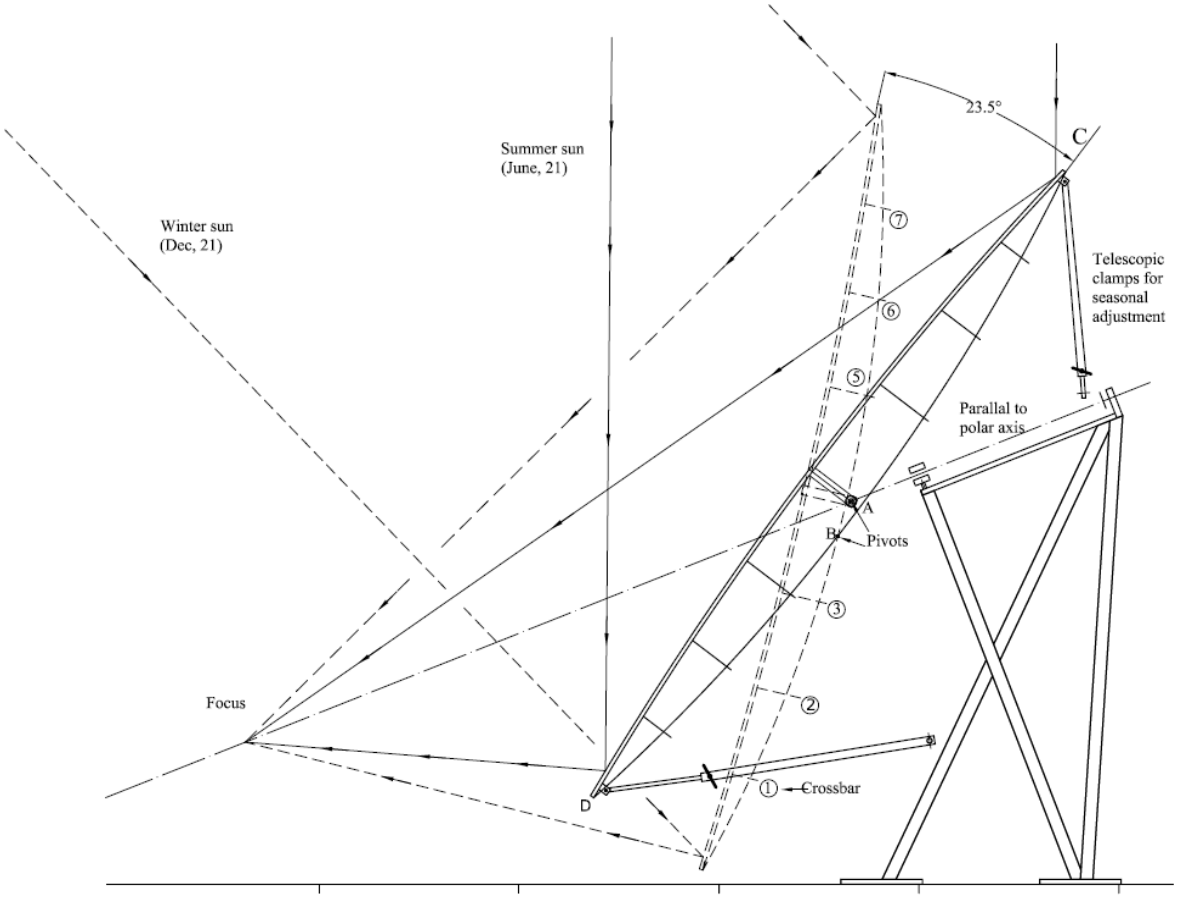

Figure 4.15: Functioning of pivot points and clamps to deform the reflector (valid for standing reflectors in the northern hemisphere)

It is evident from Fig. 4.15 that these pivot points also deform the shape of the reflector frame, which are curved outside in the summer and curved inside in the winter for the standing reflectors in the northern hemisphere. By using the three pivot points, in praxis the approximately correct shape is attained for the curvature of the crossbars. Along the parabola (center bar), the two telescopic clamps are used (at points C and D) to deform the center bar until the concentrated light is the smallest at the focal point. This is not perfect, but serves the intended purpose of heat utilization at the fixed focus in medium temperature range.

The focus remains fixed and always lies on the line passing through the axis of rotation of the primary reflector. The distance between two fixed points B and F always remain 2700 mm (for 8 m^2 reflector design). In this way, the reflected beam remains aligned with the fixed focus for all days of the year.

Although the construction and installation procedure is complicated, yet it takes only a fraction of a minute to put the system in operation by visualizing the illuminated beam at the targeted focus. Seasonal tracking is done with the help of a telescopic clamp mechanism by twisting the reflector at half the solar declination (approximately one degree after three days). The fixed focus concentrators provide an extraordinary opportunity for decentralized application in tropical countries. It can open a new land marks in small scale industrial processing especially in rural areas. It enables the stationary applications ranging from house cooking to medium temperature industrial operations.

4.3 Calculation of the required size of the Scheffler reflector

In section 4.2, the design and construction details of an 8 m^2 Scheffler reflector have been presented. In order to design the required surface area of the Scheffler, a mathematical model has been developed. This model is developed in Matlab 7 and some unusual symbols are used as per requirement of the program, so their protocol is defined. This model can also be run Microsoft Excel Spread sheet and the complete model is also provided in CD. The detail of this model in Matlab along with protocol is explained as under:

```
yp = 1.43287; y-ordinate of point Pn (main factor to change the size)
xp  = 2*yp; y-coordinate of point Pn
mp  = 1/(2*xp); slope of point Pn
Cp  = yp-mp*xp^2; y-intercept of point Pn
YP  = mp*x^2 + Cp; general equation of parabola
disp(['Yp = ' num2str(mp) ' * x^2   '  num2str(+ Cp) ]);
xe1 = 1.32387*yp/1.43287; x-coordinate of point E1
ye1 = .30578*yp/1.43287; y-coordinate of point E2
xe2 = 4.06387*yp/1.43287; x-coordinate of point E2
mg = 0.94; slope of the cutting section of the reflector frame
Cg = Ye1-mg*Xe1; y-intercept of the cutting section of the reflector frame
Yg = mg * x + Cg; equation of the cutting section of the reflector frame
disp(['Yg = ' num2str(mg) ' * x   '  num2str(+ Cg) ]);
xe1 = mg/(2*mp)+((mg/(2*mp))^2-(Cp-Cg)/mp)^0.5;
xe2 = mg/(2*mp)-((mg/(2*mp))^2-(Cp-Cg)/mp)^0.5;
a = ((mg/(2*mp))^2-(Cp-Cg)/mp)^0.5; semi-minor axis of the ellipse
b = a/cos(43.23); semi-major axis of the ellipse
xqm = (Xe1+Xe2)/2; x-cordinate of the middle crossbar
yqm = mg*xqm+Cg; y-coordinate of the middle crossbar
mqm = -1.06377; slope of the middle crossbar
cqm = yqm-xqm*mqm; y-intercept of the middle crossbar
aqm = ((mqm/(2*mp))^2-(Cp-cqm)/mp)^0.5; semi- minor axis of the middle crossbar
bqm = aqm/0.6849; semi- major axis of the middle crossbar
Iq = 0.48; distance between consecutive crossbars
Iqy = Iq/0.6849;
```

```
nc = b/0.48; no. of crossbars required
nf = fix(nc);
for i = -nf:nf;
cqm1 = cqm + i * Iqy; y-intercept of  ith crossbar
aqm1 = ((mqm/(2*mp))^2-(Cp-cqm1)/mp)^0.5; semi minor axis of  ith crossbar
bqm1 = aqm1/.6849; semi major axis of ith crossbar
Yn = cos(43.23)*(b^2-(i*Iq)^2)^0.5;
deln = (aqm1-(aqm1^2-Yn^2)^0.5)/cosd(46.77); reflector depth for ith crossbar
Rn = (deln ^2+Yn^2)/(2*deln); radius of nth crossbar
beta = 180/pi*asin(Yn/Rn); angle of ith crossbar
bn = 2*Rn*beta*pi/180; half crossbar of ith crossbar
disp(['Q' num2str(i)  '= ' num2str(mqm) ' * x   '  num2str(cqm1) ]);
end

qn = mqm*x +Cqm
n = 110; no. of day of the year
decl = 180/pi*(0.006918-0.399912*cos(2*pi/365*(n-1))...
   + 0.070257*sin(2*pi/365*(n-1))-0.006758*cos(2*(2*pi/365*(n-1)))...
   + 0.000907*sin(2*(2*pi/365*(n-1)))-0.002697*cos(3*(2*pi/365*(n-1)))...
   + 0.00148*sin(3*(2*pi/365*(n-1)))); solar declination on nth day of the year
```

For northern hemisphere

```
xdn = (2.69338*yp/1.43287)*cosd(decl)-(1.26569*yp/1.43287-1.43287)*sind(decl); x-coordinate for the seasonal equation
ydn = 2.69338* sind(decl)+(1.26569-1.43287)*cosd(decl)+1.43287; y-coordinate for the seasonal equation
mdn = tand(43.223+ decl/2)/(2*xdn); solpe of seasonal equation
Cd =ydn-(mdn)*(xdn)^2; y-intercept on nth day of the  equation
disp(['Yn = ' num2str(mdn) ' * x   '  num2str(+ Cd) ]);
```

For southern hemisphere

```
decls  = -decl;
xds = (2.69338*yp/1.43287)*cosd(decls)-(1.26569*yp/1.43287-1.43287)*sind(decls); x-coordinate for the seasonal equation
yds = 2.69338* sind(decls)+(1.26569-1.43287)*cosd(decls)+1.43287; y-coordinate for the seasonal equation
mds = tand(43.223+ decls/2)/(2*xds); slope of seasonal equation
Cds = yds-(mds)*(xds)^2;  Y-intercept on nth day of the  equation
disp(['Ys = ' num2str(mds) ' * x   '  num2str(+ Cds) ]);
disp(['Yg = ' num2str(mg) ' * x   '  num2str( Cg) ])
disp(['Yg = ' num2str(mp) ' * x   '  num2str( Cp) ])
S = yp^2*3.94; surface area of the Scheffler reflector
```

The mathematical model can be used to design different sizes of Scheffler reflectors for the desired capacities of the solar distillation system and other heat applications in medium temperature ranges. The algorithm can be used in Matlab to find out the required parabola equations for different surface areas of the Scheffler reflector. The seasonal parabola equation for any day of the year can be determined by substituting the number of

the day of the year in the model. Moreover, the major and minor axes of the reflector frame and crossbars can also be determined by using this mathematical model.

4.4 Energy distribution in the solar distillation system

The solar distillation system is designed for decentralized applications in tropical countries. The system is made simple and flexible for conducting different types of distillation experiments for post harvest processing and food applications. One way to cause economically easy terms is to design system without heat storage, the solar heat is fed directly into a suitable process (fuel saver). In this case, the maximum heat at which the solar energy systems deliver energy must not be appreciably larger than the rate at which process uses energy. It can be concluded from the results that it is more advantageous to apply solar energy to higher temperature processes than to lower temperature ones as the saving incurred are much higher (Kalogirou, 2003).

After the construction and development process, the solar distillation system was optimized thoroughly by considering the different sources of energy losses. The study also provides guidelines for other similar site specific applications. The available energy and unavailable energy/losses are indicated by black and white arrows respectively at four main points (1-4) as shown in Fig. 4.16.

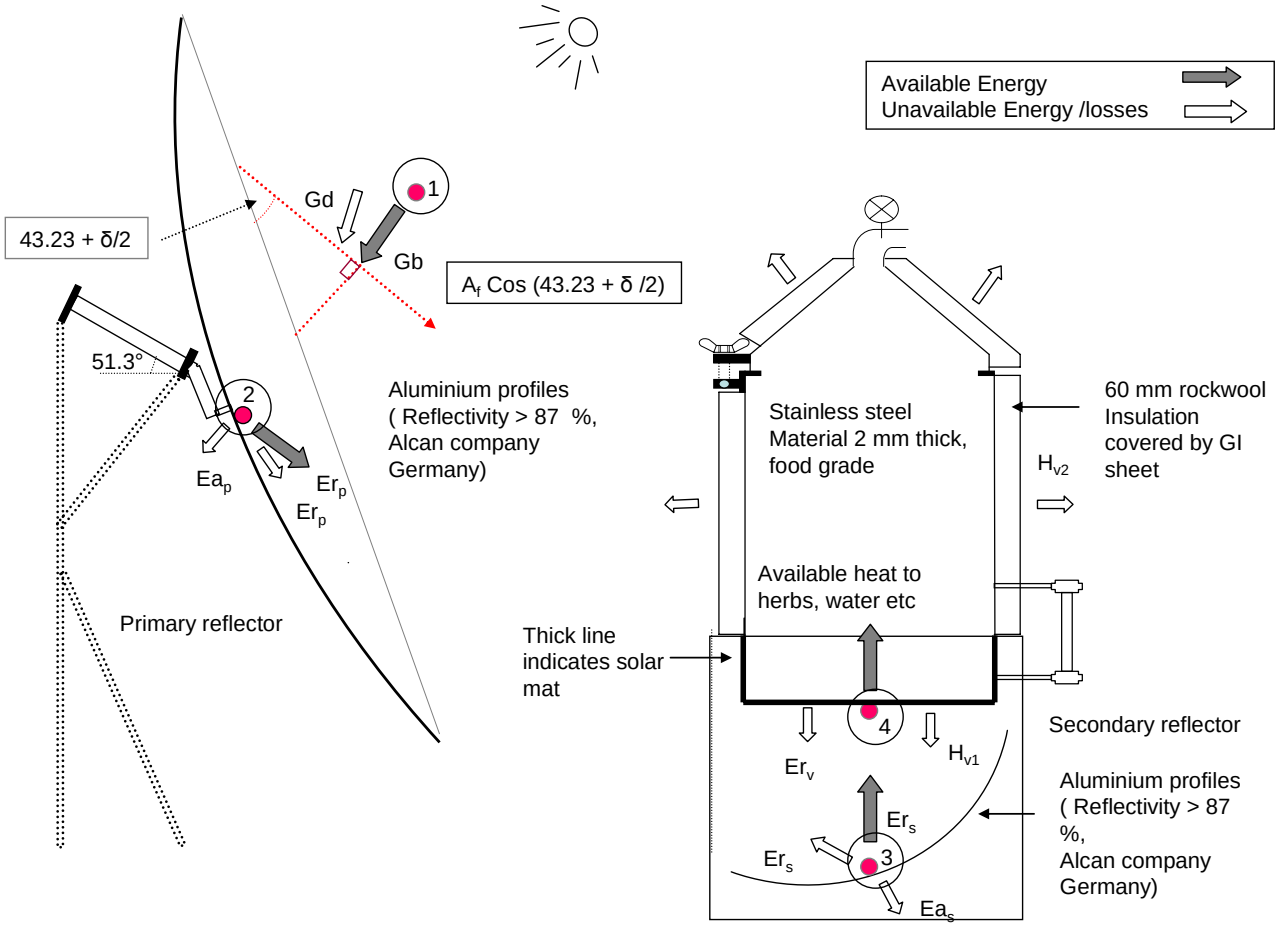

Figure 4.16: Explanation of available energy and losses in a solar distillation system

4.4.1 Available insolation from Primary reflector

Point No.1 (Fig. 4.16) indicates the available insolation for the primary reflector. Out of a total irradiance (beam radiation *Gb* plus diffuse radiation Gd) falling on the primary reflector, only beam radiation (*Gb*) is available energy for the concentrated collector. Further the frame of the Scheffler reflector (having area A_f) is not perpendicular to beam radiation but inclined downward at an angle of (43.23 ± *α*/2) degrees due to lateral part of a paraboloid (α being solar declination, positive (+) and negative (-) signs are applicable for northern and southern hemisphere respectively). Therefore, the aperture area of the primary reflector depends on solar declination and is taken as A_f*cos (43.23 ± α/2). The pyranometer is covered by black pipe so that it can record the beam radiations and is fixed on the primary reflector at a plane perpendicular to the beam radiation. Every morning, the pyranometer position is set to face the sun exactly in order to record maximum beam radiation. The pyranometer orientation accuracy can also be checked by visualizing no

shadow all around the pyranometer during the whole day. In this way, the total input energy available (E_p) at the reflector face is the beam radiation recorded by pyranometer times this fraction of the area A_f*cos (43.23 ± α/2) and is given in the mathematical form:

$$E_p == G_b\, A_f\, cos\left(43.23 \pm \frac{\alpha}{2}\right) \tag{4.28}$$

Also

$$A_s = A_f\, cos\left(43.23 \pm \frac{\alpha}{2}\right) \tag{4.29}$$

where A_s is the available aperture area of the Scheffler reflector at any day of the year
As the primary reflector is elliptical in shape, the surface area can also be expressed in semi-minor axis and semi-major axis. Eq. (4.28) can also be expressed as:

$$A_s = (\pi\, a\, b - 0.1) cos\left(43.23 \pm \frac{\alpha}{2}\right) \tag{4.30}$$

where a is the semi-minor axis of the elliptical frame of Scheffler reflector, b is the semi-major axis of the elliptical frame of the Scheffler reflector, α is the solar declination.

The semi-major axis and semi-minor axis for the elliptical frame of the Scheffler reflector are 1.88 and 1.37 m respectively. The area of the ellipse is reduced by 0.1 m^2 to allow the installation of different devices like the photovoltaic daily tracking device and the pyranometer. Equation quoted by Duffie & Beckman, (2006) with the least error (Error < 0.035°) is used for calculation of solar declination.

$$\alpha = (180/\pi)[0.006918 - 0.399912\, cos\,(n-1)2\pi/365 + 0.070257\, sin(n-1)]2\pi/365$$
$$-0.006758\, cos\, 2(n-1)2\pi/365 + 0.000907\, sin\, 2(n-1)2\pi/365 - 0.002679\ cos\, 3(n-1)2\pi/365$$
$$0.00148\, sin\, 3(n-1)2\pi/365$$

(4.31)

Solar declination “α” varies from -23.5° to +23.5° from December 21 to June 21. The variation of solar declination and aperture area for standing reflectors in the northern and southern hemispheres during the entire year is shown in Fig. 4.17 and also given in Appendix B in tabular form (for performance evaluation calculations).

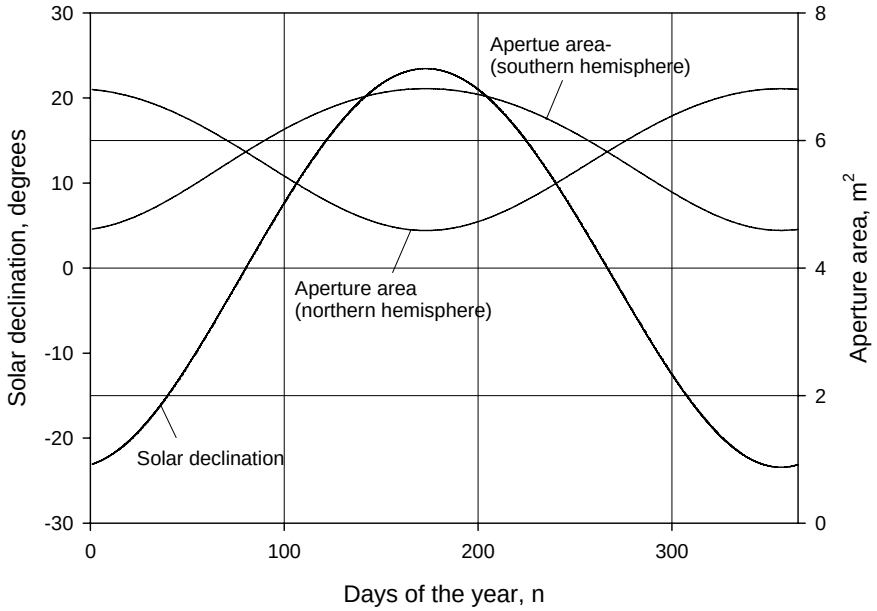

Figure 4.17: Variation of solar declination and aperture area of Scheffler reflector in the northern and southern hemisphere (valid for standings reflectors)

It is evident from figure 4.17 that aperture area is maximum (6.4 m^2) on December 21 and minimum (4.59 m^2) on June 21 in the northern hemisphere for the standing reflectors. On the other hand, the aperture area is minimum (4.59 m^2) on December 21 and maximum on June 21 (6.4 m^2) for the standing reflectors in the southern hemisphere. It is also evident from the figure that standing reflectors have the same aperture area (5.83 m^2) at equinox. For a given Scheffler reflector, more energy can be obtained from the standing reflectors designs in winter seasons as compared with the summer seasons at the same intensity of beam radiation. These reflectors are more suitable in tropical countries to maintain uniform power output throughout the year. The standing reflectors also provide an excellent opportunity to have the fixed focus well near the ground level. The variation of solar declination and aperture area for the laying reflectors in the northern and southern hemispheres during the entire year is shown in Fig. 4.18 and also given in Appendix B in the tabular form (for performance evaluation calculations)

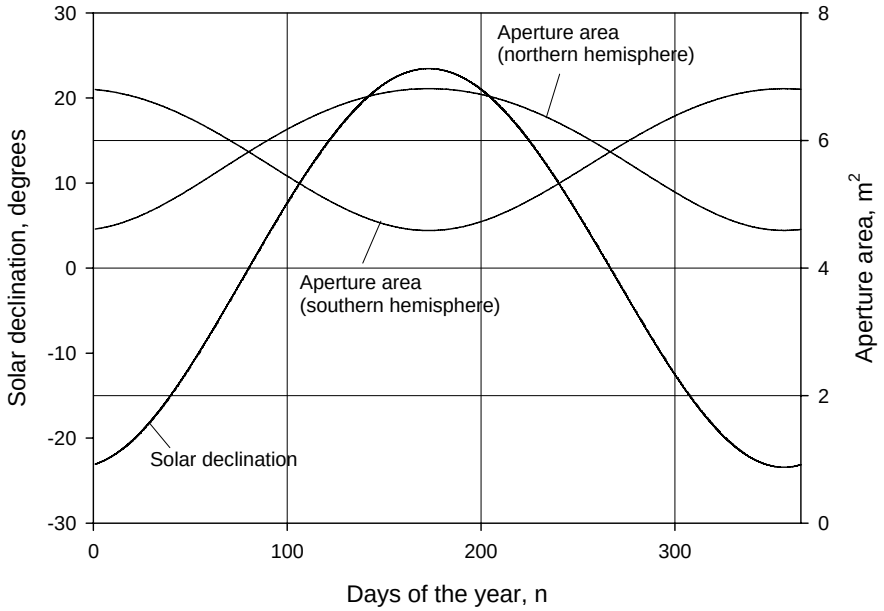

Figure 4.18: Variation of solar declination and aperture area of Scheffler reflector in the northern and southern hemisphere (valid for laying reflectors)

Figure 4.18 shows the variation of aperture area for laying reflectors. The aperture area is maximum on December 21 and minimum on June 21 in the northern hemisphere for the laying reflectors. By comparing Fig. 4.17 and Fig. 4.18, it is evident that the aperture area curve in the northern hemisphere for standing reflectors is the same as in the southern hemisphere for the laying reflector. Similarly, the aperture area curves in the southern hemisphere (standing reflectors) and in the northern hemisphere (laying reflectors) are the same. The laying reflectors are more suitable for the areas on higher latitudes to get maximum power by availing more aperture area in summer as solar intensity during winter is too low. The main drawback of the laying reflectors is that the focus is much above the ground level for big reflector designs. But these reflectors are more suitable for cooking applications as they utilize very less area of the secondary reflectors. These reflectors receive most of the beam radiations directly at the horizontal bottom of cooking vessel and thus saving a significant amount of energy which is lost by using secondary reflectors.

4.4.2 Energy distribution at primary reflector

Point No.2 (Fig. 4.16) represents the energy distribution at primary reflector. The energy is distributed as absorbed radiation (Ea_p) and reflected radiation (Er_p). The absorbed radiation component of energy (Ea_p) depends upon the reflectivity of the material used. Of the material investigated, highly secular aluminium can meet the requirements for medium concentrating technologies like parabolic troughs etc. They offer solar weighted

reflectance of 88–91 %, good mechanical properties and are easy to recycle **(**Fend et al., 2000)**.** Aluminium profiles from Alcan Company, Germany were used with reflectivity greater than 87 %. The energy available after primary reflector (E_{pr}) is given as:

$$E_{pr} = R_p E_p \tag{4.32}$$

where R_p is the reflectivity of the material used for the primary reflector

Some of the radiations are reflected from the primary reflector out of the focus. This deviation is due to the improper reflector profiles and inadequacy in daily and seasonal tracking. The accuracy of the profiles was checked with the help of a special jig designed for this purpose. Infrared camera was also used to measure the fraction of available radiations at targeted focus and out of the focus. It was found that about 12-18 % radiations are not falling on the target and are unavailable for the secondary reflector to further utilize it. The fraction available at the targeted focus (F_f) in general calculation is taken as 0.85. The energy available at the secondary reflector (E_s) is given as:

$$E_s = E_{pr} F_f \tag{4.33}$$

4.4.3 Energy distribution at secondary reflector

Point No.3 (Fig. 4.16) indicates the available energy and losses at secondary reflector. Precisely curved and high reflectivity aluminium sheets (reflectance > 87) were used to reduce the losses. The energy available after secondary reflection (E_{sr}) is given as:

$$E_{sr} = E_s R_s$$

where R_s is the reflectivity of the secondary reflector (0.87 for aluminium sheets)

A concrete foundation bed was constructed to fix the secondary reflector at optimum position with respect to calculated focal point as detailed in Fig. 3.2. Aluminium profiles of secondary reflector are designed to reflect and distribute all the beam radiations on the bottom of distillation unit. The energy available at the distillation bottom (E_v) is given as:

$$E_v = E_{sr} F_v \tag{4.34}$$

where F_v is the fraction of energy available at the distillation bottom

4.4.4 Energy losses from the distillation unit

Point No.4 (Fig. 4.16) indicates the energy losses from vessel (distillation unit). These losses include reflectivity due to incomplete absorbance (E_{rv}) and heat losses from different parts of the vessel i.e., through conduction, convection and radiation. The thermal performance of the absorber is enhanced by a selective coating with high absorptivity in the solar spectrum and low emissivity in the infrared radiation band associated with the operating temperature. The bottom part and 120 mm part of the side of the distillation still remain inside the secondary reflector and are exposed to reflected solar radiations. A heat resistant black paint (Schwarz Matt, RAL 9011) was applied to absorb maximum radiations falling on it. Prior to application, the bottom part of the distillation still was made rough with emery paper to maximize the adhesion of the paint. The heat energy available to run the distillation system (E_{ab}) is given as:

$$E_{ab} = E_v A_v$$

where A_v is the absorbance of the vessel

Other losses at point No.4 (Fig. 4.16) are due to convection and radiation losses from the vessel. H_{v1} and H_{v2} are the total heat losses from the area exposed to solar radiations (bottom and 120 mm of adjacent lateral) and area not exposed to solar radiations (lateral and top) respectively as shown in Fig. 4.16.

The thermal losses calculations are carried out under the existing sizes and conditions of the distillation unit. These calculations also provide decision making to calculate the appropriate lagging thickness. The insulation thickness is taken as a variable parameter during the calculations. The calculation of the thermal losses of the distillation unit is done by taking into account the three thermal heat transfer modes i.e., conduction, convection and radiations. The conduction heat transfer is considered through the stainless steel wall, rockwool insulation, and the galvanized iron sheet. Depending upon the heat energy utilization and geometric consideration, the distillation still is divided into the following three main parts:

1. Lateral part of the distillation still (not exposed to solar radiation and can be insulated to reduce heat losses)
2. Part exposed to solar radiation (bottom and adjacent lateral part)

3. Top cover (conical part and lateral part to sit on the seat, the conical part was insulated and the lateral part was not insulated as it is a junction to tight the two parts of the still)

The heat losses are calculated for different parts of the still and are programmed in a Matlab 7 and Microsoft Excel spreadsheet. Thereafter, losses are calculated at different insulation thicknesses to select the combination which is economically feasible and easy to handle. The model is developed in general form to apply for different sizes of the distillation still. Here, the losses are calculated for the given solar distillation prototype.

For most of the distillation experiments, the operating temperature was taken as 100 °C. The steam contacting the plant material is at 100 °C which is acceptable for most plant material and this temperature remain constant for the duration of the distillation (Dürbeck, 1997).

Following assumptions are made for the modeling of solar distillation system

- The ambient temperature (T_{amb}) is taken as 20 °C because most of the experiments were conducted at this temperature.
- The space temperature (T_{space}) is necessary to calculate the radiative losses and is taken as 15 °C by considering that the environment reacts like a black body.
- The thermal contact resistively between different layers of the insulation is neglected.
- Beam radiations are distributed on the bottom of the distillation still after reflection from the secondary reflector.

4.5 Thermal losses calculation of the distillation still

4.5.1 Conduction and convection losses

The steady state heat transfer (φ) through a cylindrical layer that are exposed to convection on both sides to fluids is given as (Cengel, 2006):

$$\varphi = \frac{T_{in} - T_{amb}}{R_{cond} + R_{conv}} \tag{4.35}$$

where T_{in} is the temperature inside the distillation still, T_{amb} is the ambient temperature, R_{cond} is the conduction resistance, R_{conv} is the convection resistance

4.5.1.1 Conduction resistance

Cylindrical part

Thermal conduction resistance for the cylindrical part is calculated by the following relation (Cengel, 2006):

$$R_{cond} = \frac{1}{2\pi \lambda L} ln\left(\frac{r_{ext}}{r_{int}}\right) \tag{4.36}$$

where λ is the thermal conductivity of the material used, L is the lateral length of the cylindrical still, r_{ext} is the external radius of the cylindrical still, r_{int} is the internal radius of the cylindrical still

Plane Wall

The conduction resistance of the bottom part is calculated by the following relation (Cengel, 2006):

$$R_{cond} = \frac{t}{\lambda A} \tag{4.37}$$

where t is the wall thickness of still bottom, A is the cross-sectional area of the still bottom

Conical part

The conduction resistance of the bottom part is calculated by the following relation.

$$R_{cond} = \frac{t\sqrt{2}}{\lambda\pi\left(L_1^2 - L_2^2\right)}$$

where t is the wall thickness. For conical part L_1=0.283 and L_2= 0.085 at 45° angle of cone

With insulation

With insulation, the conductive resistance for multilayered plane wall, cylindrical and conical segments is calculated by adding the conductive resistance for all layers and is generalized as:

$$R_{cond} = \sum R^{i}_{cond}$$

where "*i*" indicates any layer of stainless steel, rockwool and galvanized iron sheet with different thermal conductivity and thickness

4.5.1.2 Convection resistance

Convection resistance is calculated by the following relation.

$$R_{conv} = \frac{1}{hS} \tag{4.38}$$

where *S* is the external surface area, *h* is the natural convection co-efficient.

4.5.2 Radiation losses

Radiation heat losses are calculated by the following relation

$$Radiation\ losses = \varepsilon\ \delta\ S\left(T^{4}_{ext} - T^{4}_{space}\right) \tag{4.39}$$

Where ε is the emissitivity, δ is the Stephen Boltzmann constant, T_{space} is the space temperature (K), T_{ext} is the external area temperature (K) and is calculated by the following formula.

$$T_{ext} = T_{amb} + \varphi R_{conv} \tag{4.40}$$

By substituting the value of T_{ext} in Eq. (4.39), the total heat losses by radiations are calculated. By adding all the losses, the total losses of the system can be calculated.

4.5.3 Determination of natural convection co-efficient

The value of "h" depends on the characteristics of the fluid (air), geometry and position of the vessel and it is assumed. In order to calculate the actual values of natural convectional coefficients, the following equations are used (Jannot, 2003)

$$h_1 = \frac{Nu_1 \lambda_a}{L} \tag{4.41}$$

$$h_2 = \frac{Nu_2 \lambda_a}{L} \tag{4.42}$$

where

$$Nu_1 = 0.59\, Pr\, Gr^{0.25} \tag{4.43}$$

$$Nu_2 = 0.021\, Pr\, Gr^{2/5} \tag{4.44}$$

where *Pr* is Prandtl No.

$$Pr = \frac{C_a \mu_a}{\lambda_a} \tag{4.45}$$

where C_a is the air heat capacity (1009 J Kg^{-1} K^{-1}), μa is the dynamical viscosity of air (0.000020500 Pa s), λ_a is the thermal conductivity of air (0.0295 W m^{-1} K^{-1})
By substituting this value in Eq. (4.45), we get Pr = 0.7011694915

This value of Pr will remain constant as it comprises of only parameters regarding atmospheric air.
Also

$$Gr = \frac{2g(T_{ext} - T_{amb})\rho^2 L^3}{\mu^2 (T_{ext} + T_{amb} + 273.5)} \tag{4.46}$$

where T_{amb} is the air ambient temperature (20 °C), ρ is the density of air (1.050 Kg m^{-3})

By substituting the values of ρ, μ, T_{ext}, T_{amb} in Eq. (4.46), the value of *Gr* is calculated. Thereafter, the value of the product "*GrPr*" is calculated. In this way, the corresponding values of *C* and *m* are taken from the Table 4.4.

Table 4.4: Correlation coefficients for different parts of the vessels, Correlation for every fluid : $Nu = C(Gr\,Pr)^m$

Geometry	*GrPr*	*C*	*m*
Vertical wall and cylinder	10^4-10^9	0.59	1/4
	10^9-10^{13}	0.021	2/5
Horizontal cylinder	10^{-10}-10^{-2}	0.675	0.058
	10^{-2}-10^2	1.02	0.148
	10^2-10^4	0.850	0.188
	10^4-10^7	0.480	0.25
	10^7-10^{12}	0.125	0.33
Top side of a hot horizontal wall or bottom side of a cold horizontal wall	$2x10^4$-$8x10^6$	0.54	0.25
	$8x10^4$-10^{11}	0.15	0.33
Bottom side of a hot horizontal wall or top side of a cold horizontal wall	10^5-10^{11}	0.27	0.25

(Source: Adapted from Jannot, 2003)

By substituting the values of *Pr*, *Gr*, the value of *Nu* is calculated which further calculates the value of the external convective co-efficient (*h*). This value of "*h*" can not be calculated directly as it depends on T_{ext} which is calculated in Eq. (4.40) by using an assumed value of "*h*". This result is compared with the assumed value and iterative method is carried out until the assumed and calculated values become equal.

4.5.4 Parameters of the existing prototype of the distillation still

The distillation still is divided into five main sections depending on the geometry and heat application distribution. The parameters of the existing prototype are shown in Table 4.5.

Table 4.5 Input data for the existing prototype of solar distillation system

Parameters	Lateral part	Bottom		Top cover	
Geometric section	Cylindrical	Circular	Cylindrical	Cylindrical	Conical
Length (m)	0.78	-	0.120	0.050	*
Diameter (m)	0.40	0.40	0.40	0.38	0.38
Thickness (m)	0.002	0.002	0.002	0.002	0.002
λ-still (W/m°C)	15	15	15	15	15
Insulation	**	-	-	-	**
λ-insl (W/m°C)	0.4	-	-		0.4
λ-gi(W/m°C)	0.4				0.4
ε-still	0.94	0.94	0.25	0.25	0.25
ε-gi	0.35	-	-	-	0.35

* For conical part L_1=0.283 and L_2= 0.085 at 45° angle of cone

** Thickness of insulation used at 0.020, 0.040, 0.060, 0.080, 0.100 m with 0.001 mm GI sheets.

4.6 Mathematical model for the solar distillation system

The main purpose for this model is to predict the energy distribution at various sections of the existing solar distillation system as well as at varying set of conditions. The schematic diagram of solar distillation model is shown in Fig. 4.19.

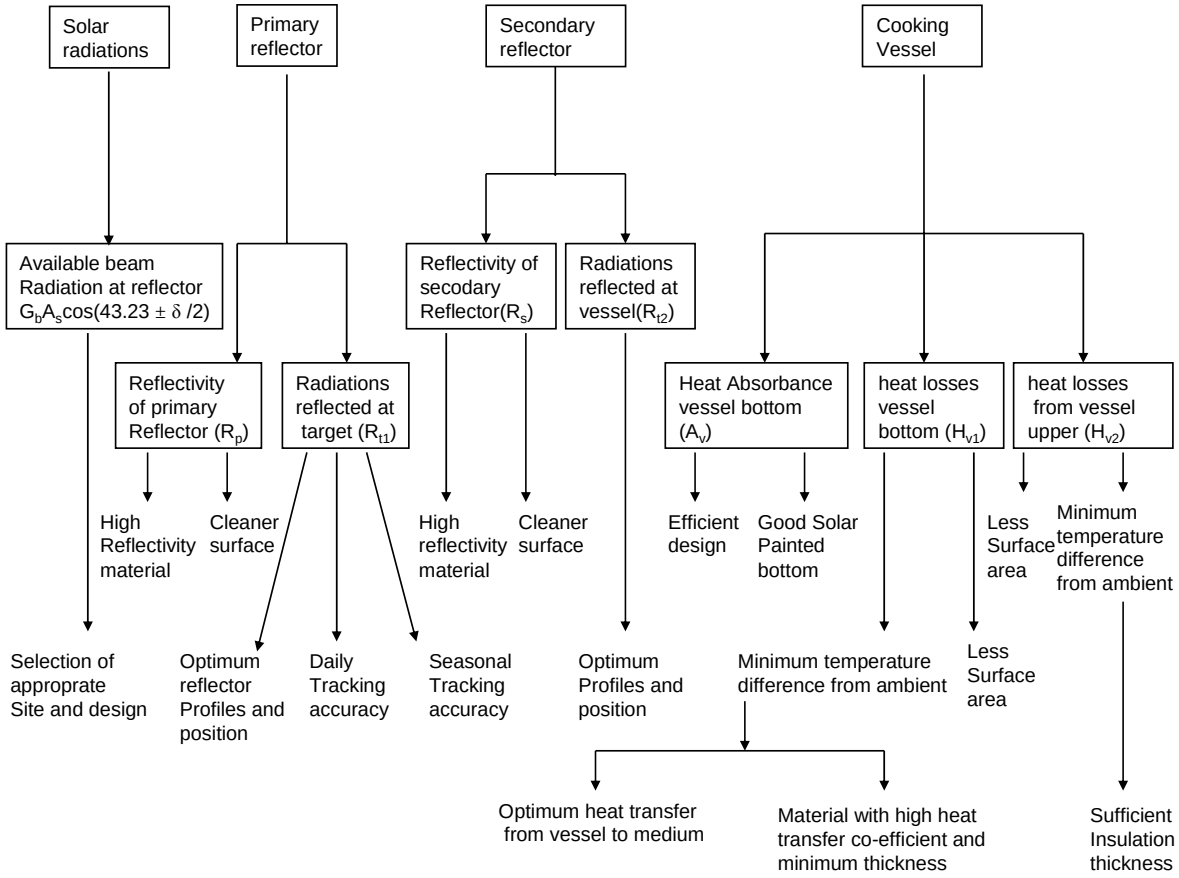

Figure 4.19: Description of the solar distillation model

All geometric considerations, variable parameters and ambient conditions were used to calculate the total heat losses for different parts of the distillation unit. This model is developed in Matlab 7 and some unusual symbols are used as per requirement of the program, so their protocols are defined. The model detail is given as under:

Distillation operating parameters

Tin = 100; Inside temperature of the distillation unit, °C
Tamb = 20; Ambient temperature, °C
Tspa = 15; Space temperature, °C
Emissivity
ua = 0.000020500; Dynamic viscosity of air, Pa.s
rho_a = 1.050; Air density, Kg /cu. m
Lam_a = 0.0295; Thermal conductivity of air, W/m°C
nu = 0.0000195238; Static viscosity of air,

Pr = 0.7011694915;

Part1 (circular)
Geometry
D1 = 0.4; External diameter, m
t1 = 0.002; Thickness, m
Thermal Parameters
Lam1 = 15; Thermal conductivity, W/mK
e1 = 0.940; Emissivity
Text1 = 150; External area temperature, °C
Calculations
Gr1 = (2/(2*273.15+Text1+Tamb)*9.81*(Text1-Tamb)*rho_a^2*D1^3)/ ua^2; Grashof number
PrGr1 = Pr*Gr1; Product of Prandtl and Grashof number
Nu1 = 0.27*PrGr1^(1/4); Correlation for the fluids
h1 = Nu1*Lam_a/D1; Natural convective coefficient (calculated), W/sq.m K
Rcond1 = t1/(Lam1*pi*D1^2/4); Conductive resistivity, K/W
Rconv1 = 1/(h1*pi*(D1)^2/4); Convective resistivity, K/W
Lcc1 = (Tin-Tamb)/(Rcond1+Rconv1);
Lr1 = e1*0.0000000567*pi*D1^2/4*((Text1+273.15)^4-(Tspa+273.15)^4); Losses due to radiation, W
Lt1 = Lcc1+Lr1; Total losses, W

Part 2 (cylindrical/bottom lateral)
Geometry
L2 = 0.120; Lateral length, m
D2 = 0.400; External diameter, m
t2 = 0.001; Thickness, m
Thermal Parameters
Lam2 = 15; Thermal conductivity, W/mK
e2 = 0.940; Emissivity
Text2 = 150; External area temperature, °C
Calculations
Gr2 = (2/(2*273.15+Text2+Tamb)*9.81*(Text2-Tamb)*rho_a^2*L2^3)/ ua^2; Grashof number
PrGr2 = Pr*Gr2; Product of Prandtl and Grashof number
Nu2 = 0.59*PrGr2^(1/4); Correlation for the fluids
h2 = Nu2*Lam_a/L2; Natural convective coefficient (calculated), W/sq.m K
Rcond2 =1/(2*pi* Lam2* L2)*log(D2/(D2-2*t2)); Conductive resistivity, K/W
Rconv2 = 1/(h2* pi *D2*L2); Convective resistivity, K/W
Lcc2 = (Tin-Tamb)/(Rcond2+Rconv2); Losses due to conduction and convection, W
Lr2 = e2*0.0000000567* pi *D2*L2*((Text2+273.15)^4-(Tspa+273.15)^4); Losses due to radiation, W
Lt2 = Lcc2+Lr2; Total losses, W

Part 3 (cylindrical without insulation)
Geometry
L3 = 0.780; Lateral length for part 3, m
D3 = 0.400; External diameter of part 3, m
t3 = 0.002; Thickness of part 3, m
Thermal Parameters
Lam3 = 15; Thermal conductivity of part 3, W/mK

e3 = 0.250; Emissivity of the distillation still of part 3
h3 = 7; Natural convective coefficient of part 3(assumed), W/sq.m K
Calculations
Rcond3 = 1/(2*pi*Lam3*L3)*log(D3/(D3-2*t3)); Conductive resistivity of part 3, K/W
Rconv3 = 1/(h3* pi *D3*L3); Convective resistivity of part 3, K/W
Lcc3 = (Tin-Tamb)/(Rcond3+Rconv3); Losses due to conduction and convection of part 3, W
Text3 = Tamb+Lcc3*Rconv3; External area temperature of Part 3 (calculated), °C
Lr3 = e3*0.0000000567* pi *D3*L3*((Text3+273.15)^4-(Tspa+273.15)^4); Losses due to radiation of part 3, W
Lt3 = Lcc3+Lr3; Total losses of part 3, W
Iteration
Gr3 = (2/(2*273.15+Text3+Tamb)*9.81*(Text3-Tamb)* rho_a ^2*L3^3)/ ua^2; Grashof number
PrGr3 = Gr3*Pr; Product of Prandtl and Grashof number for part 3
Iteration
nmax = 5; Maximum No. of Iterations
niter = 0;
while niter <= nmax
niter = niter + 1;
if PrGr3 <=1e9
Rcond3 = 1/(2*pi*Lam3*L3)*log(D3/(D3-2*t3)); Conductive resistivity of part 3, K/W
Rconv3 = 1/(h3* pi *D3*L3); Convective resistivity of part 3, K/W
Lcc3 = (Tin-Tamb)/(Rcond3+Rconv3); Losses due to conduction and convection of part 3, W
Text3 = Tamb+Lcc3*Rconv3; External area temperature of Part 3(calculated), °C
Lr3 = e3*0.0000000567* pi *D3*L3*((Text3+273.15)^4-(Tspa+273.15)^4); Losses due to radiation of part 3, W
Lt3 = Lcc3+Lr3; Total losses of part 3, W
Iteration
Gr3 = (2/(2*273.15+Text3+Tamb)*9.81*(Text3-Tamb)* rho_a ^2*L3^3)/ ua^2; Grashof number
PrGr3 = Gr3*Pr; Product of Prandtl and Grashof number for part 3
Nu3 = 0.59* (PrGr3)^(1/4); Correlation for the fluids for part 3
h3 = Nu3*Lam_a/L3; Natural convective coefficient for part 3(calculated), W/sq.m K
elseif PrGr3> 1e9
Rcond3 = 1/(2*pi*Lam3*L3)*log(D3/(D3-2*t3)); Conductive resistivity of part 3, K/W
Rconv3 = 1/(h3* pi *D3*L3); Convective resistivity of part 3, K/W
Lcc3 = (Tin-Tamb)/(Rcond3+Rconv3); Losses due to conduction and convection of part 3, W
Text3 = Tamb+Lcc3*Rconv3; External area temperature of part 3(calculated), °C
Lr3 = e3*0.0000000567* pi *D3*L3*((Text3+273.15)^4-(Tspa+273.15)^4); Losses due to radiation of part 3, W
Lt3 = Lcc3+Lr3; Total losses of part 3, W
Iteration
Gr3 = (2/(2*273.15+Text3+Tamb)*9.81*(Text3-Tamb)* rho_a ^2*L3^3)/ ua^2; Grashof number
PrGr3 = Gr3*Pr; Product of Prandtl and Grashof number for part 3
Nu3 = 0.021* (PrGr3)^(2/5); Correlation for the fluids for part 3
h3 = Nu3*Lam_a/L3; Natural convective coefficient of part 3(calculated), W/m^2K
end
end

Part 4 (cylindrical Junction)
Geometry
L4 = 0.041; Lateral length of part 4, m
D4 = 0.398; External diameter of part 4, m
t4 = 0.004; thickness of part 4, m
Thermal Parameters
Lam4 = 5; Thermal conductivity of part 4, W/mK
e4 = 0.250; Emissivity of the distillation still of part 4
h4 = 3.545; Natural convective coefficient of part 4 (assumed), W/sq.m K
Calculations
Iteration
nmax = 5;
niter = 0;
while niter <= nmax
Calculations
niter = niter + 1;
Rcond4 = 1/(2*pi* Lam4*L4)*log(D4/(D4-2*t4)); Conductive resistivity of part 4, K/W
Rconv4 = 1/(h4*pi*D4*L4); Convective resistivity of part 4, K/W
Lcc4 = (Tin-Tamb)/(Rcond4+Rconv4); Losses due to conduction and convection of part 4, W
Text4 = Tamb + Lcc4*Rconv4; External area temperature of Part 4 (calculated), °C
Lr4 = e4*0.0000000567* pi *D4*L4*((Text4+273.15)^4-(Tspa+273.15)^4); Losses due to radiation of part 4, W
Lt4 = Lcc4+Lr4; Total losses of part 4, W
Gr4 = (2/(2*273.15+Text4+Tamb)*9.81*(Text4-Tamb)*rho_a^2*L4^3)/ ua^2; Grashof number
PrGr4 = Pr*Gr4; Product of Prandtl and Grashof number for part 4
Nu4 = 0.59*PrGr4^(1/4); Correlation for the fluids for part 4
h4 = Nu4*Lam_a/L4; Natural convective coefficient of part 4 (calculated), W/m^{2}K
end

Part 5 (conical without insulation)
Geometry
D5a = 0.398; Diameter of bottom part of part 5
D5b = 0.05; Diameter of top part of part 5
L5a = D5a /2^0.5; Diameter of bottom part of part 5
L5b = D5b /2^0.5; Diameter of top part of part 5
t5 = 0.002; wall thickness of part 5
L5 = L5a-L5b; Length of cone of top cover
Thermal Parameters
Lam5 = 5; Thermal conductivity of part 3, W/mK
e5 = 0.250; Emissivity of the distillation still of part 5
h5 = 3.545; Natural convective coefficient of part 5 (assumed), W/sq.m K
Iteration
nmax = 5;
niter = 0;
while niter <= nmax
Calculations
niter = niter + 1;
Rcond5 = t5*2^(0.5)/(Lam5*pi*(L5a^2-L5b^2)); Conductive resistivity of part 5, K/W
Rconv5 = 1/(h5*pi*(L5a^2-L5b^2)); Convective resistivity of part 5, K/W

```
Lcc5 = (Tin-Tamb)/(Rcond5+Rconv5); Losses due to conduction and convection of part 5, W
Text5 = Tamb+Lcc5*Rconv5;% External area temperature of part 3(calculated), °C
Lr5 = e5*0.0000000567*pi*(L5a^2-L5b^2)*((Text5+273.15)^4-(Tspa+273.15)^4);  Losses due to radiation of part 5, W
Lt5 = Lcc5+Lr5; Total losses of part 5, W
Gr5 = (2/(2*273.15+Text5+Tamb)*9.81*(Text5-Tamb)*rho_a^2*L5^3)/ua^2; Grashof number
 PrGr5 = Pr*Gr5; Product of Prandtl and Grashof number for part 5
 Nu5 = 0.59*PrGr5^(1/4); Correlation for the fluids for part 5
 h5 = Nu5*Lam_a/L5; Natural convective coefficient of part 5(calculated), W/sq.m K
end
```

Part 3 (cylindrical with insulation)

```
Geometry
L3 = 0.780; lateral length of insulated still, m
D3 = 0.400; External diameter of still for part 3 to be insulated, m
t3 = 0.002; Wall Thickness of the still of part 3 to be insulated, m
for tt = 0.02:0.02:0.1;
 t3ins = tt; Insulation thickness used for part 3, m
t3gi = .001;
Thermal Parameters
Lam3 = 15; Thermal conductivity of the still for part 3 to be insulated, W/mK
Lamins = 0.040; Thermal conductivity of insulation for part 3, W/mK
Lamgi = 0.040; Thermal conductivity of galvanized iron sheet for part 3, W/mK
 egi = 0.350;  Emissivity of the Galvanized iron sheet for part 3
hgi3 = 13.545; Natural convective coefficient for galvanized iron part 3 (assumed), W/m2K
Iteration
nmax = 5;
niter = 0;
while niter <= nmax
Calculations
niter = niter + 1;
Rcond3ins = 1/(2*pi*Lamins*L3)*log((D3+2*t3ins)/D3); Conductive resistivity of insulated part 3, K/W
Rcond3gi = 1/(2*pi*Lamgi*L3)* log((D3+2*t3ins+2*t3gi)/(D3+2*t3ins)); Conductive resistivity of insulated part 3, K/W
Rconv3gi = 1/(hgi3*pi*(D3+2*t3ins+2*t3gi)*L3); Convective resistivity of insulated part 3, K/W
Lcc3ins = (Tin-Tamb)/(Rcond3+ Rcond3ins+ Rcond3gi+ Rconv3gi); Losses due to conduction and convection of part 3, W
Text3ins = Tamb+Lcc3ins*Rconv3gi; External area temperature of gi sheet with part 3
Lr3ins = egi*0.0000000567*pi*(D3+2*t3ins+2*t3gi)*L3*((Text3ins+273.15)^4 ...
              -(Tspa+273.15)^4); Losses due to radiation of insulated part 3, W
Lt3ins = Lcc3ins+Lr3ins; Total losses of insulated part 3, W
Gr3ins =  (2/(2*273.15+Text3ins+Tamb)*9.81*(Text3ins-Tamb)* rho_a ^2*L3^3)/ ua^2;
                    Grashof number for insulated part 3
PrGr3ins =  Pr*Gr3ins; Product of Prandtl and Grashof number for insulated part 3
Nu3ins = 0.59*PrGr3ins^(1/4); Correlation for the fluids for part 3
hgi3 = Nu3ins*Lam_a/L3; Natural convective coefficient of insulated part 3(calculated), W/m2K
end
```

Part 5 (Conical with insulation)
Geometry
D5a = 0.398; Diameter of bottom part of part 5 to be insulated
D5b = 0.05; Diameter of top part of part 5 to be insulated
L5a = D5a /2^0.5; Diameter of bottom part of part 5 to be insulated
L5b = D5b /2^0.5; Diameter of top part of part 5 to be insulated
t5 = 0.002;
t5ins = tt;
t5gi = 0.001;
Thermal Parameters
Lam5 = 15; Thermal conductivity of insulated part 5, W/mK
Lam5ins = 0.040; Thermal conductivity insulation for part 5, W/mK
Lam5gi = 0.040; Thermal conductivity of gi sheet for part 5, W/mK
e5gi = 0.350; Emissivity of the GI sheet part 5
h5gi = 3.545; Natural convective coefficient of part 5 insulated (assumed), W/m^2K
Iteration
nmax = 5;
niter = 0;
while niter <= nmax
Calculations
niter = niter + 1;
Rcond5 = t5*2^(0.5)/(Lam5*pi*(L5a^2-L5b^2)); Conductive resistivity of part 5 insulated, K/W
Rcond5ins = (t5ins*(2)^0.5)/(Lam5ins*pi*(L5a^2-L5b^2)); Conductive resistivity of insulated part 5 insulated, K/W
Rcond5gi = (t5gi*(2)^0.5)/(Lam5gi*pi*(L5a^2-L5b^2)); Losses due to conduction and convection of part 5 insulated, W
Rconv5gi = 1/(h5gi*pi*(L5a^2-L5b^2)); Convective resistivity of insulated part 5 insulated, K/W
Lcc5ins = (Tin-Tamb)/(Rcond5+Rcond5ins+Rcond5gi+Rconv5gi);
Text5ins = Tamb+Lcc5ins*Rconv5gi; External area temperature of Part 5 insulated (calculated), °C
Lr5ins = pi*(L5a^2-L5b^2)*egi*0.0000000567*((Text5ins+273.15)^4-(Tspa+273.15)^4); Losses due to radiations of part 5 insulated, K/W
Lt5ins = Lcc5ins+Lr5ins; Total losses of part 5 with insulation
Gr5ins = (2/(2*273.15+Text5ins+Tamb)*9.81*(Text5ins-Tamb)*rho_a^2*L5^3)/ ua^2; Grashof number for insulated part 5 insulated
PrGr5ins = Pr*Gr5ins; Product of Prandtl and Grashof number for insulated part 5 insulated
Nu5ins = 0.59*PrGr5ins^(1/4); Correlation for the fluids for part 5 insulated
h5gi = Nu5ins*Lam_a/L5; Natural convective coefficient of part 5(assumed), W/m^2K
Tgt = Lt1+Lt2+Lt3ins+Lt4+Lt5ins; Losses grand total with insulation
end

Complete Model (Solar distillation system)
Gb = 800; Beam radiations, $W\ m^{-2}$
Sp = 8.00; Surface area of primary reflector, m^2
n = 100; No. of day of the year
Rp = 0.87; Reflectivity of primary reflector
Ff = 0.85; Fraction available at targeted focus
Rs = 0.87; Reflectivity of secondary reflector
Fv = 0.95; Fraction available at targeted vessel

```
Av = 0.90; Absorbance of vessel
Lgt = Lt1+Lt2+Lt3ins+Lt4+Lt5ins; Grand total losses from vessel
decl = 180/pi*(0.006918-0.399912*cos(2*pi/365*(n-1))...
   + 0.070257*sin(2*pi/365*(n-1))-0.006758*cos(2*(2*pi/365*(n-1)))...
   + 0.000907*sin(2*(2*pi/365*(n-1)))-0.002697*cos(3*(2*pi/365*(n-1)))...
   + 0.00148*sin(3*(2*pi/365*(n-1))));  Solar declination
```

Energy distribution per unit time
For standing reflectors in the northern hemisphere

```
Ep1 = Gb*Sp*cosd(43.23+decl/2); Energy available at primary reflector, W
Epr1 = Ep1*Rp; Energy available after primary reflection, W
Es1 = Epr1*Ff; Energy available at secondary reflector, W
Esr1 = Es1*Rs; Energy available after secondary reflection, W
Ev1 = Esr1*Fv; Energy available at vessel surface, W
Eab1 = Ev1*Av; Energy available inside the vessel, W
Ed1 = Eab1-Lgt; Energy available for processing, W
Eff1 = 100*Ed1/Ep1; Efficiency of solar distillation system, W
```

For standing reflectors in the southern hemisphere

```
decls = - decl;
Ep2 = Gb*Sp*cosd(43.23+decls/2); Energy available at primary reflector, W
Epr2 = Ep2*Rp; Energy available after primary reflection, W
Es2 = Epr2*Ff; Energy available at secondary reflector, W
Esr2 = Es2*Rs; Energy available after secondary reflection, W
Ev2 = Esr2*Fv; Energy available at vessel surface, W
Eab2 = Ev2*Av; Energy available inside the vessel, W
Ed2 = Eab2-Lgt; Energy available for processing, W
Eff2 = 100*Ed2/Ep2; Efficiency of solar distillation system, W
```

Power Losses at different points
For standing reflectors in the northern hemisphere

```
Lpr1 = Ep1-Epr1; Losses due to reflectivity of primary reflector, W
Lpf1 = Epr1-Es1; Losses due to focus not at target of primary reflector, W
Lsr1 = Es1-Esr1; Losses due to reflectivity of secondary reflector, W
Lsf1 = Esr1-Ev1; Losses due to focus not at target of secondary reflector, W
Lab1 = Ev1-Eab1; Losses due to vessel heat absorption inefficiency, W
Lgt1 = Lgt; Losses due to vessel heat losses
```

For standing reflectors in the southern hemisphere

```
Lpr2 = Ep2-Epr2; Losses due to reflectivity of primary reflector, W
Lpf2 = Epr2-Es2; Losses due to focus not at target of primary reflector, W
Lsr2 = Es2-Esr2;   Losses due to reflectivity of secondary reflector, W
Lsf2 = Esr2-Ev2; Losses due to focus not at target of secondary reflector, W
Lab2 = Ev2-Eab2; Losses due to vessel heat absorption inefficiency, W
Lgt2 = Lgt;
end
```

The above mentioned model can be run on a specific day for the existing size of solar distillation system under the site specific parameters of Witzenhausen, Germany, (Latitude, 51.3°) by substituting the number of day of the year. The algorithm is developed

in generalized form and can be run for any set of variable parameters of the solar distillation system. This model can be used to predict the energy distribution and losses per unit time from the different components of the solar distillation system. Energy losses per unit time at different insulation thicknesses of the distillation still can also be calculated (CD is provided with the manuscript).

4.7 Output of the mathematical model for the solar distillation system

Under the available parameters and specification of the solar distillation prototype on Aug, 31 with beam radiations 800 W m^{-2}, out put of the mathematical model for the energy distribution in the solar distillation system is shown in Figure 4.20.

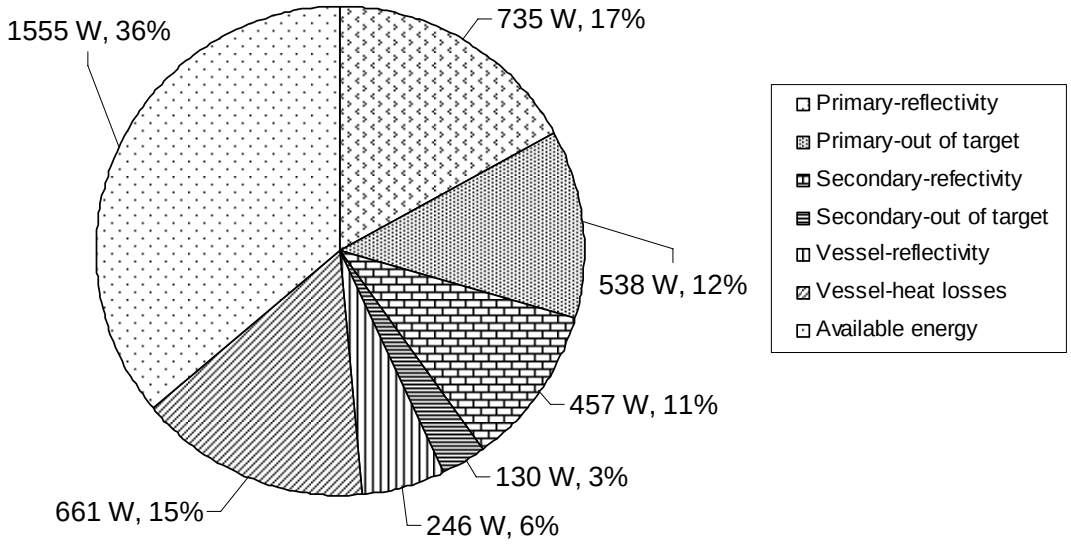

Figure 4.20: Predicted values of energy distribution per unit time from solar distillation system (for the standing reflectors in the northern hemisphere on Aug, 31 for 800 W m^{-2})

Figure 4.20 shows the heat energy losses and available energy from the existing prototype. This model can be run during any day of the year all over the world. In the present input data set, the solar distillation model is run in Witzenhausen on Aug, 31 2008 with average beam radiations 800 W m^{-2} under similar conditions. The heat energy losses per unit time (W) due to the lack of reflectivity from the primary reflector, radiations reflected out of the targeted area, lack of reflectivity from the secondary reflector, radiations reflected from secondary reflector out of the targeted distillation bottom, vessel reflectivity, and vessel heat losses (in the form of conduction, convection and radiations by

using 60 mm insulation thickness) are found to be 735, 538, 457, 130, 246 and 661 W respectively. Their corresponding percentage losses are found to be 17, 12, 11, 3, 6, 15 % respectively. The available energy for the distillation process is found to be 1555 W (36 %). In terms of components of solar distillation system, the heat losses from the primary reflector, secondary reflector, and distillation still are found to be 1273 watts, 587 and 907 W with their percentage 29, 14 and 21 % respectively. This model can be applied in the northern hemisphere under the existing condition of the plant. However, the values of beam radiations will be different at different latitudes. For southern hemisphere, the model is run under the same conditions as done for the northern hemisphere and the results obtained are shown in Figure 4.21.

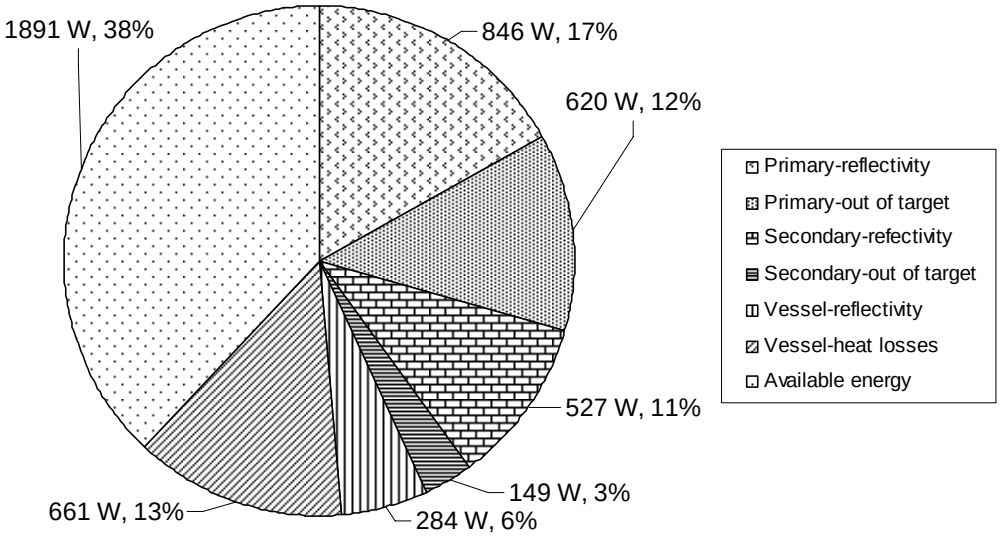

Figure 4.21: Predicted values of energy distribution per unit time from solar distillation system (for the standing reflectors in the southern hemisphere on Aug, 31 for 800 W m^{-2})

The heat energy losses per unit time (W) due to the lack of reflectivity from the primary reflector, radiations reflected out of the targeted area, lack of reflectivity from the secondary reflector, radiations reflected from secondary reflector out of the targeted distillation bottom, vessel reflectivity, and vessel heat losses (in the form of conduction, convection and radiations by using 60 mm insulation thickness) are found to be 846, 620, 527, 149, 284 and 661 W respectively. Their corresponding percentage losses are found to be 17, 12, 11, 3, 6, 13 % respectively. The available energy per unit time for the distillation process is found to be 1891 W (38 %). In terms of components of solar

distillation system, the heat losses from the Primary reflector, secondary reflector, and distillation unit are calculated to be 1466 watts, 676 and 945 watts with their percentage 29, 14 and 19 % respectively. By comparing Figures 4.20 and 4.21, it is evident that the heat losses and available energy are different under the same conditions of parameters except the heat losses from the distillation still (conduction, convection and radiation). This is due the fact that the aperture areas of the Scheffler reflector are different on the same day in northern and southern hemisphere. The constant heat losses from the distillation unit indicate that the same size of the distillation unit will have the same losses when operated under similar working temperature and ambient conditions.

The complete losses distribution from the distillation still with different insulation thickness (0.020, 0.040, 0.060, 0.080, and 0.100 m) and without insulation is shown in Figure 4.22 and also given in appendix C.

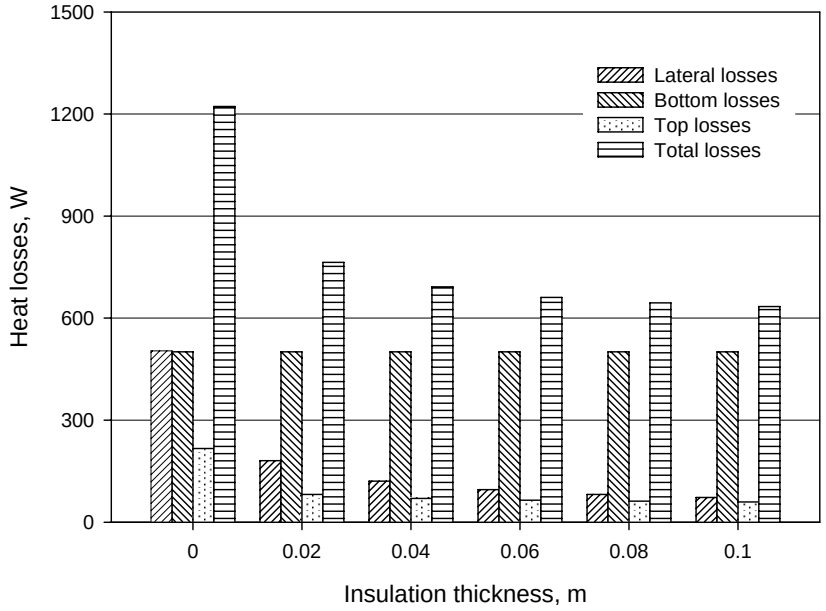

Figure 4.22: Predicted values of heat losses from the distillation still at different insulation thicknesses

These losses were calculated for lateral part, bottom part, and top cover as well as from total distillation still. The results showed that there was no significant decrease in heat losses by increasing the insulation thickness beyond 60 mm. By taking into consideration the economic benefits and easy handling (due to less weight and volume), the distillation unit was insulated with 60 mm rockwool covered by 2 mm galvanized iron (GI) sheets.

Infrared camera was also used during the optimization of solar distillation system. Heat losses from the distillation still (in the form of conduction, convection and radiations) were reduced from 1222 to 661 Watts under operating conditions of the distillation system. Out of these losses, 501 Watts are from the part exposed to solar radiations are constant as shown in the Fig. 4.22. So, the heat losses were reduced from 721 watts to 160 watts by using 60 mm rockwool insulation. Here it is worth mentioning that thermal conductivity of stainless steel is poorer than normal steel and copper. But selection of food grade Stainless steel was the first priority for good quality of essential oils. The heat losses from the distillation still are shown in Fig. 4.23.

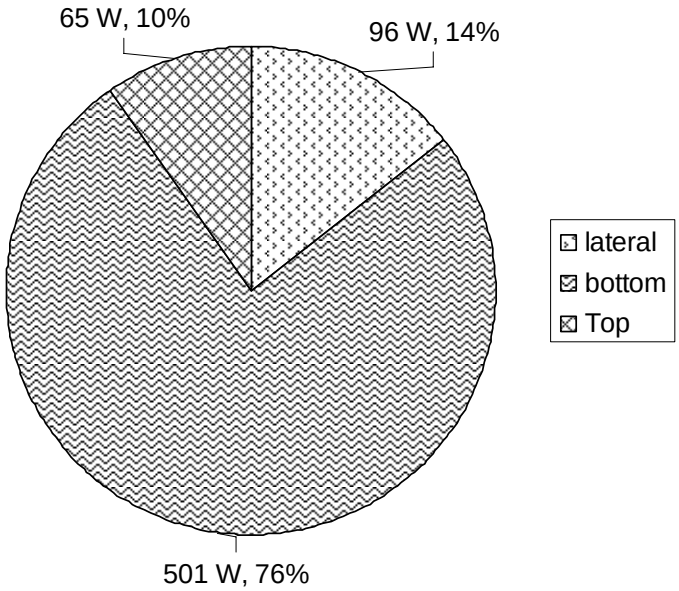

Figure 4.23: Heat losses at different parts of the distillation still

Fig. 4.23 shows that heat energy losses from bottom, lateral and top part are 501, 96 and 65 W respectively for 60 mm insulation thickness. It is also evident from Fig. 4.23 that 76 % losses are from the bottom part which is not insulated and exposed to the solar radiations. The study reveals that significant amount of heat energy can be saved which can be used to run the distillation process. This is possible by producing greenhouse effect or exposing less area of the distillation still to the atmosphere.

Energy available for the solar distillation system

The graphical presentation of total energy available at the primary reflector and energy available for the processing of the plant materials against different beam radiations (for the standing reflectors in the northern hemisphere) is shown in Fig. 4.24.

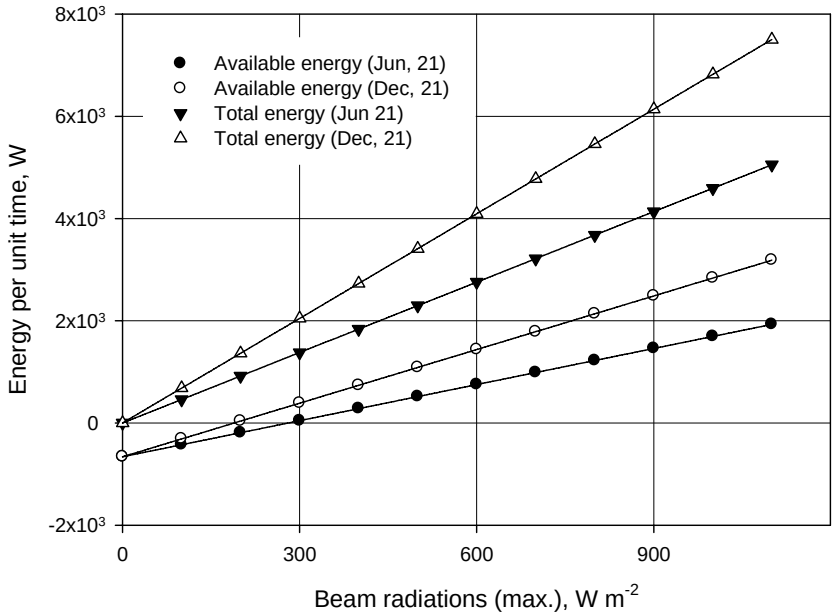

Figure 4.24 Total energy available (modeled values) at the primary reflector and for the distillation process on June 21 and December 21 against different beam radiations (for the standing reflectors in the northern hemisphere)

Fig. 4.24 shows that the total energy available on the primary reflector for an 8 m^2 Scheffler reflector increases with the increase in beam radiations. The slope for winter curve (Dec, 21) is steeper as compared to that of summer (June 21). At 1100 W m^{-2} beam radiations, power available at the primary reflector for summer (June 21) and winter (Dec, 21) were found to be 5053 and 7503 W respectively for standing reflectors in the northern hemisphere. Curves were also drawn for the available energy for the solar distillation system versus beam radiations. With the same intensity of beam radiation, the power available for the distillation process for summer (June 21) and winter (Dec, 21) were found to be 1929 and 3186 W respectively. These curves cut the x-intercept at 281 and 189 W m^{-2} beam radiations for summer (June, 21) and winter (Dec, 21) respectively. These x-intercept values indicate the minimum beam radiations required to start the distillation process for the existing prototype. If these curves are extrapolated towards the negative values of power, both of these curves cut the y-intercept at -661 W. In fact, 661 W are the constant heat losses from the distillation still when the distillation process is in operation at

100 °C. The results of solar distillation model provide useful information to predict the total energy available on the reflector and energy available for the distillation process against a wide range of beam radiations.

4.8 Performance evaluation of the solar distillation system

The principal expression for the efficiency calculation of solar distillation system is given below

$$System\ efficiency\ (\eta\ \%) = \frac{10^3 E_p}{\int_{t=0}^{t_p} Gb_{ave}\ A_s\ dt} 100 \tag{4.47}$$

Where E_p is the total heat energy during distillation process, t is the time during the distillation process, Gb_{ave} is the beam radiation at time t, A_s is the aperture area of the Scheffler reflector.

The total heat energy (E_p) during distillation process of herbs in kWh can be calculated by the following expression

$$E_p = \frac{\left[(m_w + M_w m_h) c_w + m_h (1 - M_w)\, c_f\right] \Delta T + x\, m_s\, h_{fg}}{3600} \tag{4.48}$$

where m_w is the mass of water used in the still ($m_w \geq 15$ kg, volume equivalent to the bottom area of the distillation still exposed to solar radiation), M_w is the moisture content of herbs (wet basis), m_h is the mass of herbs, ΔT is the change in temperature, c_w is the specific heat of water at constant pressure, m_s is the mass of steam produced, h_{fg} is the latent heat of vaporization (2260 kJ kg^{-1} for water at atmospheric pressure), c_f is the specific heat of fiber, x is the dryness fraction of steam.

Determination of dryness fraction

The values of dryness fraction are used to evaluate the system during the steam generation phase. The calorimeter with mass 0.0818 kg is insulated on all sides to reduce the heat losses and a thermometer is fixed on the top side to record temperature. An insulated pipe connects the top of the distillation still to the barrel calorimeter to take the steam sample. Steam is injected into 0.5 kg water sample in the barrel calorimeter. The

weight of steam added and rise in temperature are recorded when the steady state temperature of water in the calorimeter is reached. The principal formula for the dryness fraction, x, is given by Khurmi & Gupta (2005)

$$x = \frac{(m_{wc} + m_c c_c)(T_{2c} - T_{1c})}{m_{sc} h_{fg}} - \frac{c_w (T_s - T_{2c})}{h_{fg}} \tag{4.49}$$

Where m_{wc} is the mass of water in calorimeter, c_w is the specific heat of water, m_c is the mass of calorimeter, c_c is the specific heat of the calorimeter, T_{2c} is the final temperature of water and calorimeter, T_{1c} is the initial temperature of water and calorimeter, m_{sc} is the mass of steam added in the calorimeter, T_s is the temperature of steam formation at pressure P, h_{fg} is the latent heat of vaporization of water.

The mass and specific heat of the calorimeter for the existing distillation system are 0.818 kg and 0.45 kJ kg^{-1} K^{-1} respectively. For the determination of dryness fraction, 0.5 kg of water is taken in the calorimeter. The latent heat of vaporization of water at atmospheric pressure is taken as 2260 kJ kg^{-1}. Eq. (4.49) is simplified by designating these constant values under the operating conditions of the solar distillation unit and is rewritten as:

$$x = \frac{C_1 (T_{2c} - T_{1c})}{m_{sc}} - C_2 (T_s - T_{2c}) \tag{4.50}$$

where C_1 and C_2 are constants for the barrel calorimeter used during distillation experiments and are calculated to be 0.00094 and 0.00185 respectively.

In order to evaluate the performance of the solar distillation system by using herbs during small time intervals, the above equation can be re-written as:

$$E_p = C_3 \sum_{i=1}^{p} \Delta T_i + C_4 \sum_{j=1}^{q} x_j m_{sj} \tag{4.51}$$

where C_3 and C_4 are constants for the particular batch during solar distillation experiments.

The values of C_3 and C_4 are given as:

$$C_3 = \frac{(m_w + M_w m_h)c_w + m_h(1 - M_w)c_f}{3600}$$

$$C_4 = \frac{h_{fg}}{3600}$$

(C_4 =0.62777 at atmospheric pressure)

The former part of Eq. (4.51) gives the sum of total sensible heat energy (taken in small intervals ranging from the start of the experiment to reaching boiling point “p”) and the latter part of the equation gives the sum of total latent heat energy (taken in small intervals starting from the first interval of steam generation to the last interval of steam generation “q” where the distillation experiment is stopped).

Funk (2000) described the procedure for evaluation of different types of solar concentrators. He explained that the influence of test conditions on results can be minimized if uncontrolled variables are held to certain ranges. He used water for the evaluation of the cookers in terms of power. For the performance test with water only, Eq. (4.51) can be used with $C_3 = m_w c_w/3600$ for water only. The average power available, P_{ave}, during the experiment is given as

$$P_{ave} = \frac{E_p}{t_p} \tag{4.52}$$

where t_P is the total process time of the distillation experiment

Several experiments were carried out to evaluate the performance of the system under field conditions. Within the beam radiation range of 700-800 W m^{-2}, the temperature available at the focus was found to be between 300-400 °C. Scheffler (2006) showed that about half of the solar power collected by the reflector becomes finally available in the cooking vessel. Details of one performance evaluation of the solar distillation system with 20 l of water on August 31, 2008 from 9:06 to 16:00 hour (test duration = 5.9 hour) are shown in Fig. 4.25.

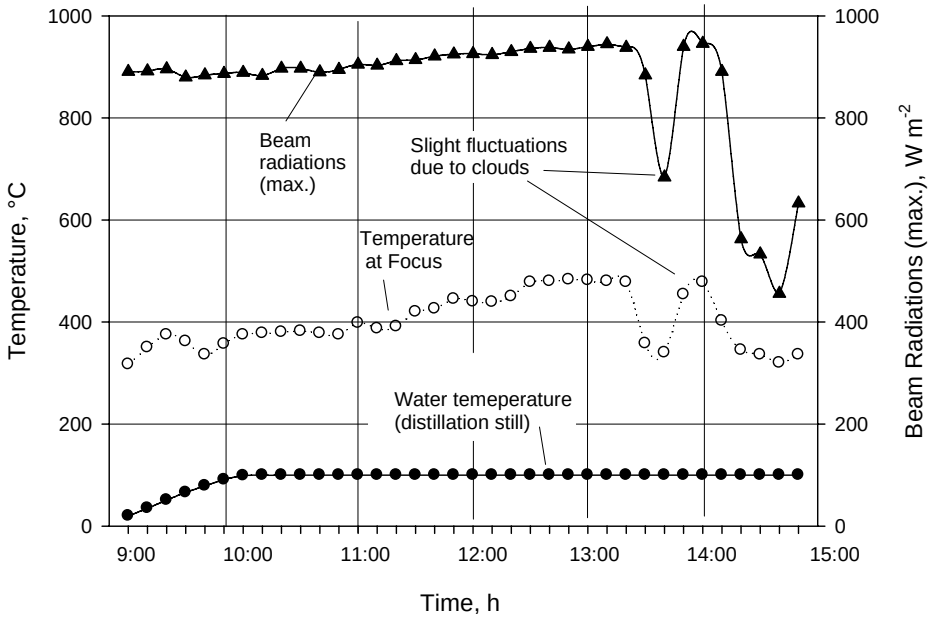

Figure 4.25 Performance evaluation of solar distillation system (on Aug, 31 2008 with 20 liters of water, 30 readings averaged)

The graph shows the variation of beam radiation, focal point temperature and the process temperature versus time. It is evident from Fig. 4.25 that within the defined range of beam radiation, the temperature at the focus is effectively constant. This shows that beam radiations are converging at the targeted focus with the changing position of the sun during the test period. From these results we conclude that the PV tracking system, axis of rotation and profiles of primary reflector have been designed sufficiently precisely. It is also clear from Fig. 4.25 that the temperature of the distillation process is well below the temperature at the focal point. This temperature gradient can be used successfully for all types of distillation processes. Fig. 4.25 shows that there is no effect on the distillation process during the slight fluctuation due to clouds. During this test, the total energy gained by the water (in sensible and latent heat phase) was calculated to be 9.136 kWh. The average power and system efficiency were found to be 1.548 kW and 33.21 % respectively at an average beam radiations of 863 W m^{-2} using Eq. (4.47) and Eqs. (4.50) - (4.52). Infrared camera was also used to evaluate the performance of the system. Two infrared photos of the bottom and top part of the solar distillation still are shown in Figure 4.26.

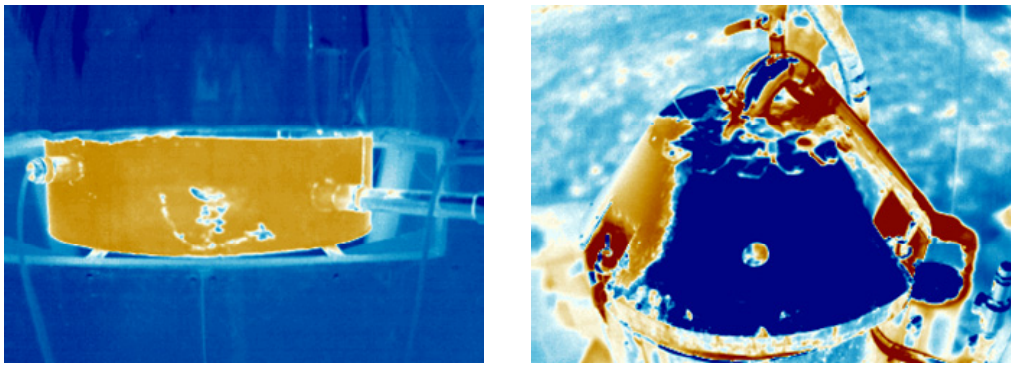

Bottom part of the still Top part of the still

Figure 4.26: Infrared photos of the bottom and top part of the solar distillation still

4.9 Evaluation of Scheffler reflector by steam receiver

In the present study, a receiver was also used to produce steam for solar-based steam distillation system. The material of the receiver was cast aluminium and has 350 mm diameter and 55 mm lateral length. The inner surface of the receiver composed of fins to increase the surface area for better heat transfer to the medium and an 8 mm thick plate was used to seal the receiver. Moreover, this receiver was also used for water boiling tests to evaluate the system. All these tests were conduced at atmospheric pressure. The tests were conducted on 31-08-09 and 01-09-09 with aperture areas of Scheffler reflector as 5.40 and 5.42 m^2 respectively. Experiments were carried out to check the performance of the solar system by using secondary reflector and without secondary reflector for water and steam trials. In order to evaluate the performance of primary reflector only, the trials were made by setting the center of receiver (black side) at the exact focus point “F” with its face adjusted perpendicular to the axis of rotation as shown in Fig. 4.27

For water tests, the receiver was filled with water to avoid from overheating (as the maximum temperature recorded up to 500 °C by the thermocouple installed at focus). For this purpose, the level of water outlet pipe was raised with respect to water inlet pipe to avoid overheating due to lack of water. A constant water flow rate was maintained and the inlet and outlet temperatures were recorded continuously. These tests were conducted to maintain the outlet temperature approximately constant. The experiment starting time was noted when the average temperature of the receiver and outlet flow was reached. The heat losses from the system were not taken into consideration in these trials. In each test, time was noted to fill 10 liters (kg) of water.

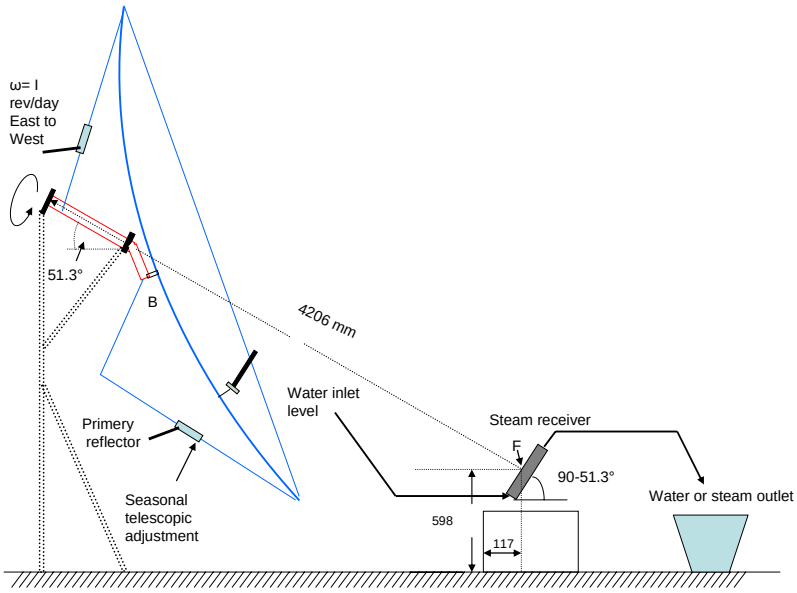

Figure 4.27: Details of steam receiver installation for the evaluation of Scheffler reflector

The beam radiations were recorded with pyranometer (Type SP Lite: response time < 1 S) simultaneously installed at primary reflector. In order to evaluate the system with the use of secondary reflector, trials were conducted by placing the receiver horizontally on the frame of secondary reflector like other cooking vessels. The other procedure and precautions were the same as discussed previously. The experimental set up during the trials is shown in Fig. 4.28

For primary reflector For primary & secondary reflector

Figure 4.28: Experimental set up of the steam receiver with and without secondary reflector

Similarly, steam tests were carried out with and without secondary reflector. In this case, the water added is measured from the inlet side and these trials were conducted with 2 liters of water. All experiments were conducted in three replications. The results for water

tests and steam tests are shown in Fig. 4.29 and are also given in Appendix “D” (Table 1 to 5)

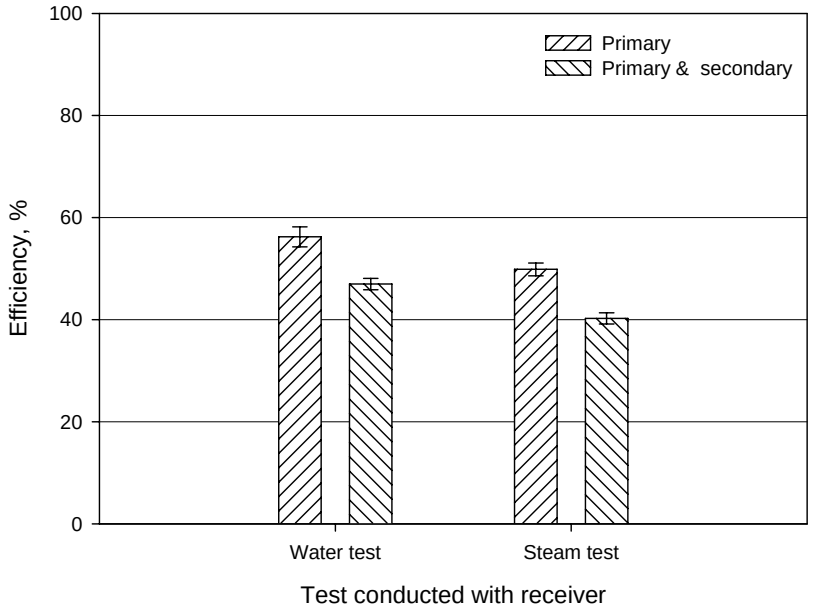

Figure 4.29: Detail of water and steam tests with and without secondary reflector

It is evident from Fig. 4.29 that system efficiency was found to be 47 % and 56 % with secondary and without secondary reflector while performing the water trials. However, the system efficiencies of the system for steam generation with “primary” and “primary & secondary” were found to be 49.8 and 40 % respectively. Lower values of standard errors and coefficient of variance for all the experiments show the consistency of the results. It can be concluded that about 9-10 % efficiency is lost by using the secondary reflector. Nevertheless, the importance of using the secondary reflectors for distillation or other cooking experiments to match the standards of cooking and distillation can not be ignored. The aluminium receiver is an efficient way for hot water and steam generation with continuous flow of water.

4.10 Essential oil extraction by solar distillation

On-farm distillation of medicinal and aromatic plants using solar energy provides an excellent opportunity to process fresh herbs for pure natural essence by using optimum harvesting time. Scheffler reflector was evaluated and then the distillation experiments were started. The distillation experiments were conducted during summer 2007, 2008 and 2009. At the beginning of 2008, the system was modified on the basis of results obtained

in 2007. The modified solar distillation system was evaluated during summer 2008 and 2009. For distillation experiments, the fresh herbs were harvested from the university farms located very near to the solar distillation system and dry herbs were purchased from the local market. Some of the medicinal plants like Melissa and Rosemary were used from the tropical green houses of the University of Kassel, Witzenhausen. In this way, the distillation system was evaluated with different kinds of medicinal and aromatic plants. Process heat energy consumption for different plant materials were calculated from the sensor system installed. In order to record data in steam generation phase, quantity of distillate (kg) and essential oils extracted (ml) were recorded with a regular interval of 10 minutes till end of the process. Beam radiations, water and steam temperatures, and temperature at focus were automatically recorded in the computer by data logger after 10 second pre-set interval. Different medicinal and aromatic plants (Melissa, Peppermint, Lavender, Fennel, Rosemary, Cumin, Basil and Cloves, Lavender etc) were processed successfully by solar distillation system (Munir & Hensel, 2007; Munir & Hensel, 2008; Munir & Hensel, 2009). The detail of some of the plant materials is gives in Table 4.6.

Table 4.6: Heat energy consumed and essential oil extracted during solar distillation of different plant material

Plant material	Part used	Weight, kg	Moistures contents (wb), %	Heat energy, kWh	Essential oil extracted, ml	Essential oil per unit plant d.m, ml kg^{-1}
Melissa	Leaves	11.6	78	3.868	1.425	0.558
Peppermint	leaves	9.1	74	3.180	28.2	11.918
Rosemary	leaves	3.0	72	4.626	4.6	5.476
Cumin	seeds	1.2	9	8.910	12.4	11.355
Cloves	buds	0.8	11	7.744	44	61.798

Table 4.6 shows the solar distillation experiments with different plant materials (Melissa, Peppermint, Rosemary, Cumin and Cloves) conducted by using different weights having different moisture contents. The heat energy consumed, essential oils extracted and essential oil obtained per unit weight of dry matter (d.m) were recorded for each experiment. The results show that different plant materials have different amounts of oils per unit dry matter. In these experiments, Melissa, Peppermint, and Rosemary plants were processed by using their leaves, Cumin plant by using seeds and Cloves plant by using buds. Under practical conditions, these specific parts of the plant materials are used for

the extraction of essential oils. These results show that the solar distillation system can also be used for the processing of different parts of the medicinal and aromatic plants.

Distillation experiments with solar based system and laboratory units were conducted simultaneously using the same plant material for comparison. In laboratory experiments, the essential oil extracted per unit weight of dry matter for Melissa, Peppermint, Rosemary, Cumin, and Cloves were found to be 0.614, 12.462, 5.786, 11.879 and 61.798 ml kg^{-1} respectively. The results show that the amounts of essential oils extracted per unit weight of dry matter by solar distillation system were found almost equal to that extracted by laboratory distillation. The study reveals that the solar energy can be successfully utilized for the solar distillation system. The distillation curves for percent of total oil extracted against heat energy (kWh) are shown in Fig. 4.30.

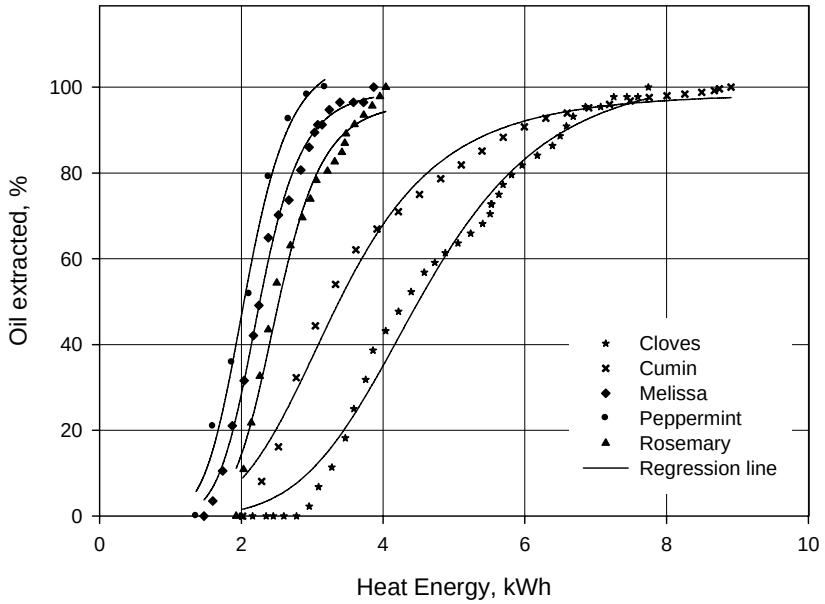

Figure 4.30: Experimental (dotted) and regression curves for percentage of essential oils extracted against different heat energy during solar distillation

The first experimental value for each herb indicates the sensible heat energy (kWh) required up to boiling point on the energy axis. Thereafter, the generated steam passes through the plant material and essential oil is separated by the process of diffusion. The experiments were carried out over a longer period (greater total energy input) than shown on the graph to observe further extraction of essential oils. For each experiment, there is a

specific energy level at which close to 100 % of essential oil is extracted as shown in the Fig. 4.30. Regression analysis was performed to fit the appropriate model for the percentage of oil extracted against heat energy required for the distillation process. The best fitted regression model for all plant materials was found to be the sigmoid/logistic curve as shown in Eq. (4.53)

$$y = \frac{k}{1+\left(\frac{z}{z_o}\right)^{l}} \tag{4.53}$$

where y and z are the variables of the regression model, k, l, z_o are the coefficients of regression model. The coefficients of the regression equation for different herbs are given in Table 4.7.

Table 4.7: Coefficient of determination (R^2) and coefficient of regression model for different herbs

Plant material	Coefficient of determination (R^2)	Coefficients of regression model		
		k	l	z_o
Peppermint	0.9906	107.5422	-6.7679	2.0809
Melissa	0.9954	99.2624	-7.5781	2.2566
Rosemary	0.9805	96.6695	-7.7536	2.5070
Cumin	0.9860	98.7476	-4.5420	3.3591
Cloves	0.9876	104.0522	-5.0884	4.5683

The reliability of the developed model was evaluated by comparing the experimental and predicted curves. The model fitted the results well as indicated by high values of coefficient of determination (R^2). A sigmoid curve is produced by a mathematical function having an "S" shape. Sigmoid function refers to the special case of the logistic function and is often used to introduce nonlinearity in the model within a specified range. These processes display a dependent progression from small beginnings that accelerates and approaches a climax over time. These results show that the higher oil extraction rates at the start of the distillation process and lower extraction rates towards the end of the process. It is also evident from Fig. 4.30 that the fresh plant materials complete the process at lower energy inputs than dry herbs. The low energy consumption for fresh herbs provides an opportunity to process more batches at farm level and hence justifying the on-farm installation of solar distillation system.

In addition to these five experiments shown in Table 4.6, many experiments were conducted with Melissa and Peppermint as a plenty of these plant materials were available at the experimental farms near solar distillation system. In summer seasons, the solar distillation system can be operated for 12 hours a day from 08:00 hours to 20:00 hours. In section 4.8, the average power and system efficiency were found to be 1.548 kW and 33.21 % respectively during a sunny day. About 18.58 kWh energy can be obtained for processing under similar conditions during 12 hours in one day. In several experiments, total energy consumptions for the processing of 10 kg batch of Melissa and Peppermint were recorded to be from 3 to 4 kWh. Therefore, 4-5 batches with 10 kg plant material were processed successfully using fresh herbs. These figures show the potential of solar distillation system during sunny days at the installed site.

The solar distillation unit behaves simultaneously as a boiler for the generation of steam as well as provides necessary column height for easy and simple oil condensation when used on the farm. The safety mountings and the instrumentation provide useful information to run the unit safely. The present research work was carried out using an 8 m^2 surface area of the solar concentrator which corresponds to 400 mm diameter for the distillation still. The capacity of the solar distillation system can be enhanced by increasing the solar concentrator area and other components of the distillation unit accordingly. This solar renewable energy technology is free of operational costs, environmental friendly and provides an excellent opportunity for on-farm processing of medicinal and aromatic plants.

A large number of experiments were conduced by using the solar distillation system. The detail of some of the plant materials are given below.

4.10.1 Distillation experiments with Lemon Balm (*Melissa officinalis L*.)

Lemon Balm (*Melissa officinalis L*.) is important due to its medical properties and its use as tea. Its essential oil is required mainly in the pharmaceutical, food and cosmetic industries. The properties of the plant extracts include sedative, relaxing, antibacterial, antiviral, and antipasmotic effects (Ayanoglu, 2005; Heeger, 1980). The main components of the essential oil are citral, citronellal and linalool. By means of gas chromatography studies of the essential oil, 70 components are known (Basta, 2005; Blum, 2005; Bomme, 2001). The lemon balm has low essential oil content ranging from 0.05 and 0.12 % volume (Basta, 2005).

Beside the solar campus, huge quantities of different herbs and medicinal plants have been planted in the University of Kassel experimental farms (one hectare area), Witzenhausen, Germany. Among all these plants, Mellissa was one of the most extensive planted medicinal plants for the research purposes on drying and distillation. Moreover, Melissa remained available during the entire period of research in the tropical green house to conduct experiment during winter season. A large number of distillation experiments were conducted with Lemon Balm (variety Citronella) during 2007, 2008 and 2009 to evaluate the performance of the solar distillation system.

These experiments were conducted with fresh, dry, and chopped Mellissa. In the experiments for fresh Melissa, 10 kg batches of fresh Melissa were taken (at 78 % moisture contents with ± 2 % variation) and they were processed just after harvesting. In order to conduct experiments with dried Melissa, 10 kg Melissa on fresh weight basis (same weight was used as for fresh experiments) were dried in the solar tunnel dryer (Hohenheim design) under optimum conditions, the design of solar tunnel drier is shown in Appendix E. The drying was carried out until a moisture content of 10 % was achieved (Cuervo & Hensel, 2008). Experiments were also conducted with chopped Melissa to increase the bulk density and to break the walls of the plants to increase the exposed surface area of the plant material. In some experiments, chopping was also done with the help of chopping machine to increase the preparatory index. The risk of losing considerable amount of essential oil exists while chopping the plant material (Öztekin & Martinov, 2007). For this purpose, the chopping was done carefully to avoid the volatile losses from the plant material into the open atmosphere. The process curves were drawn for fresh, dried and chopped Melissa with solar distillation system as shown in the Fig. 4.31.

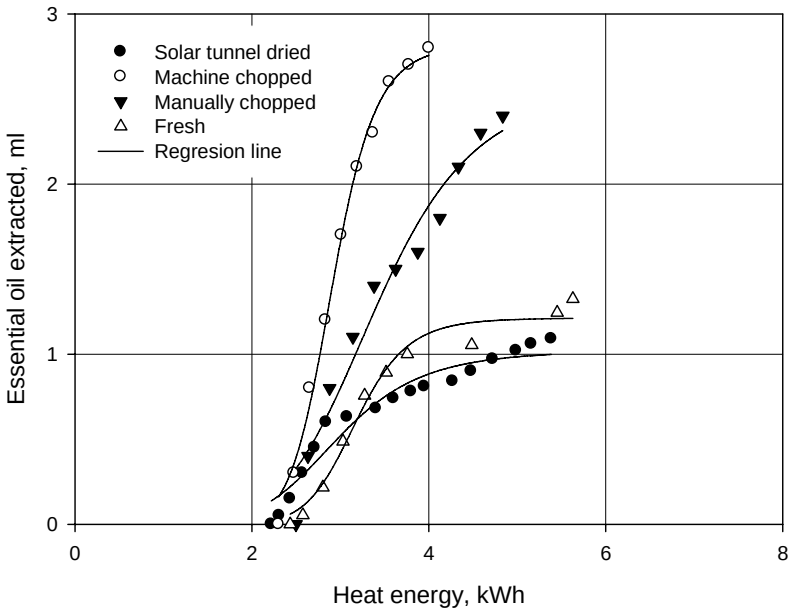

Figure 4.31 Process curves for fresh, dry and chopped Lemon Balm (*Melissa officinalis*) (10 kg batch)

It is evident from Fig. 4.31 that essential oil extraction rate for all types of curves is at faster rate at the start of the experiment and becomes slower towards the end of the processes. In conventional distillation units, the heat energy and steam generation is maintained constant as they are operated by regular sources of heat energy. Standard distillation curves are plotted for essential oil extracted (volume basis or percentage of total oil basis) versus time. These curves starts oil extraction at faster rate and then slower at the end (Dürbeck, 1997; Öztekin & Martinov, 2007; Denny, 1991). Melissa gave complete distillation in 30 minutes after the start of steam generation (Anonymous, 1998). The results obtained from the solar distillation system also give the same trends. In solar distillation, these curves are drawn for essential oils extraction versus heat energy available for the process. For this purpose, the solar distillation system was connected to thermocouples to maintain the steam temperature and barrel calorimeter was attached to measure the dryness fraction of the steam to calculate the heat energy in latent heat phase. These curves were drawn to develop the appropriate models for different medicinal and aromatic plants for the essential oils extraction against heat energy required for distillation.

Regression analysis was performed and the all the fitted models were found sigmoid/logistic curves (R^2 = 0.94-0.99). On comparison of chopped and un-chopped material, the chopped material gave better results. Similar results were obtained from the

other experiments. It has also been observed that machine chopped Melissa gave better results than manually chopped Melissa. These results show that the oil extraction from Melissa highly depends on the preparatory index of the plant material. This is due to the fact that the preparation of the finer particles of the leaves provide more chances for the steam to have a contact with the oil glands of the plant material. It is necessary that the chopping should be carried out very carefully without losing the volatile component of the plant material to the atmosphere. It is also clear from the Fig. 4.31 that fresh Melissa gave better results as compared with the dry Melissa. Results also showed that the chopped Melissa consumed less energy as compared with the fresh and dry Melissa. In order the compare the fresh, dry and chopped Melissa, a number of experiments (10 kg batch on fresh weight basis) were conducted as shown in the Figure 4.32.

Figure 4.32: Comparison of fresh, chopped and dry Melissa in different experiments (10 kg batch)

The results show that the fresh Melissa gave better results (with a mean value of 1.21 ml and standard error of 0.1413) as compared with the dry Melissa (with a mean value of 1.00 ml and standard error of 0.1648) on dry weight basis. The analysis was carried out using statistical software “SPSS 16” by using “Tukey Test”. The results were found non-significant at 5 % level of significance. However, by comparing the chopped fresh Melissa (2.251 ml) with fresh un-chopped Melissa (1.21 ml), significant results are obtained.

According to Jud (Cited in Müller, 1992), by increasing the drying temperature from 30 °C to 55 °C, essential oil losses increase by 15 percent and the drug color changes from green to gray. Drying temperature usually has an influence on the temperature sensible components of essential oil. Cuervo & Hensel (2008) have also concluded the similar results. Moreover, the drying process necessitates an enormous amount of thermal and electrical energy (Fargali et al., 2008). In the present study, many experiments were conducted to compare the fresh and dry Melissa per unit dry matter. Even though fresh herbs gave better results but statistically these results were found non-significant. In fact, these drying trials were conducted using solar tunnel dryer in the permissible temperature range to avoid the burning and decomposition of the essential oil of the plant material. The study concludes that the dry Melissa can also be distilled successfully for essential oil extraction if dried in the permissible temperature range.

Öztekin & Martinov (2007) investigated that during distillation experiments, the plant materials get denser by absorbing water and the fresh steam is not able to move it, and the pores in the randomly places material at the beginning gets larger. In this way, only some part of the material is in touch with the steam and absorbing essential oil is far from complete. This can be prevented by using mixers such as an auger inside the still body or chopping of plant material before processing. Many experiments were performed to compare chopped and un-chopped Melissa per unit weight of dry matter, highly significant results were obtained. These results show that chopping is an effective way to get the full contents of the essential oils by exposing the more surface area of the plant material to the steam.

4.10.1.1 Distillation experiments with Peppermint varieties (Mentha piperita L, Mentha spec., Mentha spicata)

Three varieties of Peppermint were available to conduct the distillation experiments at the solar distillation experimental site. These varieties were Mentha Piperita L, Mentha spec. and Mentha spicata as shown in Appendix F. The health benefits of Peppermint oil include its ability to treat indigestion, respiratory problems, headache, nausea, fever, dental care, urinary track infection, stomach and bowel spasms and pain. It also increase immunity to diseases, improve blood circulation, It is further believed that peppermint oil is useful for treating cancer and tuberculosis. Due to the presence of menthol, menthone and menthyl esters, peppermint and peppermint oil find wide applications in manufacture of soap, shampoo, cigarette, toothpaste, chewing gum, tea and ice cream. Peppermint is a cross

between watermint and spearmint and is native to Europe. Historically, the herb has been known for its medicinal uses. Hence it is often termed as the world's oldest medicine. Unlike many other herbs and essential oils, numerous health benefits of peppermint and peppermint oil have been studied and proved by the scientific community. As a result, peppermint oil is also sold in the form of capsules and tablets. Peppermint oil is also used as a flavoring agent. Peppermint oil contains numerous minerals and nutrients including manganese, iron, magnesium, calcium, folate, potassium, and copper. It also contains omega-3 fatty acids, Vitamin A and Vitamin C.

All three different varieties were processed by solar distillation system and the process curves for all these varieties (10 kg weight on fresh weight basis) are shown in Figure 4.33.

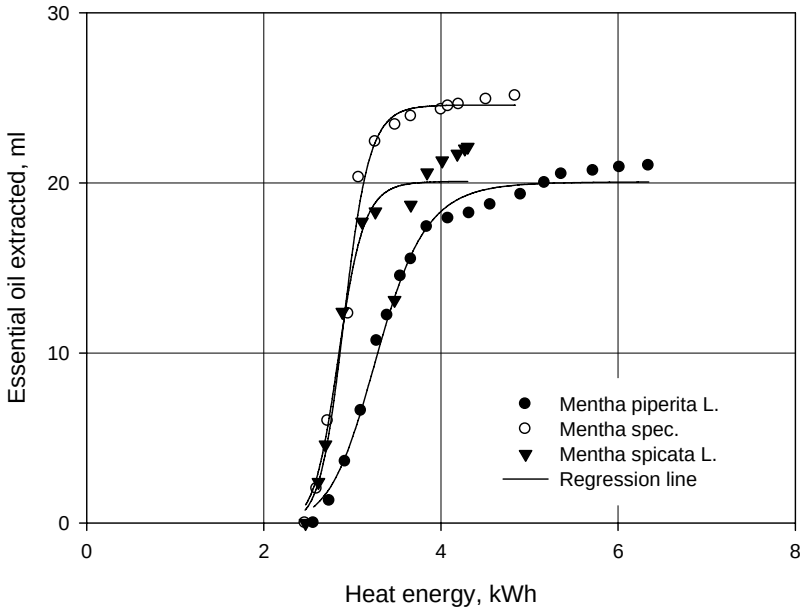

Figure 4.33: Process curved of Peppermint verities (Mentha piperita L., Mentha spec., and Mentha spicala) for 10 kg batch (Fresh weight basis)

Regression analysis was performed and the best fitted regression model for all the experiments with peppermint was found to be sigmoid/logistic with three parameters. The reliability of the developed model was evaluated by comparing the experimental and predicted curves. The results revealed that the model fitted very well with the experimental data for different plant materials which are indicated by high values of coefficient of determination (R^2 =0.9834-0.9916). Peppermint gave distillation in 30 minutes after the

start of steam generation (Anonymous, 1998). Similar results were obtained from solar distillation of Peppermint. These results show that the higher oil extraction rates at the start of the distillation process and lower extraction rates towards the end of the process. Frequent experiments were carried out with all these three varieties of Peppermint (Mentha piperita L, Mentha spec., and Mentha spicala), a comparison of 10 kg batch on fresh weight basis is shown in Figure 4.34.

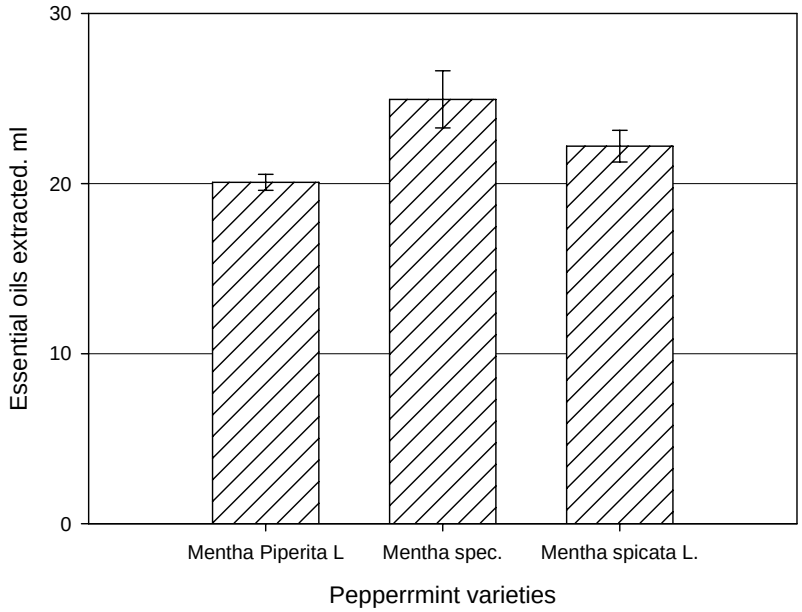

Figure 4.34: Comparison of Peppermint varieties (Mentha Piperta L, Mentha spec., and Mentha Spicala) (10 kg batch, fresh weight basis)

The mean values of and standard errors for Mentha Piperta L, Mentha spec.and Mentha Spicala L were found to be 20.07, 24.95, 22.20 ml respectively. Their corresponding standard errors were found to be 0.4676, 1.6791, and 0.9338 respectively. Low values of standard errors indicate the consistency of the results. Anonymous (1998) concluded that 1 kg fresh peppermint with I kg steam in 30 minutes gave 3 ml of essential oil. Although the results obtained by solar distilled peppermint are lowers but were comparable with the laboratory experiments conducted with the same plant material simultaneously. Research concluded that the peppermint varieties (Mentha piperta L, Mentha spec., and Mentha spicala) can be successfully processed by using solar distillation system.

4.10.2 Oregano (*Origanum vulgare SSP.*)

Oregano is an important culinary herb. It is particularly widely used in Turkish, Greek, Portuguese, Spanish, Latin American, and Italian cuisine. It has an aromatic, warm and

slightly bitter taste. Oregano is high in antioxidant activity, due to a high content of phenolic acids and flavonoids. In the Philippines, oregano is not commonly used for cooking but is rather considered as a primarily medicinal plant, useful for relieving headaches and coughs. Main constituents include carvacrol, thymol, limonene, pinene, ocimene, and caryophyllene. The leaves and flowering stems are strongly antiseptic, antispasmodic, carminative, cholagogue, diaphoretic, emmenagogue, expectorant, stimulant, stomachic and mildly tonic. Aqueous extracts, capsules, or oil extracts of oregano are taken by mouth for the treatment of colds, influenza, mild fevers, fungal infections, indigestion, stomach upsets, enteric parasites, and painful menstruation. Practitioners of alternative medicine often recommend oregano as an herb essential to aid in the recovery of a variety of ailments.

Oregano was planted in the University experimental plants for the research purpose and distillation experiments. Experiments were carried out with Oregano to extract the oil with solar distillation system. A process comparison of 10 kg (fresh weight basis) chopped and un-chopped Oregano is presented in Fig. 4.35.

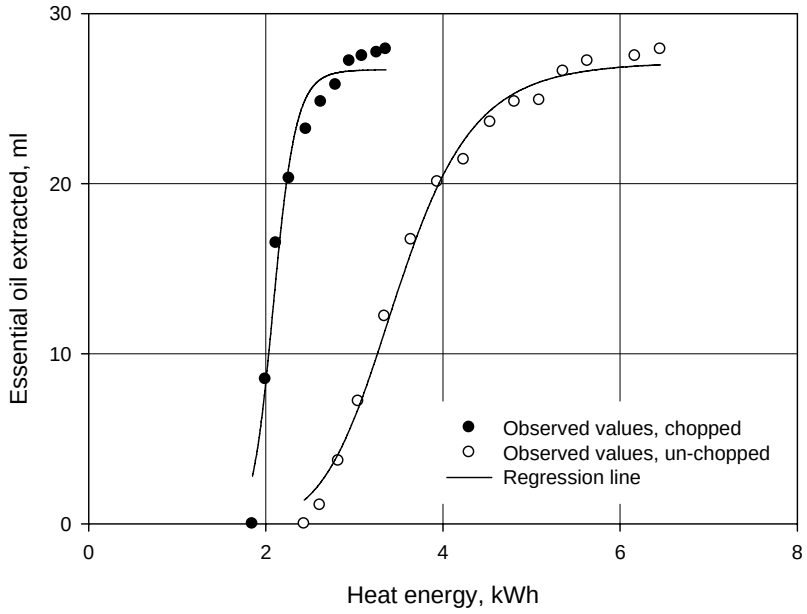

Figure 4.35 Process comparison for chopped and un-chopped Oregano (10 kg batch)

Regression analysis was performed and the best fitted regression model was found to be sigmoid/logistic curve with three parameters. The reliability of the developed model was evaluated by comparing the experimental and predicted curves. The results revealed that

the model fitted very well with the experimental data for different plant materials which are indicated by high values of coefficient of determination (R^2 = 0.9738-0.9930). These results show that the higher oil extraction rates at the start of the distillation process and lower extraction rates towards the end of the process.

It is clear from the Fig. 4.35 that in the processing of Oregano, almost same contents of essential oils were obtained by chopped (27.9 ml) and un-chopped material (27.9) ml) but the energy consumptions for un-chopped and chopped Oregano were found to be 6.46 kWh and 3.36 kWh to extract 100 % essential oil. These results show that there is no significant effect of chopping on the extraction of oil but results are significant in terms of energy consumption. These results revealed that same contents of essential oils can be obtained from Oregano without doing any chopping practice as it is highly volatile material to release essential oils. However, the chopping facilitates to extract this volatile material with saving of energy and time. A number of experiments were conducted with chopped and un-chopped material (10 kg batch on fresh weight basis) are shown in Figure 4.36

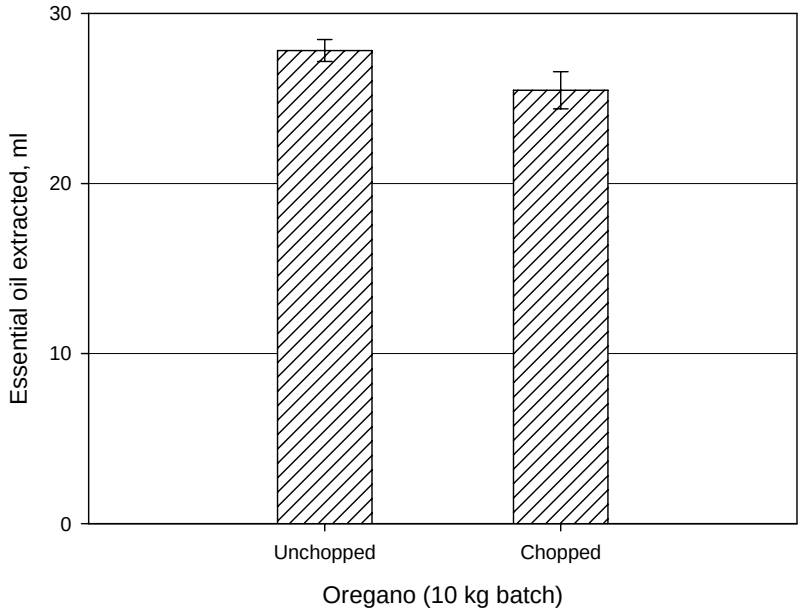

Figure 4.36: Comparison for chopped and un-chopped Oregano (Origanum Vulgare SSP.) (10 kg batch, fresh weight basis)

The analysis was carried out using statistical software “SPSS 16”. The results show that essential oil extraction from both un-chopped (with a mean value of 27.82 ml and standard error of 0.6227) and chopped Oregano (with a mean value of 25.48 ml and standard error

of 1.10905) gave non-significant results at 5 % level of significance. These results show that chopping of Oregano has no significant effect on the oil extraction.

4.10.3 Cloves (*Eugenia caryophyllata*)

Cloves (*Eugenia caryophyllata*) are the aromatic dried flower buds of a tree in the family Myrtaceae. Cloves are native to Indonesia and used as a spice in cuisines all over the world. Cloves are now harvested primarily in Indonesia, Madagascar, Zanzibar, Pakistan, Sri Lanka and India. The clove tree is an evergreen which grows to a height ranging from 8-12 m, having large square leaves and sanguine flowers in numerous groups of terminal clusters. The flower buds are at first of a pale color and gradually become green, after which they develop into a bright red, when they are ready for collecting. Cloves are harvested when 1.5–2 cm long, and consist of a long calyx, terminating in four spreading sepals, and four unopened petals which form a small ball in the centre. Cloves are used as a carminative, to increase hydrochloric acid in the stomach and to improve peristalsis. Cloves are also said to be a natural anthelmintic. The essential oil is used in aromatherapy when stimulation and warming are needed, especially for digestive problems. Topical application over the stomach or abdomen are said to warm the digestive tract. Clove oil, applied to a cavity in a decayed tooth, also relieves toothache. It also helps to decrease infection in the teeth due to its antiseptic properties.

In Chinese medicine cloves or *ding xiang* are considered acrid, warm and aromatic, entering the kidney, spleen and stomach meridians, and are notable in their ability to warm the middle, direct stomach qi downward, to treat hiccough and to fortify the kidney yang (Bensky et al., 2004). Clove oil is used in various skin disorders like acne, pimples etc. It is also used in severe burns, skin irritations and to reduce the sensitiveness of skin. It is used as a tea and topically as oil for hypotonic muscles, including for multiple sclerosis. Western studies have supported the use of cloves and clove oil for dental pain. However, studies to determine its effectiveness for fever reduction, as a mosquito repellent and to prevent premature ejaculation have been inconclusive. Cloves are traditionally used in winter to help warm the body. Cloves warm the spleen and stomach. Cloves are used for nausea, vomiting and hiccupping due to Cold. Cloves warm the kidneys. They are used for lumber aches. The normal doses are 1-3 gram a day. Cloves are not recommended to use when there are heat symptoms and Yin deficiency (Chmelik, 1999).

Water distillation is generally used to extract the essential oils of the dried or powdered plant material, that is, spice powders, ground woody plants like cinnamon bark as well as some flowers such as rose and orange and very tough material such as roots, woods, or nuts. During the boiling process, the volatile component of the plant material is mostly extracted at temperature just below 100 °C by diffusion mechanism (Öztekin & Martinov, 2007).

The distillation experiments with cloves were conducted by using the water distillation. For this purpose, 20 kg of water was filled during distillation experiments and additional water was used to make up the level of the distillation tank from the heat recovery by condenser. The cloves were dipped into it for 2-3 hours prior to the start of the experiment so that all oil contents can easily be extracted from the dried material. When distilling dry material, pre soaking has been found to increase the yields, and to reduce the time required for completion the distillation (Dürbeck, 1997). Thereafter distillation process is started. In case of dry spices, the lower quantities of the plant material are taken so that it should be dipped in water easily. The essential oil extraction against heat energy by solar distillation system is shown in figure 4.37

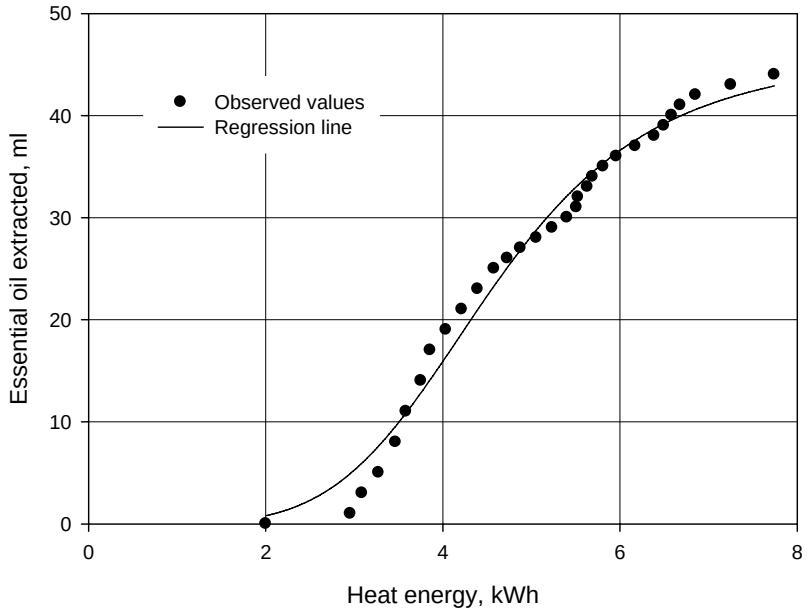

Figure 4.37: Experimental results for the essential oils extracted against different heat energy during solar distillation of Cloves (0.8 kg)

It is evident from Fig. 4.37 that the oil extraction rate is slower at the start, then becomes faster and at the end also becomes slower. In this experiment, 0.8 kg of the cloves were used and 44 ml of the oil were extracted and the process consumed 7.74 kWh total heat

energy. Regression analysis was performed and the best fitted model was found to be sigmoid/logistic with 3 parameters. The coefficient of determination (R^2) was found to be 0.984 showing the best relation of observed and predicted values. Frequent experiments were carried out with the clove buds and the similar results were obtained. These results show that dry herbs and spices can also be successfully processed by water distillation using solar energy.

4.10.4 Cumin (*Cuminum cyminum*)

Cumin is the second most popular spice in the world after black pepper. Cumin seeds are used as a spice for their distinctive aroma, popular in Indian, Pakistani, North African, Middle Eastern, Sri Lankan, Cuban, Northern Mexican cuisines, and the Western Chinese cuisines of Sichuan and Xinjiang. The health benefits of Cumin essential oil can be attributed to its properties like bactericidal, carminative, digestive, diuretic, anti septic, anti spasmodic, detoxifier, emenagogue, stimulant, nervine and tonic. Essential Oils of Cumin is extracted from its dried and crushed seeds through steam distillation. Nearly all the medicinal properties of Cumin come from its essential oils, which, in its pure form, is far more effective and beneficial than cumin seeds. The Cumin essential oil is composed mainly of Cuminic Acid, Cymene, Dipentene, Limonene, Phellandrene and Pinene. It can be used in treatment of diarrhea and cholera which are caused by bacteria. Cumin oil has strong carminative properties and efficiently drives away gases from intestines. Cumin oil aids digestion, promotes discharge of bile and gastric juices and also stimulates peristaltic motion of the intestines. Cumin oil increases urination, both in frequency and in quantity. It removes excess water from the body and reduces swelling etc. Its biggest contribution is that it removes toxins from the body and also reduces blood pressure. Cumin oil can help maintain a regular menstruation cycle and can open obstructed menses. It particularly stimulates the digestive and the excretory system and keeps them in order. Cumin oil is good on nerves and helps cure nervous disorders such as convulsions, anxiety, stress etc. Tones up muscles, tissues and skin as well as the various systems functioning inside the body, such as respiratory system, circulatory system, nervous system, digestive system and the excretory system. This tonic effect helps retain youth for a long.

The distillation experiments with cumin were conducted by using the water distillation. For this purpose, 20 kg of water was filled during distillation experiments and additional water was used to make up the level the distillation tank from the heat recovery by condenser. The cumin was soaked into it for 2-3 hours prior to the start of the experiment so that all oil

contents can easily be extracted from the dried material. In case of dry spices, the lower quantities of the plant material are taken for better results.

The essential oil of cumin is extracted by water distillation process. The process curve for 1.2 Kg of dry cumin is shown in Figure 4.38.

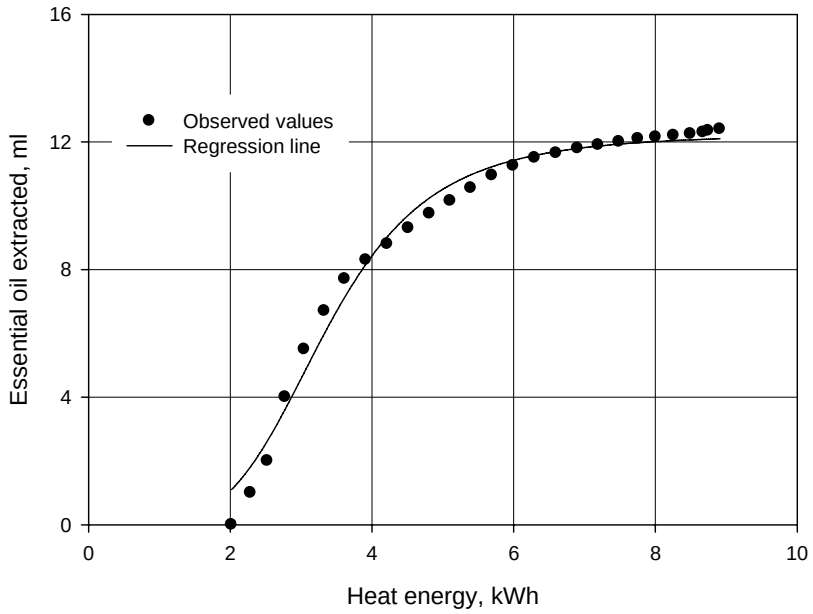

Figure 4.38: Experimental results for the essential oils extracted against different heat energy during solar distillation of Cumin (1.2 kg)

Figure 4.38 shows that oil extraction curve for the cloves. In this experiment, 1.2 kg of the cumin was used and 12.4 ml of essential oil was extracted with heat energy consumption 8.91 kWh. Regression analysis was performed and the best fitted model was found to be sigmoid logistic with three parameters. The values of R^2 were found to be 0.985 showing the best relation of observed and predicted values. A number of experiments were conducted with Cumin by using water distillation technique and successful results were obtained by using solar energy.

4.10.5 Rosemary (*Rosmarinus officinalis*)

Rosemary oil is extracted from Rosmarinus officinalis (also known as Rosmarinus coronarium) of the Labiatae family and is also known as incensier. This crisp and clean smelling essential oil is great for stimulating the brain, improving memory and mental clarity, while helping with a variety of congested respiratory tract problems, stiff muscles,

coldness as well as boosting the liver and gall bladder. It is also used for improving hair and scalp health. Rosemary oil has a clear, powerful refreshing herbal smell, is clear in color and watery in viscosity. It is a shrubby evergreen bush that grows up to 1.5 meters high with green-gray needle-shaped leaves and pale blue/lilac flowers that bees just love and is originally from Asia, but is now cultivated in France, Tunisia and Yugoslavia. Rosemary oil is extracted from the fresh flowering tops by steam distillation and yields 1.0-2.0 %. The therapeutic properties of rosemary oil are analgesic, antidepressant, astringent, carminative, cephalic, cholagogue, cordial, digestive, diuretic, emmenagogue, hepatic, hypertensive, nervine, rubefacient, stimulant, sudorific and tonic. Rosemary oil has a pronounced action on the brain and the central nervous system and is wonderful for clearing the mind and mental awareness, while having excellent brain stimulant properties, as well as improving memory. It helps with headaches, migraines, neuralgia, mental fatigue and nervous exhaustion and the antiseptic action of rosemary oil is especially suitable for intestinal infections and diarrhea, easing colitis, dyspepsia, flatulence, hepatic disorders and jaundice and relieving pain associated with rheumatism, arthritis, muscular pain and gout. It also helps for arteriosclerosis, palpitations, poor circulation and varicose veins. The diuretic properties of rosemary oil are useful with reducing water retention during menstruation, and also with obesity and cellulite. On the respiratory system, it is effective for asthma, bronchitis, catarrh, sinus and whooping cough. Because of its astringent action, it is also effective for countering sagging skin. Its stimulating action benefits scalp disorders and encourage hair growth. On the skin, it helps to ease congestion, puffiness and swelling and can also be used for acne, dermatitis and eczema, but a very popular use of this oil is the use in hair care products, as it has a pronounced positive effect on the health of the hair and scalp. It increases the circulation to the scalp and is therefore also effective for promoting hair growth.

The distillation experiments with Rosemary were conducted by using the “water and steam distillation” using solar energy. For this purpose, 20 kg of water was filled during distillation experiments and additional water was used to make up the level the distillation tank from the heat recovery by condenser. The material was placed on the perforated grid to be processed with steam. One example with 3 kg of Rosemary is explained in Figure 4.39.

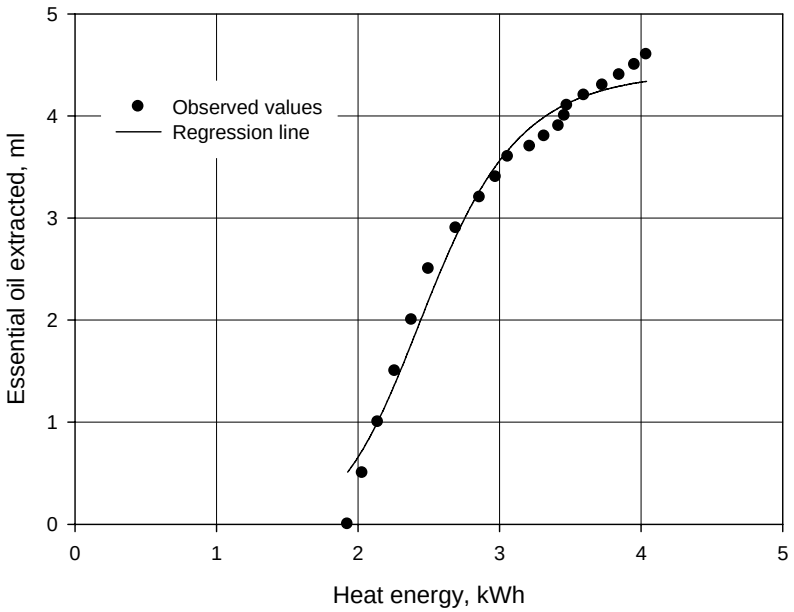

Figure 4.39: Experimental results for the essential oils extracted against different heat energy during solar distillation of Rosemary (3 kg batch)

Figure 4.39 shows that oil extraction curve for rosemary with steam distillation. In this experiment, 3 kg of the Rosemary and 4.6 ml of the oil was extracted against energy of 4.038 kWh. Regression analysis was performed and the best fitted model was found to be sigmoid logistic with 3 degrees. The coefficient of determination (R^2) was found to be 0.981 showing the best relation of observed and predicted values.

4.10.6 Fennel (*Foeniculum valgure Mill.*)

Seeds (fruits) are used to flavor liqueurs, vinegars, breads, pastries, candies and pickles. Leaves and stems occasionally serve as vegetable, salad, or Potherb. The herb has long been an important adjunct for cooking with strong fish. Oil is used in culinary articles, cordials, and toilet articles. The oil can be used to protect the stored fruits and vegetables against infection by pathogenic fungi. It is reported to be abortifacient, anodyne, aphrodisiac, balsamic, cardiotonic, carminative, diaphoretic, digestive, emmenagogue, expectorant, lactogogue, pectoral, restorative, stimulant, stomachic, tonic, and vermicide. The fennel is a folk remedy for aerophagia, amenorrea, hernia, nausea, nephrosis, parturition, snakebite, sore, spasm, splenosis, stomachache, strangury, tenesmus, toothache, and virility. Fennel juice was once a popular cough remedy. The oil is recommended for hookworm. Lea are said to be diuretic, roots purgative, and oil carminative and vermicidal. Resies remaining after oil extraction contain 14 to 22 % protein and 12 to 18.5 % fat. Fruits contain 1.5 to 3.0 % essential oils and 9 to 21 % fatty

oil, high in petroselinic acid (67 to 69 %), and 6.5 % unsaponifiables containing 6-oxychroman derivatives. Per 100, the leaves contain 31 calories, 80.2 g water, 2.9 g protein. Fennel is like many herbs with combined medicinal and culinary uses. The properties are pungent and warming. Channels affected are Spleen, stomach, Liver and Kidneys. It dispels cold. For abdominal pains and distension due to cold, including period pain, hernia pain and the pains in the testicles. It warms the spleen and stomach and is used for poor digestion. The normal dosage is 3-8 g a day (Chmelik, 1999). Experiments were conducted with Fennel using steam distillation as shown in Figure 4.40.

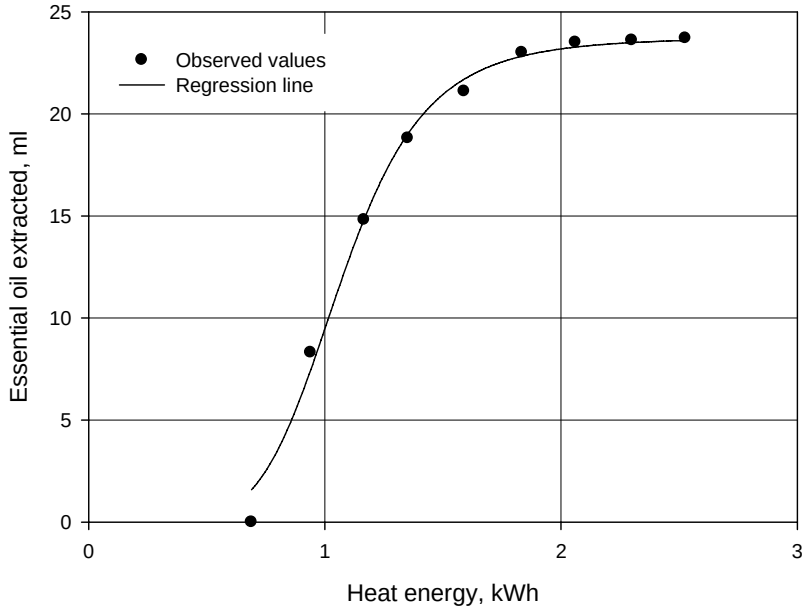

Figure 4.40: Experimental results for the essential oils extracted against different heat energy during solar distillation of Fennel (10 kg batch, fresh weight basis)

Figure 4.40 shows that oil extraction curve for the steam distillation of Fennel. At start, the oil extraction rate is slow, them becomes faster and at the end also becomes slower. In this experiment, 10 kg of the Fennel Rosemary and 23.7 ml of the oil was extracted against energy of 2.53 kWh. Regression analysis was performed and the best fitted model was found to be sigmoid logistic with 3 parameters. The values of R^2 were found to be 0.9933 showing the best relation of observed and predicted values. The results shows that Fennel can be successfully processed by solar distillation system.

4.11 Comparison of results-laboratory versus solar

Several experiments were carried out for solar distillation system and successful results were achieved. While conducting solar experiments, laboratory experiments were also conducted simultaneously using the same plant materials for comparison. Under laboratory conditions 100 gram of different herbs were taken (200 gram for Melissa), while the field experiments were conducted with different weight. For comparison, detail of some of the experiments with Cloves, Cumin, Rosemary and Melissa at 11, 9, 72 and 78 % on wet basis respectively as shown in Table 4.8.

Table 4.8: Comparison of distillation experiments- laboratory versus solar

Experiment	Cloves		Cumin		Rosemarie		Melissa	
Description	Lab.	Solar	Lab.	Solar	Lab.	Solar	Lab.	Solar
Weight, kg	0.1	0.8	0.1	1.2	0.1	3.0	0.2	11.6
Oil extracted, ml	5.5	44	1.081	12.4	0.162	4.600	0.027	1.425
Essential oil per unit of d.m, ml/kg	61.8	61.8	11.9	11.4	5.79	5.48	0.614	0.558
kWh/ ml of oil	0.133	0.176	0.574	0.719	1.000	1.006	2.667	2.714
% decrease in oil	-	0	-	4.20	-	5.35	-	9.12
% increase Energy	-	32.33	-	25.26	-	0.60	-	1.76

Table 4.8 shows the quantity of essential oils per 100 g of herbs, energy consumption (kWh) per ml of oil, percent decrease in essential oils (compared with the laboratory) and percent increase in energy consumption. In most of the experiments, the percent decrease in essential oil extraction by solar distillation was found up to 5 % than that of laboratory. In some cases, almost same results were also achieved. In case of Melissa, the percentage decrease of essential oil was found to be 9.12 %. In several experiments, only 1-2 % more energy consumption per unit weight of the herbs was observed. However, more energy consumptions were observed in some of the experiments as in case of Cumin (25.26%) and cloves (32.33 %). This variation in energy is due to the fluctuations of solar radiations at the site which resulted in more energy consumption. Moreover, the energy consumption depend on the characteristics of the material used for the distillation still, quantity of water added in the still etc. So, the energy consumption for the field distillation cannot be compared with that of laboratory results. However, satisfactory results were obtained by solar distillation system. These results show that completes distillation process for essential oils extraction can be done successfully using Scheffler reflector. However, the solar system needs an auxiliary heat source to compensate for bad weather conditions.

4.12 Need of auxiliary energy for the solar distillation system

The solar distillation system worked quite effectively during sunny hours as it is operated by a concentrated solar collector. The present study was conducted in Witzenhausen, Germany (Latitude 51.3°) where sunny days are not so often. Many distillation experiments were suffered adversely during bad weather conditions. As the present research was conducted without any energy storage consideration, so the temperature during distillation process drops rapidly with the drop of beam radiations as shown in Fig. 4.41

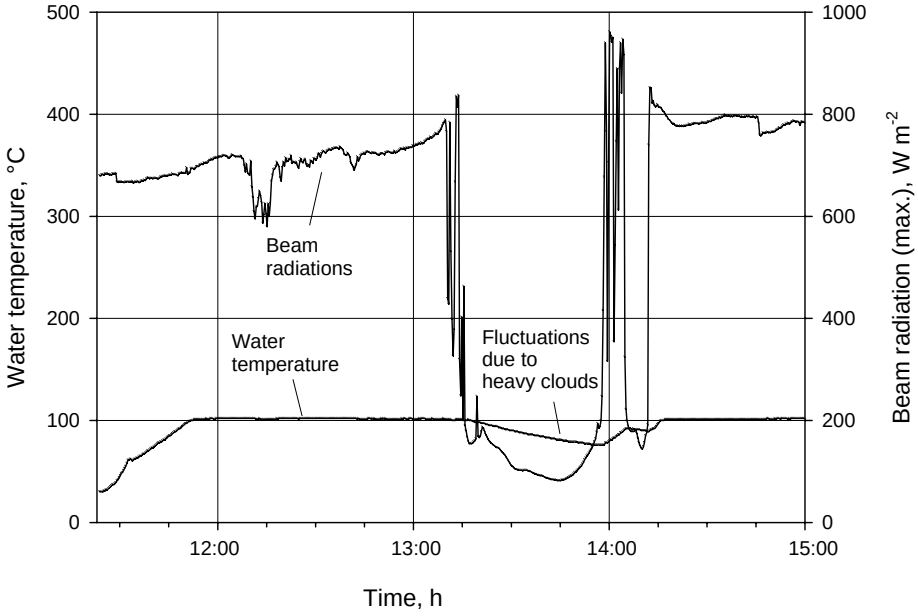

Figure 4.41: Water temperature and beam radiations (max.) from 11:23 to 15:00 hours on Aug, 24 2007 (Real time data sample taken for 10 seconds intervals during distillation experiments, Location, Am Sande Witzenhausen, Latitute:51.3°)

The degree of reliability desired of a solar process to meet a particular load can be provided by a combination of properly sized collector and an auxiliary energy source. In the most climates, auxiliary energy is needed to provide high reliability and avoid gross over design of the solar system (Duffie & Beckman, 2006). By keeping all these facts in view, the existing solar system was connected with the biomass energy to continue the distillation process under variable climatic conditions. For this purpose, the steam connections are provided to the steam coils of the distillation still in order to operate solar-biomass hybrid system as shown in Fig. 4.42.

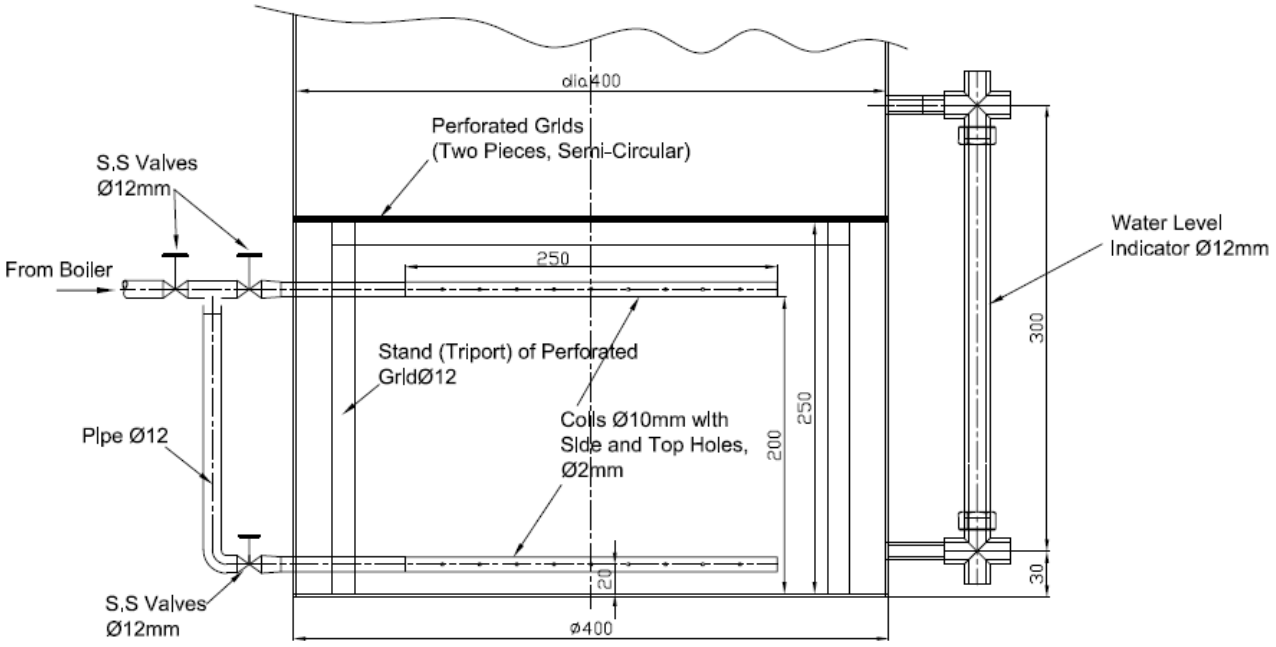

Figure 4.42: Distillation still with coils and steam connections to operate the unit with solar-biomass hybrid system

4.12.1 Distillation experiments with solar-biomass hybrid system (European Silver Fir (*Abies alba*) as sample)

European Silver Fir (*Abies alba*) is a fir native to the mountains of Europe, from the Pyrenees north to Normandy, east to the Alps and the Carpathians, and south to southern Italy and northern Serbia, where it intergrades with the closely related Bulgarian Fir. It is a large evergreen coniferous tree growing to 40–50 m tall and with a trunk diameter of up to 1.5 m. The leaves are needle-like, flattened, 1.8–3 cm long and 2 mm wide by 0.5 mm thick, glossy dark green above, and with two greenish-white bands of stomata below. The buds are antibiotic, antiseptic and balsamic (Chiej, 1984). The bark is antiseptic and astringent. It can be harvested as required throughout the year. The leaves are expectorant and a bronchial sedative. They are best harvested in the spring and can be dried for later use. The resin is antiseptic, balsamic, diuretic, eupeptic, expectorant, vasoconstrictor and vulnerary. Both the leaves and the resin are common ingredients in remedies for colds and coughs, either taken internally or used as an inhalant. The leaves and the resin are used in folk medicine to treat bronchitis, cystitis, leucorrhoea, ulcers and flatulent colic. The resin is also used externally in bath extracts, rubbing oils etc for treating rheumatic pains and neuralgia. Oil of Turpentine, which is obtained from the trunk of the

tree, is occasionally used instead of the leaves or the resin. The oil is also rubefacient and can be applied externally in the treatment of neuralgia.

It is harvested in the summer and used fresh, dried or distilled for oil (Bown, 1995). The resin extracted from it is used in perfumery, medicine and for caulking ships (Usher, 1974). It is called 'Strasburg Turpentine. Oil of turpentine is an important solvent in the paint industry. The residue, known as 'rosin oil', is used in making varnishes, lacquers and carbon black (for pigments and ink). Resin is tapped from trees about 60-80 years old in the spring and used for the distillation of oil. An essential oil obtained from the leaves is used as a disinfectant and also in medicine and perfumery (Usher, 1974). It is a common ingredient in many bath products, giving them their familiar pine scent (Chiej, 1984). The timber of this tree is especially sought after for its lightness, it is used for construction, furniture, boxes, pulp etc.

Many experiments were carried out with European Silver Fir (*Abies alba*). These experiments were conducted with solar energy and with solar biomass hybrid system using “water and steam distillation”, and “steam distillation” technique during cloudy conditions. Experiments were also conducted with un-chopped and chopped plant material. In each experiment, 10 kg batch on fresh weight basis (at the same moisture contents) was used for comparison. The detailed process lines for essential oil extracted (ml) against heat energy used (kWh) for three identical experiments (10 kg batch) with European Silver Fir is shown in the Figure 4.43.

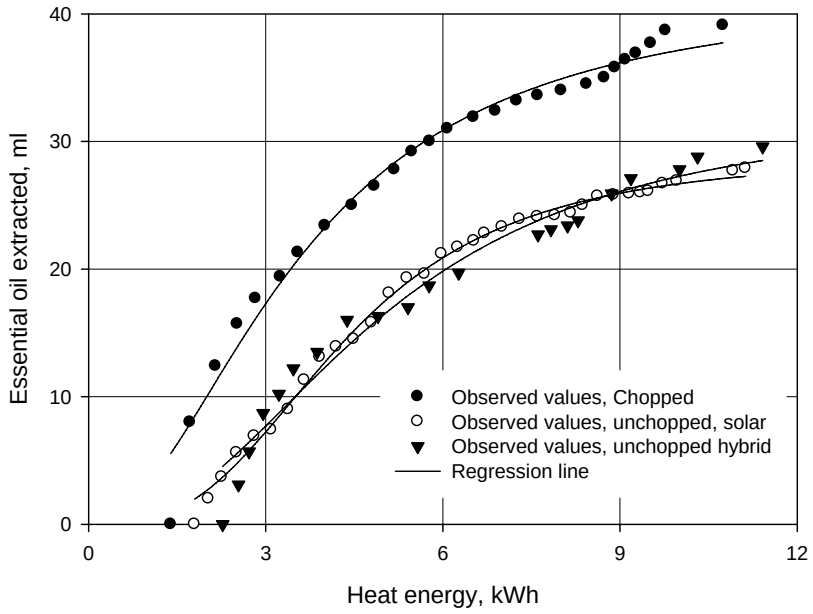

Figure 4.43: Process comparison for solar and solar-biomass hybrid system with European Fir (10 kg batch)

The dotted values indicate the observed values during the entire experiment. The data were conducted after 10 minute interval. Regression analysis was performed to calculate the appropriate trend. The best fitted model was found the Sigmoid/logistic with high co-efficient of determination (R^2 = 0.964-0.996). This model shows the high extraction rate at the start of the experiment and then decreases towards the end of experiment. It is also clear from the Figure 4.43 that the plant material processed with "water and steam distillation" by using solar energy and with "steam distillation" by using solar-biomass hybrid system gave the similar process curves. In this comparison, the process curves are almost overlapping each other from start to end of the process. The quantities of essential oils extracted from solar based system and solar-biomass hybrid system were found to be 27.9 and 29.6 ml respectively. Their energy consumptions to complete the process were found to be 11.13 and 11.42 kWh respectively. These results show that distillation experiments with solar and solar-biomass hybrid systems were conducted successfully and gave almost the same oil contents and energy consumptions. It is also evident from the Fig. 4.43 that the essential oil contents and energy consumption to process 10 kg of chopped Silver Fir were recorded to be 39.1 and 10.74 kWh respectively. These results show that chopped European silver Fir gave better results in terms of oil extraction and the curve is well above the process lines of un-chopped material (for both solar and hybrid system). Similar results were obtained from the other experiment and are detailed in Figure 4.44.

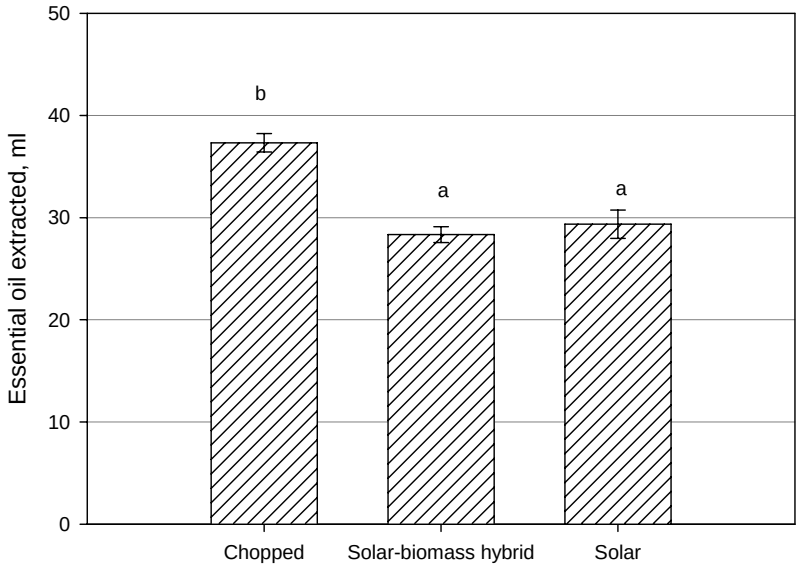

Figure 4.44: Comparison of chopped and un-chopped European Silver Fir (*Abies Alba*) with solar based and solar-biomass hybrid system

Figure 4.44 shows the statistical analysis for the Europeans Silver Fir (*Abies alba*). The mean values of the essential oil extracted for the un-chopped solar distilled, un-chopped solar-biomass distilled and solar chopped was found to be 29.35, 28.34, 37.33 ml respectively. Their standard errors were found to be 1.39, 0.771, and 0.896 respectively. The statistical analysis was conducted at 5 % level of significance and Tukey test was performed to compare the means. It was found that the chopped Silver Fir gave significant results. On the other hand, the both solar and solar biomass hybrid system gave the similar results. The study concludes that the solar system can be successfully operated by using the hybrid system. The study also concludes that chopped material gave better results than the un-chopped material. Chopping of the material increases the bulk density and makes the material finer where all the plant materials have a chance to release the oil. In case of un-chopped material, some of the oil can not be extracted due to the hard material. The results conclude that European Silver Fir can be successfully distilled with solar energy and by solar biomass hybrid system. These results also show that not only very delicate leaves and flowers are processed but solar energy can be successfully utilized to process the hard tree plants as well. However, the material should be chopped for better results.

Several experiments were carried out during adverse climatic conditions using solar distillation system integrated with biomass energy. During these experiments, the distillation still was filled with water to produce steam by reflected beam radiations on the still bottom and the extra energy was taken from the biomass boiler. The experiments were conducted with different plant material like Melissa, Peppermint, Lavender, European Silver Fir etc (10 kg batch) are shown in the Figure 4.45.

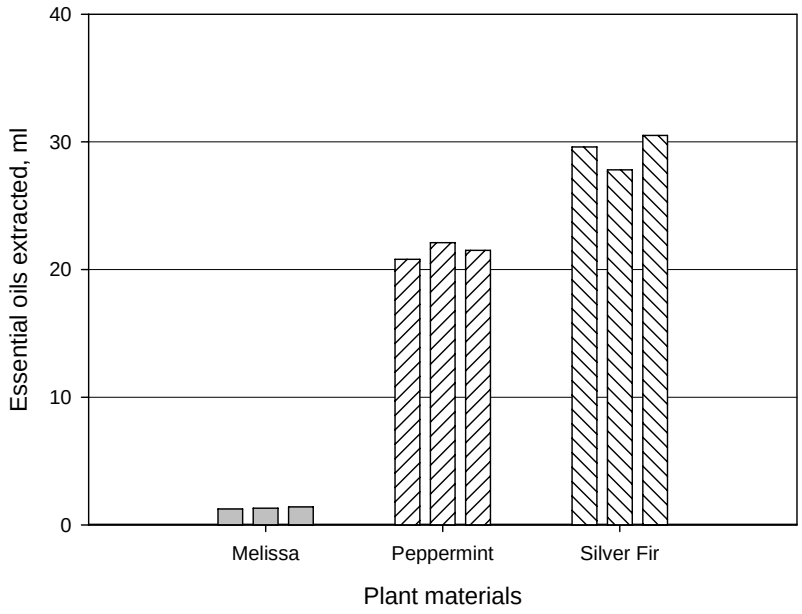

Figure 4.45: Results of solar-biomass hybrid distillation system for Peppermint, Melissa, European Silver Fir (10 kg batch)

The average amount of oil extracted for Peppermint, Melissa and European Silver Fir were 21.46, 1.317 and 29.3 ml. The energy ratio of biomass to solar energy was varied from 0.3 to 0.5 during most of the experiments conducted by solar-biomass hybrid distillation system. The results reveal that biomass energy can be successfully utilized in the solar distillation system to operate the distillation experiments during adverse climatic conditions.

In order to recover energy from the steam, the quantity of inlet cold water to the condenser is controlled to get maximum outlet temperature. This water is stored and recycled to make up any deficiency in the distillation still during experiments as well as to recharge the distillation unit for the next batch. The schematic diagram for solar-biomass hybrid distillation system with heat recovery unit is shown in Figure 4.46

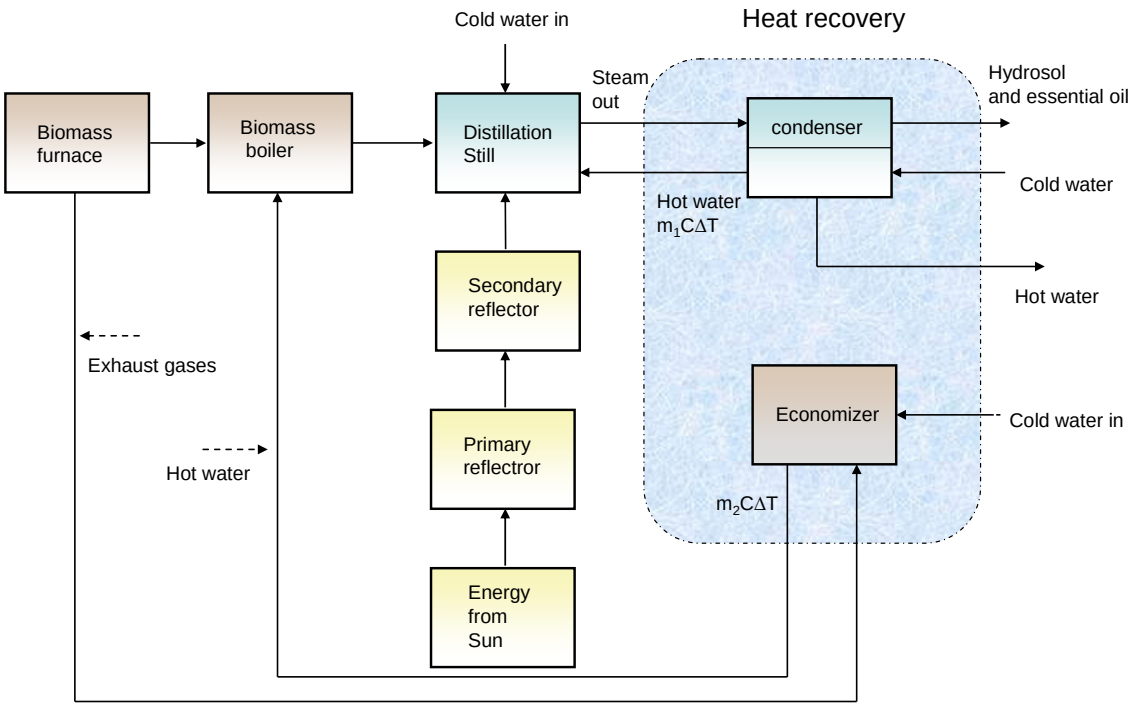

Figure 4.46: Schematic diagram of solar-biomass hybrid system with heat recovery

Distilleries consume considerable energy in the form of heat, most of which inevitably is lost in the heated cooling water discharged from the condenser. Up to about 12 % of this can be saved by preheating the water used for recharging the boiler or the water bath (Denny, 1991). While performing distillation experiments, the outlet water of the condenser water was taken in a big tank. This hot water was used to make up the level in the distillation still during distillation process as well as to refill the distillation still for new charge while performing experiments with “water distillation” and “water & steam distillation”. It has been found experimentally that 85 to 90 °C temperature is achievable from the condenser by maintaining the optimum temperature 35-40 °C of the distillate (condensate). The addition of heat recovery from condenser reduced the energy consumption which is used in sensible heat range during the distillation process.

5 Overall discussion

The design, development, experimental results of a solar distillation system have been presented. The main components of solar distillation system are primary reflector, secondary reflector, distillation still, condenser, and Florentine vessels. Solar distillation system was designed as a fixed installation and all parts of the reflector stand were prepared and assembled with respect to the latitude of Witzenhausen (51.3°). The complete solar based distillation system was constructed in the Agricultural Engineering workshop, University of Kassel, Witzenhausen, Germany.

Many research papers were reviewed on production, uses, drying and processing of medicinal and other plant materials. Design and develop of different types of distillation plants were also studied for the processing of medicinal and aromatic plants using the conventional fuels. A large number of papers are available on different innovative solar collectors in the medium temperature range. In the light of the research work conducted, the present research was focused to integrate the standard distillation techniques with the solar energy for the processing of medicinal and aromatic plants in such a way that it can be applicable for the on-farm processing of medicinal and aromatic plants by using a solar based distillation system.

Laboratory experiments were conducted to investigate the optimal thermal and physical parameters. Heat energy consumptions to process 100 grams of Cloves buds, Fennel, Cumin, Melissa, Patchouli, Cassia, Orange barks, Lavender and Peppermint were ranged between 0.163 and 0.718 kWh. This energy span is remarkable showing that different plant materials have different energy consumptions per unit weight of plant material during the distillation process. Laboratory results also concluded that fresh herbs needed short duration for processing and were less energy consuming. The study reveals that the on-farm processing of fresh medicinal and aromatic plants is necessary for functional and economic reasons. From the recorded data, energy consumptions to extract one ml of the oil were calculated. The heat energy consumptions to extract one ml from Cloves buds, Fennel, Cumin, Melissa, Patchouli, Cassia, Orange barks, Lavender, Peppermint were ranged between 0.133 and 2.807 kWh respectively. The laboratory experiments were carried out to extract the full contents of the plant material. However, the energy consumptions of the field distillation stills cannot be compared with that of the laboratory as they differ in material, geometry and environmental conditions. Moreover, amount of

water taken per unit mass varies in both types of distillation units. The study concludes that the laboratory setup is only useful to compare the oil extraction but cannot be used for energy comparison. Under laboratory condition, 0.2 kg of different plant materials were processed successfully in 2 liter glass boiler. For the field experiments, 100 liter capacity distillation still was fabricated with 400 mm diameter and 1210 mm column height to process 10 kg of different plant materials. Thereafter a solar system was selected which can provide the required power to conduct different distillation experiments.

Next step of the study was the selection of an efficient solar collector which can provide the required temperature range to conduct different distillation experiments successfully. The solar system can also facilitate “water distillation” and “water and steam distillation” by a continuous and uniform heat distribution on the entire circumference of the distillation still. The distillation still should be easy to charge and clean when integrated with the solar system. The options of vacuum tube collectors with integrated circuits were also studied. These reflectors are more efficient and can provide the required range of the temperature but can not meet the required heat distribution at the bottom of the distillation still. Selection of a Scheffler reflector with secondary reflector arrangement facilitates to conduct different distillation experiments by providing the heat at the bottom like conventional distillation system. In the present study, an 8 m^2 Scheffler fixed focus concentrator was selected for distillation experiments. Up to now, no mathematical description of the design process of a Scheffler reflector has been done. The study explains the design principle and construction detail of an 8 m^2 Scheffler fixed focus concentrator. The results have proved mathematically that it is possible to construct a concentrator that can provide fixed focus for all the days of the year. The slope and y-intercepts for the 8 m^2 surface area Scheffler reflector with respect to equinox (solar declination = 0) are calculated to be 0.17447 and 0 respectively. The slopes of the parabola equations for two extreme position of summer (solar declination = +23.5) and winter (solar declination = -23.5) in the northern hemisphere (standing reflectors) are calculated to be 0.28123, and 0.12736 respectively. The y-intercepts of the parabola curves for summer and winter are calculated to be 0.54394, and -0.53004 respectively. By comparing with the equinox parabola curve, the summer parabola is found to be smaller in size and uses the top part of the parabola curve, while the winter parabola is bigger in size and uses the lower part of a parabola curve to give the fixed focus. In conclusion, the parabola equations on June 21 and December 21 in the southern hemisphere are found to be the same as the parabola equations on December 21 and June 21 in the northern

hemisphere respectively for the standing reflectors. In laying reflectors, the parabola equations for the northern hemisphere are found to be the same as the parabola equations for the southern hemisphere (standing reflectors). Similarly, the parabola equations for laying reflectors in the southern hemisphere are the same as the parabola equations in the northern hemisphere for standing reflectors. For this purpose, the reflector assembly is composed of flexible crossbars and a frame to induce the required change of parabola curves with the changing solar declination. The study also concludes that the concentrator is to be installed at the required site by setting its axis of rotation equal to the latitude of the site in north-south directions to make the axis of the reflector paraboloid parallel to the beam radiations. For daily tracking, these concentrators rotate along an axis parallel to the polar axis of the earth at an angular velocity of one revolution per day with the help of self-tracking devices. The seasonal tracking rotates the reflector at half the solar declination angle to induce the required change of the shape of the reflector paraboloid to track the sun at the fixed focus. Aluminium sheets (with solar weighted reflectance of 88-91 %) from Alcan Company Germany were used successfully for the Scheffler reflector. This material is not available in most of the Asian and African countries. In order to construct a solar distillation system using a Scheffler reflector economically, small plan mirror strips can also be used. By using these mirrors, the material cost of a Scheffler reflector also becomes significantly lowered and this technique fits to the rural areas for on-farm processing of perishable products in most of the underdeveloped countries. Moreover, the construction and fabrication of these reflectors are also possible in an ordinary workshop. This offers a huge potential for its application in domestic as well as industrial configurations. These constructional and installation procedures are applicable all over the world. Scheffler reflector needs little maintenance and can be used for many years provided the reflectors should be free from dirt and other weathering hazards. The main drawback of these reflectors is that a slight inaccuracy during construction will result in poor performance of the reflectors. In fact, the fixed focus is achieved by the combined effect of precisely shaped profiles as well as daily and seasonal tracking accuracy. The distillation experiments can also be carried out with other conventional concentrators which are cheaper but more labor intensive.

Two mathematical models were also developed. First mathematical model was developed in Matlab 7 and Microsoft Excel to calculate the required size of the Scheffler reflector. The second model was developed to calculate the energy distribution and heat losses from different parts of the solar distillation system which provides useful information to optimize

the system. The model can be run for any set of variables to predict the energy losses from the solar distillation system. These models are easy to calculate and predict the feasibility at the desired site. The accuracy of the models was checked with the field experiments using solar distillation system. On a sample day Aug, 31 2008 with average beam radiations 800 W/m^2, the heat losses from the primary reflector, secondary reflector, and distillation still of the solar distillation system were found to be 1273, 587 and 907 Watts with their percentage losses were found to be 29, 14 and 21 % respectively under the available conditions of the solar distillation unit. The available energy for the distillation process was found to be 1555 W with 36 %. Energy losses from bottom, lateral and top part of the distillation unit were found to be 501, 96 and 65 Watts respectively. These results conclude that 76 % losses are taking place from the bottom part which is not insulated and exposed to the solar radiations. This exposed area of the distillation still is 0.277 m^2 due the addition of secondary reflector to avail maximum beam radiations. In normal heat applications with Scheffler reflector, the area required is 0.096 m^2 by placing the receiver inclined before the primary reflector. The main drawbacks of the present distillation system are the losses due to more bottom area of the distillation unit exposed to the open atmosphere and heat losses due to addition of secondary reflector to facilitate the conventional distillation system. The beam radiations required to start the steam generation in the existing solar distillation prototype at atmospheric pressure from June 21 to December 21 was calculated to be 189 to 281 W respectively. This model can be used to predict the results for any required set of data.

Under field conditions, several experiments were carried out to evaluate the performance of the system. In the conventional distillation system, oil extraction rates are recorded versus time. In the present study, the solar distillation system was equipped with pyranometer and thermocouples and to record oil extraction rates of different plant materials versus heat energy. Results revealed that under the constant range of beam radiations, the temperature at focus was also found constant. Within the beam radiation range of 700-800 W m^{-2}, temperature available at focus was found between 300 and 400 °C. The data were recorded for the variation of beam radiations, focal point temperature and the process temperature during distillation process in the still versus time. These results show that the profiles of primary reflector, tracking system, and inclinations of the axis of rotation are precise and converging the beam radiations at the targeted focal point with the changing sun position during the test period. It is also concluded that the temperature line of distillation process is quite below than the temperature line of focal

point. During this test, the total energy gained by water (in sensible and latent heat phase) was calculated to be 9.136 kWh. In this trial, the average power and system efficiency were found to be 1.548 kW and 33.21 % respectively at an average solar radiations of 863 W m^{-2}. The actual efficiency figure from the instrumentation installed in solar distillation system showed approximately the same results as calculated from modeling under similar conditions. The efficiency of the system is lowered as compared with the other solar systems. The energy output per unit area of the Scheffler reflector is lower that other solar collectors due to less aperture area available. The available aperture varies from 4.59 to 6.4 m^2 throughout the year for an 8 m^2 surface area Scheffler reflector.

In the present research, a cast aluminium receiver was used to produce steam for solar-based steam distillation system. Moreover, this receiver was also used for water to evaluate the system. All tests were conduced at atmospheric pressure. Frequent experiments were carried out to check the performance of the solar system by using secondary reflector and without secondary reflector for water and steam trials. The system efficiency was found to be nearly 47 % and 56 % with secondary and without secondary reflector while performing the water trials. However, the system efficiencies of the system for steam generation with and without secondary reflector were found to be 49.8 and 40 % respectively. Low values of “standard errors” and “co-efficient of variance” for all the experiments show the consistency of the results. It can be concluded that about 9-10 % efficiency is lost by using the secondary reflector. The study concludes that the aluminium receiver is an efficient way for hot water and steam generation with continuous flow of water. The study concludes that a significant amount of energy is wasted by using the secondary reflector.

On-farm solar distillation of medicinal and aromatic plants provides an excellent opportunity to process fresh herbs for pure natural essence by availing optimum harvesting time. In conventional distillation system, although distillation is carried out on large scale, yet a part of the volatile components of the plant materials evaporate during traveling and handling. The distillation experiments were conducted during summer 2007, 2008 and 2009. For distillation experiments, the fresh herbs were harvested from the university farms located very near to the solar distillation system and dry herbs purchased from the local market. Process heat energy consumptions for different herbs were calculated from the sensor system installed. Different medicinal and aromatic plant like Melissa, Peppermint, Oregano, Silver Fir, Lavender, Fennel, Rosemary, Cumin, Basil and

Cloves, Lavender etc were processed successfully by solar distillation system. The results showed that different plant materials have different contents of oils and depend on the weight, moisture contents, part of plant material used. During sunny days, 4-5 batches can be processed with 10 kg of fresh plant material per batch. About 40-50 kg fresh plant material (un-chopped) can be processed by using the existing solar distillation prototype during sunny days. With the chopped plant material, even more plant material can be processed per batch due to increase in bulk density. In Pakistan and many other Asian and African countries, the farm sizes are smaller and fragmented; the small scale solar distillation systems best fit to these small farm sizes for on-farm distillation with solar energy and can provide a good opportunity to the farmers for small-scale business.

The distillation curves for percentage of total oil extracted against heat energy (kWh) were drawn. For each experiment, there is a specific energy level at which 100 % of essential oil is extracted. Regression analysis was performance an all predicted curves indicated the regression model of Sigmoid logistic with three parameters with high coefficient of determination ($R^2 > 0.90$). These processes display a dependent progression from small beginnings that accelerates and approaches a climax over time. These figures provide guidelines for the farmers to best utilize the resources while performing distillation experiments. The low energy consumptions for fresh herbs provide an opportunity to process more batches at farm level and hence justifying the on-farm installation of solar distillation system. The study also concludes that the chopped material gave better oils extraction results during experiments with Melissa, Peppermint, European Silver Fir. However, in some of the experiments, the same oil extraction results were obtained but these were less energy consuming comparatively. The solar distillation unit behaves simultaneously as a boiler for the generation of steam as well as provides necessary column height for easy and simple utilization of distillation technique at the farm level. The safety mountings and the instrumentation provides information to run the unit in safe working level. Sensor system also leads to extract full contents of the essential oils by monitoring the operational physical and thermal parameters. Results of essential oils contents per unit weight of dry matter of different plant materials were found almost similar to that of laboratory results.

The same procedure can be used at site specific location to get the optimum results for decentralized application of solar distillation system. On commercial scale, very large distillation units are available for the processing of medicinal and aromatic plants. This

technology is applicable for on-farm processing to promote rural development. It is economical and more suitable for the farm scale. In order to compensate the solar energy for bad weather conditions, a biomass boiler was also connected with the solar distillation system to compensate for bad weather conditions. In case of poor solar intensity, the solar biomass hybrid system worked quite satisfactorily. The energy ratio of biomass to solar energy was varied from 0.3 to 0.5 during most of the experiments conducted by hybrid solar-biomass distillation system. Essential oil extraction from herbs is sensitive and sophisticated process in terms of temperature and energy control. Successful results of distillation processes conclude that solar energy can be used successfully for different agro-based industrial processing by selecting appropriate solar systems. This solar renewable energy technology is free of operational costs, environmental friendly and provides an excellent opportunity for on-farm processing of medicinal and aromatic plants.

6 Outlook

In the article 4.10, results of some the distillation experiments with solar energy have been presented. Experiments were also conducted with water and steam distillation processes with Lavender (*Lavedula L*.), Basel, Calendula and other plant materials. For all experiments, successful results were obtained. The successful results concluded that the solar energy can be successfully used for the distillation of all kinds of medicinal and aromatic plants. These experiments were conducted with a specific size of the distillation still (100 liter capacity) which is capable to process 10 kg fresh plant material on fresh weight basis (un-chopped) and 15-20 kg chopped plant material.

The main object of the research is to develop an on-farm distillation system for essential oils extraction from different herbs and plant materials. However, provision was also given to the solar system for the on-farm food processing. For this purpose, special food grade pots (40 liters capacity) were used after modifying them according to the existing design of solar system. The back plate of secondary reflector was fabricated as a removable assembly which facilitates easy replacing of distillation still by food vessels. On the experimental farms near solar campus, a variety of fruits (Apples, Plums, Johannesburg, tomatoes etc) were available. Experiments were conducted for the manufacturing of jams from Johannesburg, and plums and tomato peeling from tomato using solar energy. The sterilization processes of the vessel and glass bottles were also carried out with solar energy before the food processing. These products were sealed and preserved. These food products were successfully processed by solar energy. The purpose of these trials was to introduce the farmers about the multifunctional use of solar energy in a very simple and easy method so that they may process their perishable products at the farm level.

7 Recommendations and suggestions

- The current study is conducted with only one batch type distillation still. It is recommended to use another identical distillation still to make one still always in operation and other on charging position to best utilize the solar energy and to distill more batches. The study also suggests a continuous type distillation system should be used to save the heat losses and time while charging a new batch.
- Laying reflectors provide an elevated focus directly on the receiver and thus need very small area of the secondary reflector to reflect these radiations to the bottom of distillation still. A significant amount of energy can be saved and can be used during distillation experiments.
- Out of the total losses from the distillation still, about 76 % losses are from the bottom part exposed to the solar radiations. The green house effect should be considered in secondary reflector to minimize these heat losses.
- Heat recovery system was used intermittently for the charging of new batches and to make up the water. It is suggested that the system should be modified to refill the distillation still continuously.
- As a solar concentrator is used for distillation experiments, these kinds of solar based systems are best suited for the regions with high beam radiations.
- The existing size of the distillation system is smaller as compared with the conventional field distillation units. It is recommended to develop big size solar distillation systems by using bigger size reflectors to save time and energy. Scheffler reflectors can be constructed up to 60 m^2 successfully.
- The existing solar distillation system was operated at atmospheric pressure. The system should be modified to run the distillation experiments at different pressures.

8 Summary

Processing of medicinal and aromatic plants by distillation method is one of the agro-based industries which lie in the medium temperature range. Essential oils extracted from these plant materials have been used throughout the world in foods, fragrances, perfumery, cosmetics and medicines and these oils are very expensive. With the introduction of innovative solar collectors, it is possible to use solar energy in the medium temperature range. The study was initiated to develop a de-centralized solar distillation system for the processing of medicinal and aromatic plants for functional, environmental and economic reasons. The system was installed at solar campus, University of Kassel, Witzenhausen, Germany to avail the fresh supply of herbs. Scheffler fixed focus concentrator (8 m^2 surface area) was used for solar distillation system. The system comprises of a primary reflector, secondary reflector, distillation still, condenser unit and Florentine flasks. The primary reflector rotates along an axis parallel to the earth axis of rotation and keeps the reflected beam aligned with the fixed secondary reflector as the sun moves. The secondary reflector further reflects the beam radiation to the targeted distillation still bottom. The distillation still was fabricated of a food grade stainless steel vessel having 1210 mm column height, 400 mm diameter, and 2 mm thickness. Stainless steel condenser is connected to the distillation still via a pipe. The distillation unit has provision to operate for “water distillation” and “water and steam distillation”. The solar distillation system is equipped with thermocouples and Pyranometer to control and optimize the distillation processes.

During the first phase of the research, laboratory experiments were conducted to determine the heat energy required per unit weight of different plant materials. Scheffler fixed focus concentrator was selected for the processing of medicinal and aromatic plants. A mathematical procedure has been explained to calculate the parabola equations for an 8 m^2 surface area Scheffler reflector for all the days of the year in the northern and southern hemisphere. The construction, installation and tracking details of the solar distillations system are also explained in the manuscript.

Two mathematical models were developed in Matlab and Microsoft Excel. First model is used to calculate the required size of the Scheffler reflector and the second model is applied to predict the energy distribution and heat losses from the solar distillation system. Under field experiments, several experiments were carried out to evaluate the

performance of the system. Within the beam radiation range of 700-800 W m^{-2}, temperature available at focus was found between 300 and 400 °C. These results show that profiles of primary reflector, tracking system, and inclinations of the axis of rotation are precise and converging the beam radiations at the targeted focal point with the changing sun position during the test period. During trials, average power and system efficiency were found to be 1.548 kW and 33.21 % respectively at an average solar radiations of 863 W m^{-2}. These results were found approximately the same as calculated from modeling under similar conditions. During the research, a steam receiver is also evaluated to produce steam for solar-based steam distillation system. The system efficiencies for the generation of steam by using only primary reflector and by using both primary and secondary reflectors were found to be 49.8 and 40 % respectively. It was concluded that about 9-10 % efficiency is lost by using the secondary reflector

Different medicinal and aromatic plant like Melissa, Peppermint, Oregano, Silver Fir, Lavender, Fennel, Rosemary, Cumin, Basil and Cloves, Lavender etc were processes successfully by solar distillation system. The results showed that different plant materials have different contents of oils and depend on the weight, moisture contents, part of plant material used. During sunny days, 4-5 batches can be processed with 10 kg of fresh plant material per batch. Experiments were also conducted with chopped plant material and the results were compared. The distillation curves for percent of total oil extracted against heat energy (kWh) were drawn. For each experiment, there is a specific energy level at which 100 % of essential oil is extracted. Regression analysis was performance and all predicted curves indicated the regression model of Sigmoid logistic with high coefficient of determination (R^2 > 0.90). The low energy consumptions for fresh herbs provide an opportunity to process more batches at farm level and hence justifying the on-farm installation of solar distillation system. Results of essential oils contents of different plant materials were found similar to that of laboratory results.

In order to run the distillation experiments during adverse climatic conditions, a biomass boiler was connected with the solar distillation system to make up any steam. Successful results were obtained by the solar-biomass hybrid system. This solar renewable energy technology is free of energy costs, environmental friendly and provides an excellent opportunity for on-farm processing of medicinal and aromatic plants.

Zusammenfassung

Die Verarbeitung von Arznei- und Gewürzpflanzen durch Destillation ist eine der landwirtschaftsnahen Nacherntetechnologien, die im mittleren Temperaturbereich betrieben werden. Ätherische Öle, extrahiert aus Pflanzen und zur Verwendung in der Nahrungsmittelindustrie, bei Duftstoffen, Parfums, Kosmetika und Arzneimitteln sind außergewöhnlich wertvoll. Mit der Einführung innovativer Solarkollektoren ist es möglich, Solarenergie für Prozesse im mittleren Temperaturbereich einzusetzen. Diese Arbeit beschreibt die Entwicklung und den Einsatz einer dezentralen solaren Destillationsanlage zur Verarbeitung von Arznei- und Gewürzpflanzen. Das System wurde auf dem Solar-Versuchsgelände der Universität Kassel in Witzenhausen installiert, wo auch erntefrische Kräutern verfügbar waren. Es wurde ein Scheffler Reflektor nach dem Fix-Focus Prinzip verwendet. Das System besteht aus Primär- und Sekundärreflektor sowie dem Destillationskessel mit Kondensator und Florentiner Flasche. Der Primärreflektor dreht sich entlang einer Achse parallel zur Rotationsachse der Erde der Sonnenbahn folgend und reflektiert die einfallende direkte Strahlung auf einen feststehendem Sekundärreflektor, der die Strahlung auf den Boden der Destillationsanlage spiegelt. Diese ist aus Edelstahl gefertigt, und hat eine Säulenhöhe von 1210 mm bei einem Durchmesser von 400 mm. Die Anlage kann durch einen Einlegeboden sowohl zur "Wasser-Destillation" als auch zur „Wasserdampf-Destillation" genutzt werden. Die solare Destille ist mit entsprechender Meßtechnik ausgestattet (Thermoelemente und Pyranometer), um eine Kontrolle und Optimierung des Prozesses zu ermöglichen.

Zu Beginn der Untersuchungen wurden Laborexperimente durchgeführt, um die notwendige Wärmeenergie pro Einheit der verschiedenen zu verarbeitenden pflanzlichen Materialien zu bestimmen. Anschließend wurde ein Scheffler - Konzentrator der Baugröße 8 m² ausgewählt und über ein mathematisches Verfahren die Parabel Gleichungen für alle Tage des Jahres sowohl in der nördlichen als auch der südlichen Hemisphäre berechnet. Der Bau, die Installation und die Nachführungs-Werte wurden ausführlich dokumentiert.

Zwei mathematische Modelle wurden unter Verwendung der Software-Pakete Matlab und Microsoft Excel entwickelt. Das erste Modell wird verwendet, um die erforderliche Größe des Scheffler-Reflektors berechnen zu können. Das zweite Modell wird angewandt, um die Energieverteilung und die Wärmeverluste bei dem solaren Destillations-System vorherzusagen. In anschließenden Feldversuchen wurde die Leistung des Systems

gemessen und bewertet. Innerhalb des Strahlungsbereiches von 700-800 W m^{-2} konnten Temperaturen zwischen 300 und 400 °C erreicht werden. Die Versuche zeigen, dass das Primär-Reflektor-System durch die Nachführung und die Neigung der Drehachse der Sonnenbahn folgend präzise die Strahlung auf den gewünschten Punkt bündeln kann. Die Leistung bei einer durchschnittlichen solaren Strahlung von 863 W m^{-2} betrug 1,548 kW bei einem Wirkungsgrad von 33,21%. Diese Ergebnisse entsprechen den Berechnungen aus der Modellierung unter ähnlichen Bedingungen. Zusätzlich wurde das System zur Produktion von Dampf unter Fortfall des Sekundärreflektors untersucht. Der Wirkungsgrad betrug hier mit dem Primärreflektor 49,8 %, mit beiden Reflektoren 40 %, so dass etwa 9-10 % Effizienz durch die Verwendung der Sekundärreflektors verloren gehen.

Anschließend wurden aromatische Pflanzen wie Melisse, Pfefferminze, Oregano, Edeltanne, Lavendel, Fenchel, Rosmarin, Kümmel, Basilikum und Nelken mit dem solaren Destillations-System verarbeitet. Die Ergebnisse zeigen, dass die verschiedenen pflanzlichen Rohstoffe unterschiedliche Ölgehalte haben und diese auch vom Feuchtigkeitsgehalt, der Vorbereitung (geschnitten) und dem verwendeten Pflanzenteil abhängen. An sonnigen Tagen kann die Anlage 4 - 5 Chargen mit je 10 kg frischem Pflanzenmaterial pro Durchlauf verarbeiten. Die Kurven für den Destillationsprozess wurden als Prozentzahl der Gesamtölmenge gegenüber der notwendigen Wärmeenergie (kWh) dargestellt, so dass für jeden Versuch der spezifische Energiebedarf, bei dem 100 % des enthaltenen ätherischen Öls gewonnen wird, dargestellt werden kann. Mittels einer Regressionsanalyse wurde für die Experimente ein hoher Determinationskoeffizient (R^2>0,90) berechnet. Um die Destillation auch bei ungünstigen klimatischen Bedingungen zu ermöglichen wurde zusätzlich ein Biomasse-Ofen an das solare Destillations System angeschlossen und erfolgreich betrieben. Insgesamt konnte die Funktionsfähigkeit des solaren Destillations-Systems und seine Eignung zum On-Farm-Betrieb nachgewiesen werden, so dass sich neue Möglichkeiten für die dezentrale Verarbeitung von empfindlichen aromatischen Pflanzen ergeben.

Literature Cited

Abdel-Dayem, A.M., Mohamad, M.A., 2001. Potential of solar energy utilization in the textile industry-a case study. Renewable Energy 23, 685-694

Akerele, O., 1993. Summary of WHO guidelines for the assessment of herbal medicines. HerbalGram 28, 13-19

Anonymous, 1970. Solar distillation as a mean of meeting small-scale demands, UNITED NATIONS, New York, USA

Anonymous, 1998. Waserdampf-Destillation ätherischer Öle aus frischen oder angewelkten Pflanzen

Aslam, M., 2002. Conservation, cultivation and trade of medicinal herbs and spices in Pakistan, International workshop on health Challenges of 21st Century and Traditional medicines in SAARC Region

Ayanoglu, F., Arslan, M., Hatay, A. 2005 Effects of harvesting stages, harvesting hours, and drying methods on essential oil content of Lemon Balm in Eastern Mediterranean. International Journal of Botany 1(2) (2005) 138-142

Balzar, A., Stumpf, P., Eckhoff, S., Ackermann, H., Grupp, M., 1996. A solar cooker using vacuum-tube collectors with integrated heat pipes, Solar Energy 58 (1996) 63-68

Baser, K.H.C., 1999. Industrial utilization of medicinal and aromatic Plants. Proceedings of Second World Congress on Medicinal and Aromatic Plants for Human Welfare, 10-15 November 1997, Mendoza, Argentina. Martinov M, Bandoni A, Blaak G, Capelle N, editors. Acta Hort. 503: 21-29

Basta, A., Tzakou, O., Couladis, M. 2005. Composition of the leaves essential oil of Melissa officinalis L. S.I. from Greece. Flavor and Fragrance Journal 20 (2005) 642-644

Bensky, D., Clavey, S., Stoger, E., Gamble A., 2004. Chinese Herbal Medicine: Materia Medica, Third Edition by Dan Bensky, Steven Clavey, Erich Stoger, and Andrew Gamble

Benz, N., Gut, M, Rub W. 1998. Solar process heat in breweries and dairies, Proceedings of EuroSun 98, Portoroz, Slovenia, 1998 (on CD-Rom)

Bhirud, N., Tandale M.S., 2006. Field evaluation of a fixed-focus concentrators for industrial oven, Advances in Energy Research (AER – 2006)

Blum, H., Lorenz, J., 2005. Ergebnisse der vergleichenden Prüfung von drei Sorten der Zitronenmelisse (*Melissa officinalis L.).* In: Zeitschrift für Arznei-und Gewürzpflanzen 10(3) (2005), S. 133-139

Bomme, U., 2001.Kulturanleitung für Zitronenmelisse. 4. Grundlegend überarbeitete. Bayerische Landesanstalt für Bodenkultur und Pflanzenbau.

Bown. D., 1995. Encyclopaedia of herbs and their uses. Dorling Kindersley, London. ISBN 0-7513-020-31

Bruce, S., 2001. Introduction to growing herbs, for essential oils, Medicinal and Culinary purposes, Crop & Food Research, Number 45

Busse, W., 2000. The significancy of quality for efficacy and safety of herbal medicinal products. Drug Inf. J. 34, 15-23

Calixto, J.B., 2000. Efficacy, safety, quality control, marketing and regulatory guidelines for herbal medicines (phytotherapeutic agents). Braz. J. Med. Biol. Res. 33, 179-189

Cengel, A.Y.,, 2006. Heat and mass transfer, A practical approach, third Edition, McGraw-Hill Companies, Inc, 1221 Avenue of the Americas, New York, NY 10020

Challa, A., Ahmad, N., Mukhtar, H., 1997. Cancer prevention through sensible nutrition (Commentary). International journal of Oncology, 11, 1387-1392

Chan, K., 2003. Some aspects of toxic contaminants in herbal medicines. Chemosphere 52, 1361-1371

Chiej. R. 1984 Encyclopaedia of Medicinal Plants. MacDonald 1984 ISBN 0-356-10541-5

Chmelik, S., 1999. Chinese Herbal Secrets, The key to total health. New Leaf an imprint of Gill & Macmillan Ltd, Goldenbridge Dublin 8, The IVY Press Limited 2/3 str. Andrews place, Lewes, East Sussex

Clark, J.A., 1982. An analysis of the technical and economic performance of a parabola trough concentrator for solar industrial process heat application. International journal of heat and mass transfer, 1427-1438

Cordeiro, D.S., Oliveira, W.P., 2005. Technical aspects of the production of dried extracts of Maytenus ilicifolia leaves by jet spouted bed drying

Cuervo, S.P., Hensel, O., 2008 Conference on International Research on Food Security, Natural Resource Management and Rural Development, Tropentag 2008 University of Hohenheim, October 7-9, 2008

Dachler, M.. Pelzman, H., 1989. Heil- und Gewürzpflanzen, Anbau-Ernte-Aufbereitung: Östterreichischer Agrarverlag, Wien;40p

Delaney, D. 2003. Scheffler's community solar cooker, www.solar-bruecke.org

Denny, E.F.K., 1991. Field distillation for Herbaceous Oils, second Edition, Denny, McKenzie associates, Lilydate, Tasmania 7268, Australia

Diplock, T.A., Charleux, J.L., Crozier-Willi, G., Kok, F.J., Rice-avans, C., Roberfroid, M., Staul, W., Vina- Ribes, J., 1998. Functional food science and defence against reactive oxidative species, British Journal of Nutrition, 80, 77-112

Dürbeck, K., 1997. The distillation of essential oils, manufacturing and plant construction handbook, Protrade:Department Foodstuffs and agricultural products, Deutsche Geselschaft für Technische Zuzammenarbeit (GTZ) GmbH. P.O box 5180 D-65726 Eschborn, Federal republic of Germany

Duffie, J., Beckman, W., 2006. Solar engineering of thermal processes, 3rd edition, John Wiley& Sons, Inc.Hoboken, New Jersey ISBN -13 978-0-471-69867-8

Esen, M., 2004. Thermal performance of a solar cooker integrated vacuum-tube collector with heat pipes containing different refrigerants, Solar Energy 76 (2004) 751-757

Eskin, N., 2000. Performance analysis of solar process heat system. Energy conservation and management. 41, 1141-1154

Essandoh-Yeddu, J.J., 1993. Prospects for using solar energy power systems to meet energy requirements of agricultural facilities located in remote areas. Proceeding of National Energy Symposium 93, vol. 5. 1993

ESTIF (European Solar Thermal Industry Federation), 2004 A study on key issues for renewable heat in Europe (K4RES-H). Solar industrial process heat–WP3 Task 3.5, Contact EIE/04/204\S07.38607

Estrada, C.A., Jaramillo, O.A., Acosta, R., Arancibia-Bulnes, C.A., 2007. Heat transfer analysis in a calorimeter for concentrated solar radiation measurements, Solar Energy 81, 1306-1313

FAO., 1992. Minor Oil Crops, Essential Oils, Part III. Minor Oil Crops, Part I-Edible Oils, Part II-Non Edible Oils, Part III- Essential Oils. FAO Agricultural Services Bulletin; 94: 175-2417

Fargali, H.M., Nafeh, A.A., Fahmy, F.H., Hassan, M.A., 2008. Medicinal herb drying using a photovoltaic array and a solar thermal system. Solar Energy 82, 1154-1160

Fend, T., Jorgensen, G., Küste, H., 2000. Applicability of highly reflective aluminium coil for solar concentrators, Solar Energy 2000, 361-370

Funk, P.A., 2000. Evaluating the international standard procedure for testing solar cookers and reporting performance. Solar Energy 2000, 1-7

Garg, H.P., Kumar, R., 2001. Developments in solar drying, In: Proceedings of the Second Asian-Oceania Drying Conference (ADC 2001), Batu Feringhi, Pulau Pinang, Malaysia, pp. 297–319

Garg, H.P., Prakash, J., 2006. Solar energy for industrial process heat, in “Solar energy fundamentals and applications”, Tata McGraw-Hill, New Delhi

Goswami, D.Y., 1999. Principle of Solar Engineering, George H.Bchanan Co., Philadelphia. USA

Heeger, E., 1980. Handbuch des Arznei-und Gewürzpflanzen Drogengewinnung. VEB Deutscher Landwirtschaftsverlag, 1980

Hu, F.B., Willet, W.C., 2002. Optimal diets for prevention of coronary heart diseases. Journal of American Medical Association, 2888, 2569-2578

Jannot, Yves, 2003. Cours de transert thermique (Downloaded on 05-02-2010)

Jayasimha, B.K., 2006. Application of Scheffler reflectors for process industry, International Solar Cooker Conference 2006 in Granada, Spain

Jenkins, N., 1995. Photovoltaic systems for small-scale remote power supplies. Power Engineering Journal 1995, 9(2):89–96

Kalogirou, S., 2003. Potential of solar industrial process heat applications, Applied Energy 76, 337-361

Kalogirou, S.A., 2004. Optimization of solar systems using artificial neural networks and genetic algorithm. Applied Energy 77, 383-405

Kapecka, E., Mareczek, A., Leja, M., 2005. Antioxidant activity of fresh and dry herbs of some Lamiaceae species. Food chemistry 93 (2005) 223-226

Khurmi, R.S., Gupta, J.K., 2005. A text book of thermal Engineering, Ram Nagar, New Delhi-110055

Klein, S.A., Beckman, W.A., 1979. A general design method for closed loop solar energy systems. Solar Energy 22, 269-282

Klein, S.A., Beckman, W.A., Duffie, J.A., 1976. A design procedure for solar heating systems. Solar Energy 18, 113-127

Koller, W.D., 1987. Problems with the flavour of herbs and spices. Proceeding of the fifth Int. Flavour conference, Porto Karras, Chalkidiki, Greece, 123-132

Kulkarni, G.N., Kedare, S.B., Bandyopadhyay, S., 2007. Determination of design space and optimization of solar water heating systems , Solar Energy 81, 958-968

Kulkarni, G.N., Kedare, S.B., Bandyopadhyay, S., 2008. Design of solar thermal systems utilizing pressurized hot water storage for industrial applications. Solar Energy 82, Issue 8, August 2008, 686-699

Kumar, N.S., Reddy K.S., 2007. Numerical investigation of natural convection heat loss in modified cavity receiver for fuzzy focal solar dish concentrator. Solar Energy 81, 846-855

Kutscher, C.F., Davenport, R.L., Dougherty, D.A., Gee, R.C., Masterson, M.P., Kenneth, M., 1982. Design approaches of solar industrial process heat systems. Solar Energy Research Institude, USA

Lawrence, B.M., 1978. Essential Oils, Allured publishing Corporation, P.O Box 318, Wheaton, Illinois 60187, USA. pp16

Lawrence, B.M., 1995. The isolation of aromatic materials from natural plant products. In: A manual on the essential oils industry. K Tulrey De siva, Editor. UNIDO, Vienna, Austria. 57-154

Madsen, H.L., & Bertelsen, G., 1995. Species as antioxidants. Trends in food Science and Technology, 6, 271-276

Malle, B., Schmickl, H., 2005. Ätherische Öle selbst herstellen, Verlag Die Werkstatt GmbH Lotzestraße 24 a, D- 37083 Göttingen pp 23-27

Mills, D., 2004. Advances in solar thermal electricity technology. Solar Energy 76, 19–31

Morrison, G.L., Di, J., Mills, D. R., 1993. Solar stove for developed countries. Kaboldy E (Ed) , Proceedings of ISES World Congress, August 23-27, Budapest, Hungry, Hungarian Energy Society, Vol 5, pp 491-496

Müller, J., 1992. Trocknung von Arzheip Pflanzen mit Solar Energy. Dissertation. Ulmer Verlag. Germany

Munir, A., Hensel, O., 2007. Development of solar distillation system for essential oils extraction from herbs in the international conference “Utilization of diversity in land use systems: Sustainable and organic approaches to meet human needs (Tropentag 2007), Germany

Munir, A., Hensel, O., 2008. Development and experimental results of solar distillation system for essential oils extraction from herbs, Paper published and oral presentation in “CIOSTA XXXIII CIGR CONFERENCE 2009 and Workshop IUFRO, Technology

and management to ensure sustainable agriculture, agro-system, forestry and safety". University Mediterranea of Reggio Calabria, Italy on 16-06-09 to 19-06-09

Munir, A., Hensel, O., 2008. Development and optimization of solar distillation system for essential oils extraction from herbs in the international conference " Sustainable use of natural resources in developing countries" organized by Czech university of Life Sciences, Prague, Czech Republic. The conference was held on November 20-21, 2008

Munir, A., Hensel, O., 2008. Experimental results of essential oils extraction from herbs using solar energy in the international conference "Competition for resources in a changing world: New drive for rural development (Tropentag 2008) organized by University of Hohenheim, Stuttgart on October 7-9, 2008

Munir, A., Hensel, O., 2008. Solar distillation for essential oils extraction - a decentralized approach for rural development, Paper published in "International Solar Food Processing Conference 2009", in Indore, India (CD Rom)

Munir, A., Hensel, O., 2009. Biomass energy utilization in solar distillation system for essential oils extraction from herbs, International conference for "Biophysical and Socio-economic Frame Conditions for the Sustainable Management of Natural Resources" (Tropentag 2009) on October 6 - 8, 2009 in university of Hamburg, Germany

Munir, A; Hensel, O., 2008. Investigation of optimal thermal parameters during distillation of essential oils from herbs in the international conference "Competition for resources in a changing world: New drive for rural development (Tropentag 2008) organized by University of Hohenheim, Stuttgart, Germany on October 7-9, 2008

Norten, B., 1999. Solar process heat: Distillation drying, agricultural and industrial uses. In: Proceedings of ISES Solar world congress 1999, Jerusalem, Israel (on CD-ROM, P. 1334-8)

Okoro, O.I., Madueme, T.C., 2004. Solar energy investments in a developing economy, Renewable Energy 29, 1599-1610

Oparaku, O.U., Iloeje, O.C., 1991. Design considerations for a photovoltaic-powered water-pumping facility in a rural village near Nsukka. Nigerian Journal of Renewable Energy 1991; 10, 64–69

Oyen L.P.A., Dung., N.X., 1999. Plant Resources of South-East Asia No. 19. Essential-oils plants. Backhuys Publishers, Leiden. P.O Box 321, 2300 AH Leiden, the Netherlands

Öztekin, S., Martinov, M., 2007. Medicinal and aromatic crops, harvesting, drying and processing, Haworth Food & Agricultural Products Press™ , An Imprint of the Haworth Press, Inc., 10 Alice Street, Binhamton, New York 13904-1580 USA

Pareira, M.C., Gordon, J.M., Rabi, A., Zarmi, Y., 1984. Design and optimization of solar industrial hot water systems with storage. Solar Energy 32, 121-133

Proctor, D., Morse, R.N., 1977. Solar energy for the Australian food processing industry. Solar Energy, 19, 63-72

Runha, F.P., Cordeiro, D.S., Pereira, C.A.M., Vilegas, J., Olivera.W.P., 2001. Production of dry extracts of medicinal Brazilian plants by spouted bed process: Development of process and evaluation of thermal degradation during the drying operations. TransIchemE 79, 160-168, Part C

Scheffler, W., 2006. Introduction to the revolutionary design of Scheffler, SCIs International Solar cooker conference, 2006 in Granada, Spain

Sharma, S.D., Iwata, T., Kitano, H., 2005. Thermal performance of a solar cooker based on an evacuated tube collector with a PCM storage unit, Solar Energy, 78 (2005), 416-426

Shilcher, H., 1987. Chamamile (In German). Wissenschaftliche Verlaggesllschaft mbH, Stuttgard, Germany

Solar heat for industrial processes, SHE Annex 33, Solar PACES Annex 4. International Energy Agency, pp. 2-7

Soysal, Y., 2000. Research on Fundamental of MAF Drying and developing a Field Scale Cabinet Dryer (In Turkish). PhD. Thesis. Cukurova University , Adana, Turkey

Spate, F., Hafner, B., Schwarzer, K., 1999. A system for solar process heat for decentralized applications in developing countries. In: Proceedings of ISES Solar World Congress 1999, Jerusalem, Israel

Stumpf, P., Balzar, A., 2001. Comparative measurements and theoretical modeling of a single - and double-stage heat pipe coupled solar cooking systems for high temperatures, Solar Energy 71 (2001) 1-10

Sutter, C., 1996. Evaluation of solar community kitchen in Gujrat, Group ULOG, Morgartenring 18 CH-4054 Basel, Switzerland

Usher, G., 1974. A Dictionary of Plants Used by Man. Constable 1974 ISBN 0094579202

Vukik, R., Perunicic, Mi., Brujic, B. 1995. Distillation and extraction plants in a single unit. Plant report (In Serbian) ;2(2): 39-43

Wang, X.D., Zhao, L., Wang, J.L., Zhang, W.Z., Zhao, X.Z., Wu, W., 2010. Performance evaluation of a low-temperature solar Rankine cycle system utilizing R245fa, Solar Energy 84 (2010) 353–364

Weiss, W., Rommel, M., 2005. Medium Temperature collectors, State of the art within task 33/IV, subtask C, Solar Heat for Industrial processes. International Energy Agency

Winter, C.-J., Sizman, R.L., Van-Hull, L.L., 1991. Solar Power Plants, Fundamentals, Technology, Systems, Economics, ISBN 3-540-18897-5 Springer-Verlag Berlin Heidelberg New York

Yahya, M., Sopian, K., Daud, W.R.W., Othman, M.Y., Yatim, B., 2001. Design of solar assisted dehumidification of air drying system for medicinal herbs: pegaga leaf, In: Proceedings of the Second Asian-Oceania Drying Conference (ADC 2001), Batu Feringhi, Pulau Pinang, Malaysia, pp. 383–392

Appendices

Appendix A

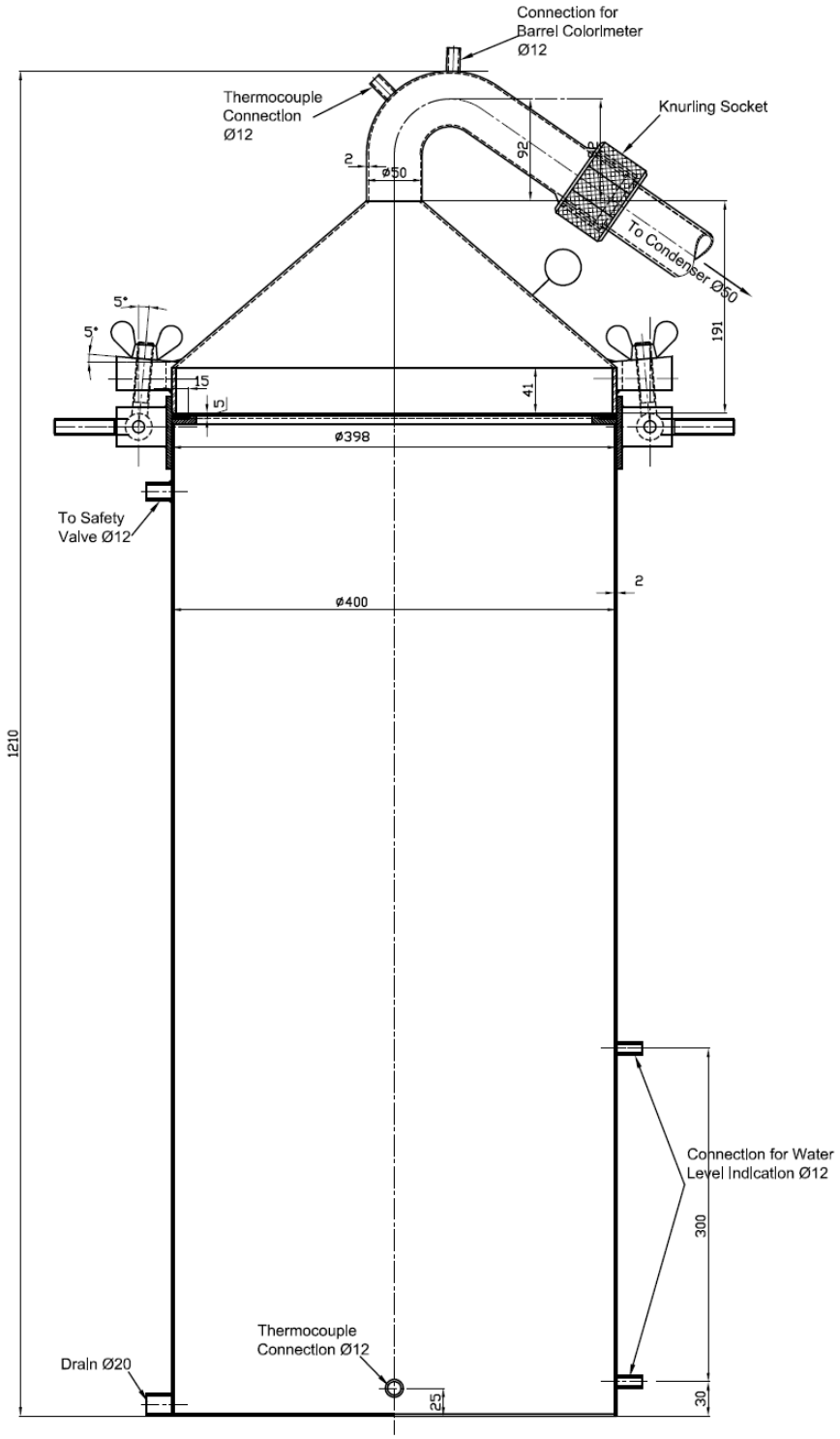

Figure 1-A Distillation still for the solar distillation system

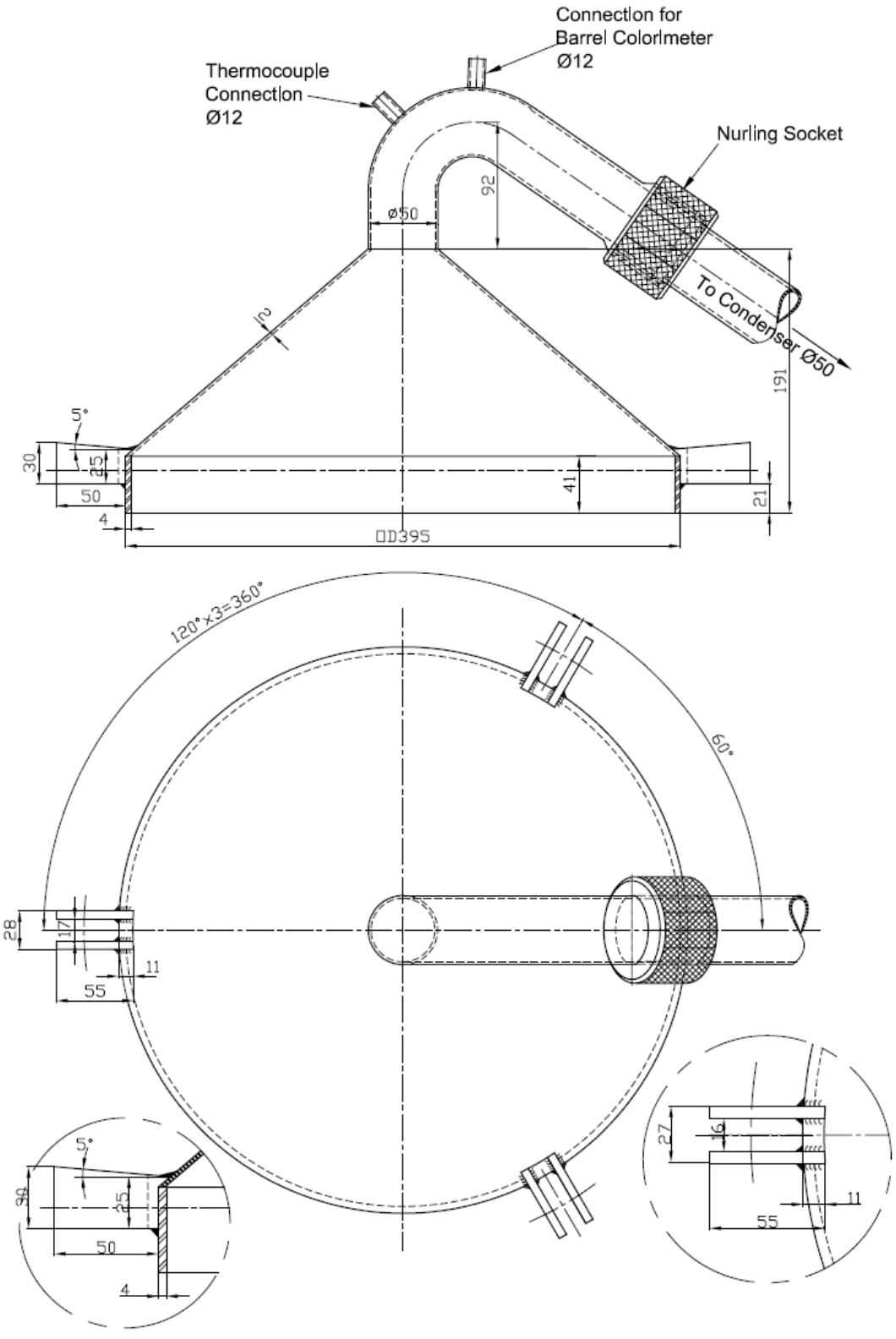

Figure 2-A Top cover of the distillation still

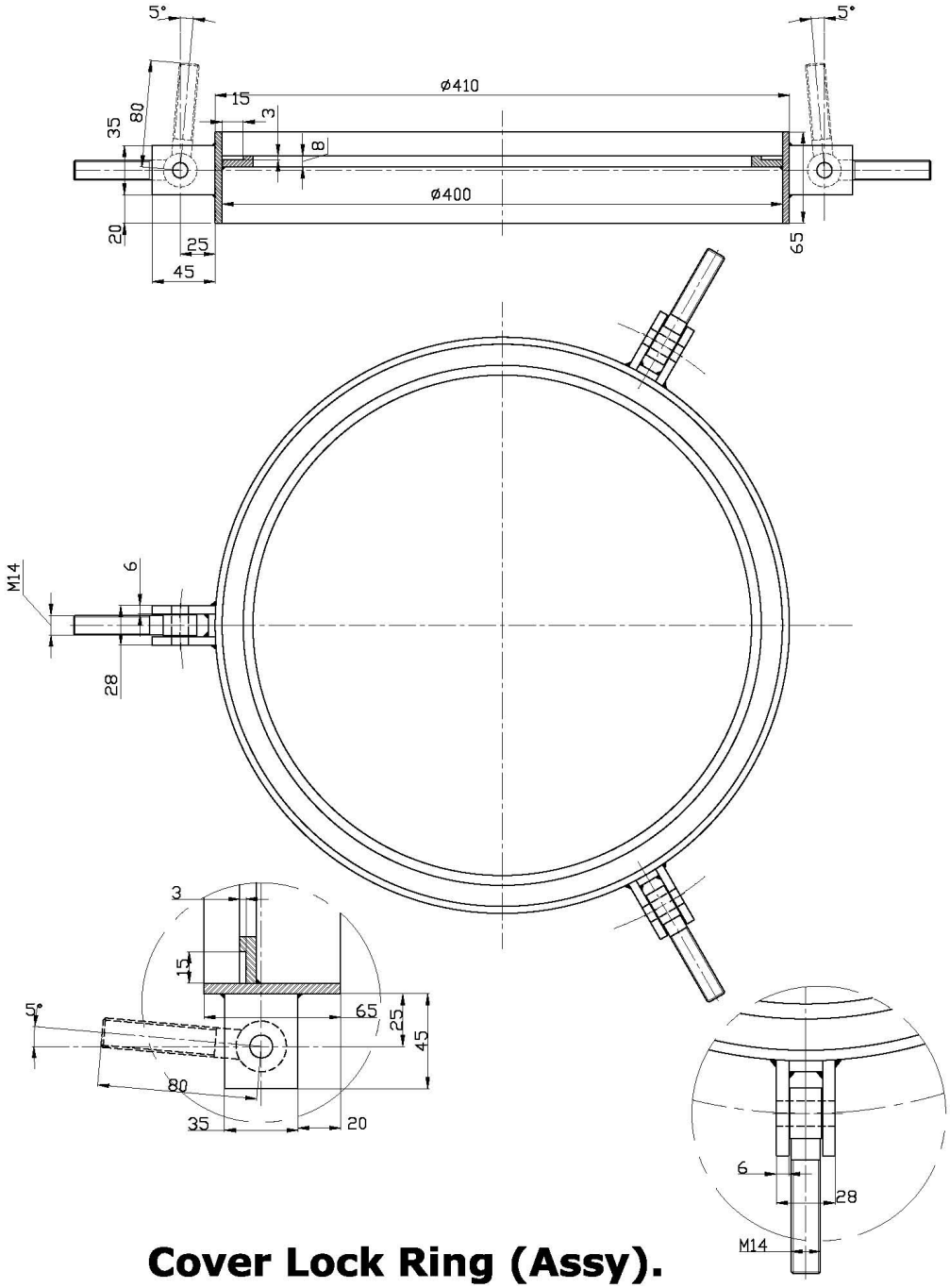

Figure 3-A Description of cover lock assembly of the distillation still

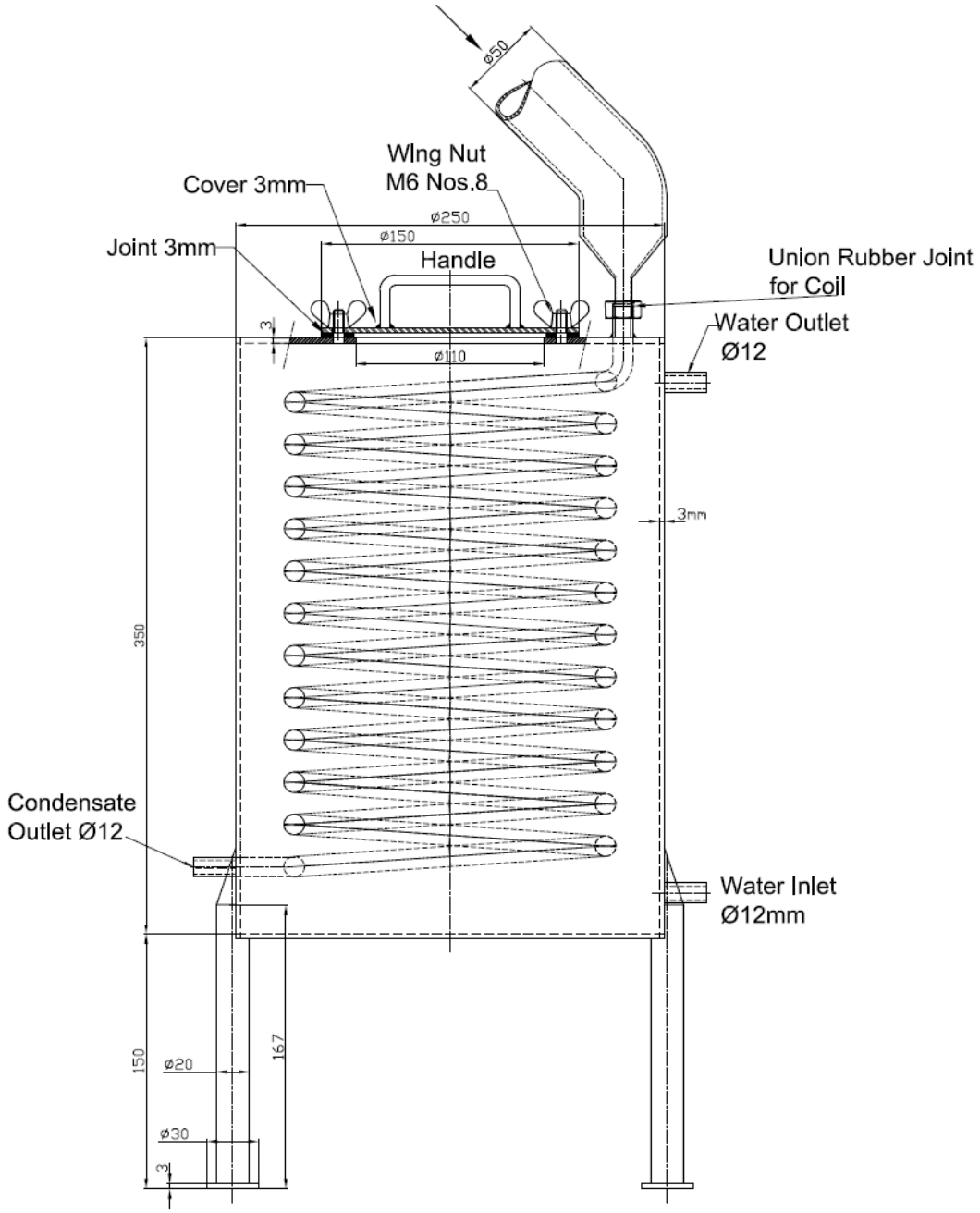

Figure 4-A Condenser for the solar distillation system

Appendix B

Date	Day of the year “n”	Delta “δ” (degrees)	Aperture in Northern hemisphere “As” (m^2)	Aperture in Southern hemisphere “As” (m^2)
1-Jan	1	-23.06	6.80	4.61
2-Jan	2	-22.98	6.80	4.62
3-Jan	3	-22.89	6.79	4.62
4-Jan	4	-22.80	6.79	4.63
5-Jan	5	-22.70	6.79	4.63
6-Jan	6	-22.59	6.78	4.64
7-Jan	7	-22.47	6.78	4.64
8-Jan	8	-22.35	6.77	4.65
9-Jan	9	-22.21	6.77	4.66
10-Jan	10	-22.07	6.76	4.67
11-Jan	11	-21.93	6.76	4.68
12-Jan	12	-21.77	6.75	4.68
13-Jan	13	-21.61	6.75	4.69
14-Jan	14	-21.45	6.74	4.70
15-Jan	15	-21.27	6.73	4.71
16-Jan	16	-21.09	6.73	4.72
17-Jan	17	-20.90	6.72	4.73
18-Jan	18	-20.71	6.71	4.74
19-Jan	19	-20.51	6.70	4.76
20-Jan	20	-20.30	6.70	4.77
21-Jan	21	-20.09	6.69	4.78
22-Jan	22	-19.87	6.68	4.79
23-Jan	23	-19.64	6.67	4.80
24-Jan	24	-19.41	6.66	4.82
25-Jan	25	-19.17	6.65	4.83
26-Jan	26	-18.92	6.64	4.84
27-Jan	27	-18.67	6.63	4.86
28-Jan	28	-18.42	6.62	4.87

29-Jan	29	-18.15	6.61	4.89
30-Jan	30	-17.89	6.60	4.90
31-Jan	31	-17.61	6.59	4.92
1-Feb	32	-17.34	6.58	4.93
2-Feb	33	-17.05	6.57	4.95
3-Feb	34	-16.76	6.56	4.96
4-Feb	35	-16.47	6.55	4.98
5-Feb	36	-16.17	6.53	4.99
6-Feb	37	-15.87	6.52	5.01
7-Feb	38	-15.56	6.51	5.03
8-Feb	39	-15.25	6.50	5.04
9-Feb	40	-14.93	6.48	5.06
10-Feb	41	-14.61	6.47	5.08
11-Feb	42	-14.29	6.46	5.10
12-Feb	43	-13.96	6.44	5.11
13-Feb	44	-13.63	6.43	5.13
14-Feb	45	-13.29	6.42	5.15
15-Feb	46	-12.95	6.40	5.17
16-Feb	47	-12.61	6.39	5.19
17-Feb	48	-12.26	6.37	5.20
18-Feb	49	-11.91	6.36	5.22
19-Feb	50	-11.56	6.34	5.24
20-Feb	51	-11.20	6.33	5.26
21-Feb	52	-10.84	6.31	5.28
22-Feb	53	-10.48	6.30	5.30
23-Feb	54	-10.12	6.28	5.32
24-Feb	55	-9.75	6.27	5.34
25-Feb	56	-9.38	6.25	5.36
26-Feb	57	-9.01	6.23	5.37
27-Feb	58	-8.63	6.22	5.39
28-Feb	59	-8.26	6.20	5.41
29-Feb	60	-7.88	6.18	5.43
1-Mar	61	-7.50	6.17	5.45
2-Mar	62	-7.12	6.15	5.47

3-Mar	63	-6.73	6.13	5.49
4-Mar	64	-6.35	6.12	5.51
5-Mar	65	-5.96	6.10	5.53
6-Mar	66	-5.57	6.08	5.55
7-Mar	67	-5.19	6.06	5.57
8-Mar	68	-4.79	6.05	5.59
9-Mar	69	-4.40	6.03	5.61
10-Mar	70	-4.01	6.01	5.63
11-Mar	71	-3.62	5.99	5.65
12-Mar	72	-3.23	5.97	5.67
13-Mar	73	-2.83	5.96	5.69
14-Mar	74	-2.44	5.94	5.70
15-Mar	75	-2.04	5.92	5.72
16-Mar	76	-1.65	5.90	5.74
17-Mar	77	-1.25	5.88	5.76
18-Mar	78	-0.86	5.86	5.78
19-Mar	79	-0.46	5.84	5.80
20-Mar	80	-0.07	5.83	5.82
21-Mar	81	0.33	5.81	5.84
22-Mar	82	0.72	5.79	5.86
23-Mar	83	1.12	5.77	5.88
24-Mar	84	1.51	5.75	5.89
25-Mar	85	1.90	5.73	5.91
26-Mar	86	2.30	5.71	5.93
27-Mar	87	2.69	5.69	5.95
28-Mar	88	3.08	5.67	5.97
29-Mar	89	3.47	5.65	5.99
30-Mar	90	3.86	5.64	6.00
31-Mar	91	4.24	5.62	6.02
1-Apr	92	4.63	5.60	6.04
2-Apr	93	5.01	5.58	6.06
3-Apr	94	5.40	5.56	6.07
4-Apr	95	5.78	5.54	6.09
5-Apr	96	6.16	5.52	6.11

6-Apr	97	6.53	5.50	6.13
7-Apr	98	6.91	5.48	6.14
8-Apr	99	7.28	5.46	6.16
9-Apr	100	7.66	5.44	6.18
10-Apr	101	8.03	5.43	6.19
11-Apr	102	8.39	5.41	6.21
12-Apr	103	8.76	5.39	6.22
13-Apr	104	9.12	5.37	6.24
14-Apr	105	9.48	5.35	6.26
15-Apr	106	9.84	5.33	6.27
16-Apr	107	10.19	5.31	6.29
17-Apr	108	10.55	5.30	6.30
18-Apr	109	10.89	5.28	6.32
19-Apr	110	11.24	5.26	6.33
20-Apr	111	11.58	5.24	6.35
21-Apr	112	11.92	5.22	6.36
22-Apr	113	12.26	5.20	6.37
23-Apr	114	12.60	5.19	6.39
24-Apr	115	12.93	5.17	6.40
25-Apr	116	13.25	5.15	6.42
26-Apr	117	13.57	5.13	6.43
27-Apr	118	13.89	5.12	6.44
28-Apr	119	14.21	5.10	6.45
29-Apr	120	14.52	5.08	6.47
30-Apr	121	14.83	5.07	6.48
1-May	122	15.13	5.05	6.49
2-May	123	15.43	5.04	6.50
3-May	124	15.73	5.02	6.52
4-May	125	16.02	5.00	6.53
5-May	126	16.31	4.99	6.54
6-May	127	16.59	4.97	6.55
7-May	128	16.87	4.96	6.56
8-May	129	17.14	4.94	6.57
9-May	130	17.41	4.93	6.58

10-May	131	17.67	4.91	6.59
11-May	132	17.93	4.90	6.60
12-May	133	18.18	4.88	6.61
13-May	134	18.43	4.87	6.62
14-May	135	18.67	4.86	6.63
15-May	136	18.91	4.84	6.64
16-May	137	19.14	4.83	6.65
17-May	138	19.37	4.82	6.66
18-May	139	19.59	4.81	6.67
19-May	140	19.81	4.79	6.68
20-May	141	20.02	4.78	6.69
21-May	142	20.23	4.77	6.69
22-May	143	20.43	4.76	6.70
23-May	144	20.62	4.75	6.71
24-May	145	20.81	4.74	6.72
25-May	146	20.99	4.73	6.72
26-May	147	21.16	4.72	6.73
27-May	148	21.33	4.71	6.74
28-May	149	21.50	4.70	6.74
29-May	150	21.65	4.69	6.75
30-May	151	21.80	4.68	6.75
31-May	152	21.95	4.67	6.76
1-Jun	153	22.09	4.67	6.76
2-Jun	154	22.22	4.66	6.77
3-Jun	155	22.34	4.65	6.77
4-Jun	156	22.46	4.65	6.78
5-Jun	157	22.58	4.64	6.78
6-Jun	158	22.68	4.63	6.79
7-Jun	159	22.78	4.63	6.79
8-Jun	160	22.87	4.62	6.79
9-Jun	161	22.96	4.62	6.80
10-Jun	162	23.04	4.61	6.80
11-Jun	163	23.11	4.61	6.80
12-Jun	164	23.18	4.60	6.80

13-Jun	165	23.23	4.60	6.81
14-Jun	166	23.29	4.60	6.81
15-Jun	167	23.33	4.60	6.81
16-Jun	168	23.37	4.59	6.81
17-Jun	169	23.40	4.59	6.81
18-Jun	170	23.42	4.59	6.81
19-Jun	171	23.44	4.59	6.81
20-Jun	172	23.45	4.59	6.81
21-Jun	173	23.46	4.59	6.81
22-Jun	174	23.45	4.59	6.81
23-Jun	175	23.44	4.59	6.81
24-Jun	176	23.42	4.59	6.81
25-Jun	177	23.40	4.59	6.81
26-Jun	178	23.37	4.59	6.81
27-Jun	179	23.33	4.60	6.81
28-Jun	180	23.29	4.60	6.81
29-Jun	181	23.24	4.60	6.81
30-Jun	182	23.18	4.60	6.80
1-Jul	183	23.11	4.61	6.80
2-Jul	184	23.04	4.61	6.80
3-Jul	185	22.96	4.62	6.80
4-Jul	186	22.88	4.62	6.79
5-Jul	187	22.78	4.63	6.79
6-Jul	188	22.69	4.63	6.79
7-Jul	189	22.58	4.64	6.78
8-Jul	190	22.47	4.64	6.78
9-Jul	191	22.35	4.65	6.77
10-Jul	192	22.23	4.66	6.77
11-Jul	193	22.09	4.67	6.76
12-Jul	194	21.96	4.67	6.76
13-Jul	195	21.81	4.68	6.75
14-Jul	196	21.66	4.69	6.75
15-Jul	197	21.51	4.70	6.74
16-Jul	198	21.35	4.71	6.74

17-Jul	199	21.18	4.72	6.73
18-Jul	200	21.00	4.73	6.72
19-Jul	201	20.82	4.74	6.72
20-Jul	202	20.64	4.75	6.71
21-Jul	203	20.44	4.76	6.70
22-Jul	204	20.25	4.77	6.69
23-Jul	205	20.04	4.78	6.69
24-Jul	206	19.84	4.79	6.68
25-Jul	207	19.62	4.80	6.67
26-Jul	208	19.40	4.82	6.66
27-Jul	209	19.18	4.83	6.65
28-Jul	210	18.95	4.84	6.64
29-Jul	211	18.71	4.86	6.63
30-Jul	212	18.47	4.87	6.63
31-Jul	213	18.22	4.88	6.62
1-Aug	214	17.97	4.90	6.61
2-Aug	215	17.72	4.91	6.60
3-Aug	216	17.46	4.92	6.59
4-Aug	217	17.19	4.94	6.58
5-Aug	218	16.92	4.95	6.56
6-Aug	219	16.65	4.97	6.55
7-Aug	220	16.37	4.98	6.54
8-Aug	221	16.09	5.00	6.53
9-Aug	222	15.80	5.02	6.52
10-Aug	223	15.51	5.03	6.51
11-Aug	224	15.21	5.05	6.50
12-Aug	225	14.91	5.06	6.48
13-Aug	226	14.61	5.08	6.47
14-Aug	227	14.30	5.10	6.46
15-Aug	228	13.99	5.11	6.45
16-Aug	229	13.67	5.13	6.43
17-Aug	230	13.36	5.15	6.42
18-Aug	231	13.03	5.16	6.41
19-Aug	232	12.71	5.18	6.39

20-Aug	233	12.38	5.20	6.38
21-Aug	234	12.05	5.22	6.36
22-Aug	235	11.71	5.23	6.35
23-Aug	236	11.38	5.25	6.34
24-Aug	237	11.03	5.27	6.32
25-Aug	238	10.69	5.29	6.31
26-Aug	239	10.34	5.31	6.29
27-Aug	240	9.99	5.32	6.28
28-Aug	241	9.64	5.34	6.26
29-Aug	242	9.29	5.36	6.25
30-Aug	243	8.93	5.38	6.23
31-Aug	244	8.57	5.40	6.22
1-Sep	245	8.21	5.42	6.20
2-Sep	246	7.85	5.43	6.18
3-Sep	247	7.48	5.45	6.17
4-Sep	248	7.11	5.47	6.15
5-Sep	249	6.74	5.49	6.13
6-Sep	250	6.37	5.51	6.12
7-Sep	251	6.00	5.53	6.10
8-Sep	252	5.62	5.55	6.08
9-Sep	253	5.25	5.57	6.07
10-Sep	254	4.87	5.58	6.05
11-Sep	255	4.49	5.60	6.03
12-Sep	256	4.11	5.62	6.02
13-Sep	257	3.73	5.64	6.00
14-Sep	258	3.34	5.66	5.98
15-Sep	259	2.96	5.68	5.96
16-Sep	260	2.57	5.70	5.94
17-Sep	261	2.19	5.72	5.93
18-Sep	262	1.80	5.74	5.91
19-Sep	263	1.41	5.75	5.89
20-Sep	264	1.03	5.77	5.87
21-Sep	265	0.64	5.79	5.85
22-Sep	266	0.25	5.81	5.83

23-Sep	267	-0.14	5.83	5.82
24-Sep	268	-0.53	5.85	5.80
25-Sep	269	-0.92	5.87	5.78
26-Sep	270	-1.31	5.88	5.76
27-Sep	271	-1.70	5.90	5.74
28-Sep	272	-2.09	5.92	5.72
29-Sep	273	-2.48	5.94	5.70
30-Sep	274	-2.87	5.96	5.68
1-Oct	275	-3.25	5.98	5.66
2-Oct	276	-3.64	5.99	5.65
3-Oct	277	-4.03	6.01	5.63
4-Oct	278	-4.42	6.03	5.61
5-Oct	279	-4.80	6.05	5.59
6-Oct	280	-5.19	6.06	5.57
7-Oct	281	-5.57	6.08	5.55
8-Oct	282	-5.95	6.10	5.53
9-Oct	283	-6.33	6.12	5.51
10-Oct	284	-6.71	6.13	5.49
11-Oct	285	-7.09	6.15	5.47
12-Oct	286	-7.47	6.17	5.45
13-Oct	287	-7.84	6.18	5.43
14-Oct	288	-8.22	6.20	5.42
15-Oct	289	-8.59	6.22	5.40
16-Oct	290	-8.96	6.23	5.38
17-Oct	291	-9.33	6.25	5.36
18-Oct	292	-9.69	6.26	5.34
19-Oct	293	-10.06	6.28	5.32
20-Oct	294	-10.42	6.30	5.30
21-Oct	295	-10.77	6.31	5.28
22-Oct	296	-11.13	6.33	5.26
23-Oct	297	-11.48	6.34	5.25
24-Oct	298	-11.83	6.36	5.23
25-Oct	299	-12.18	6.37	5.21
26-Oct	300	-12.52	6.38	5.19

27-Oct	301	-12.86	6.40	5.17
28-Oct	302	-13.20	6.41	5.16
29-Oct	303	-13.53	6.43	5.14
30-Oct	304	-13.86	6.44	5.12
31-Oct	305	-14.19	6.45	5.10
1-Nov	306	-14.51	6.47	5.08
2-Nov	307	-14.83	6.48	5.07
3-Nov	308	-15.14	6.49	5.05
4-Nov	309	-15.46	6.51	5.03
5-Nov	310	-15.76	6.52	5.02
6-Nov	311	-16.06	6.53	5.00
7-Nov	312	-16.36	6.54	4.98
8-Nov	313	-16.65	6.55	4.97
9-Nov	314	-16.94	6.57	4.95
10-Nov	315	-17.22	6.58	4.94
11-Nov	316	-17.50	6.59	4.92
12-Nov	317	-17.77	6.60	4.91
13-Nov	318	-18.04	6.61	4.89
14-Nov	319	-18.30	6.62	4.88
15-Nov	320	-18.56	6.63	4.86
16-Nov	321	-18.81	6.64	4.85
17-Nov	322	-19.06	6.65	4.84
18-Nov	323	-19.30	6.66	4.82
19-Nov	324	-19.53	6.67	4.81
20-Nov	325	-19.76	6.68	4.80
21-Nov	326	-19.98	6.68	4.78
22-Nov	327	-20.20	6.69	4.77
23-Nov	328	-20.41	6.70	4.76
24-Nov	329	-20.61	6.71	4.75
25-Nov	330	-20.81	6.72	4.74
26-Nov	331	-21.00	6.72	4.73
27-Nov	332	-21.18	6.73	4.72
28-Nov	333	-21.36	6.74	4.71
29-Nov	334	-21.53	6.74	4.70

30-Nov	335	-21.69	6.75	4.69
1-Dec	336	-21.85	6.75	4.68
2-Dec	337	-22.00	6.76	4.67
3-Dec	338	-22.14	6.77	4.66
4-Dec	339	-22.27	6.77	4.66
5-Dec	340	-22.40	6.78	4.65
6-Dec	341	-22.52	6.78	4.64
7-Dec	342	-22.64	6.78	4.64
8-Dec	343	-22.74	6.79	4.63
9-Dec	344	-22.84	6.79	4.62
10-Dec	345	-22.93	6.79	4.62
11-Dec	346	-23.01	6.80	4.61
12-Dec	347	-23.09	6.80	4.61
13-Dec	348	-23.16	6.80	4.61
14-Dec	349	-23.22	6.81	4.60
15-Dec	350	-23.27	6.81	4.60
16-Dec	351	-23.32	6.81	4.60
17-Dec	352	-23.35	6.81	4.59
18-Dec	353	-23.38	6.81	4.59
19-Dec	354	-23.41	6.81	4.59
20-Dec	355	-23.42	6.81	4.59
21-Dec	356	-23.43	6.81	4.59
22-Dec	357	-23.42	6.81	4.59
23-Dec	358	-23.41	6.81	4.59
24-Dec	359	-23.40	6.81	4.59
25-Dec	360	-23.37	6.81	4.59
26-Dec	361	-23.34	6.81	4.60
27-Dec	362	-23.30	6.81	4.60
28-Dec	363	-23.25	6.81	4.60
29-Dec	364	-23.19	6.80	4.60
30-Dec	365	-23.13	6.80	4.61

Appendix C

Table Heat energy losses at different parts of the distillation still

Part	Description	Without insulation	0.020	0.040	0.060	0.080	0.100
Still shell-not solar	Lateral	504	181	121	96	83	74
Still shell- Solar	bottom	101	101	101	101	101	101
	lateral	249	249	249	249	249	249
	Total	350	350	350	350	350	350
Top cover-not solar	conical	139	30	19	14	11	10
	Lateral	35	35	35	35	35	35
	Total	174	66	54	49	47	45
Grand Total		1028	597	525	495	479	469

Appendix D

Table1 System evaluation test with water using primary reflector only –Data set 1

Parameters	Trial 1	Trial 2	Trial 3	Ave	St. Error	COV
Gb_{ave}	861	857	842	-		
P_{in}, kW	4.669	4.647	4.566	-		
T1, °C	20	20	20	-		
T2, °C	50	48	47	-		
m, kg	10	10	10	-		
t, sec	449	474	446	-		
P_{out} kW	2.798	2.473	2.535			
Eff., %	59.922	53.221	55.511	56.228	1.967	0.061

Table2 System evaluation test with water using primary reflector only –Data set 2

Parameters	Trial 1	Trial 2	Trial 3	Ave	St. Error	COV
Gb_{ave}	804	776	794			
P_{in}, kW	4.356	4.204	4.304			
T1, °C	21.5	21.5	22			
T2, °C	49	50	51			
m, kg	10	10	10			
t, sec	450	518	502			
P_{out} kW	2.559	2.304	2.419			
Eff., %	58.738	54.799	56.205	56.581	1.153	0.035

Table 3 System evaluation with water using primary & secondary reflector

Parameters	Trials 1	Trial 2	Trial 3	Ave	St. Error	COV
Gb_{ave}	836	840	834			
P_{in}, kW	4.529	4.552	4.522			
T1, °C	21.5	21.5	21.5			
T2, °C	42	42	41			
m, kg	10	10	10			
t, sec	401	386	403			
P_{out} kW	2.140	2.224	2.026			
Eff., %	47.258	48.855	44.806	46.973	1.177	0.043

Table 4 Steam generation test (with primary reflector only)

Parameters	Trials 1	Trial 2	Trial 3	Ave	St. Error	COV
Gb_{ave}	853	819	841			
T1, °C	20	20.5	20.5			
T2, °C	100	to100	100			
m, kg	2	2	2			
t, sec	2166	2352	2395			
P, kW	2.40	2.20	2.17			
Eff., %	52.02	49.85	47.68	49.85	1.253	0.044

Table 5 Steam generation test (with primary and secondary reflectors)

Parameters	Trials 1	Trial 2	Trial 3	Ave	St. Error	COV
Gb	864	821	841			
T1, °C	21	21	21.5			
T2, °C	100	100	100			
m, kg	2	2	2			
t, sec	2716	2802	2992			
P, kW	1.91	1.85	1.73			
Eff., %	40.89	41.71	38.10	40.23	1.092	0.047

Appendix E

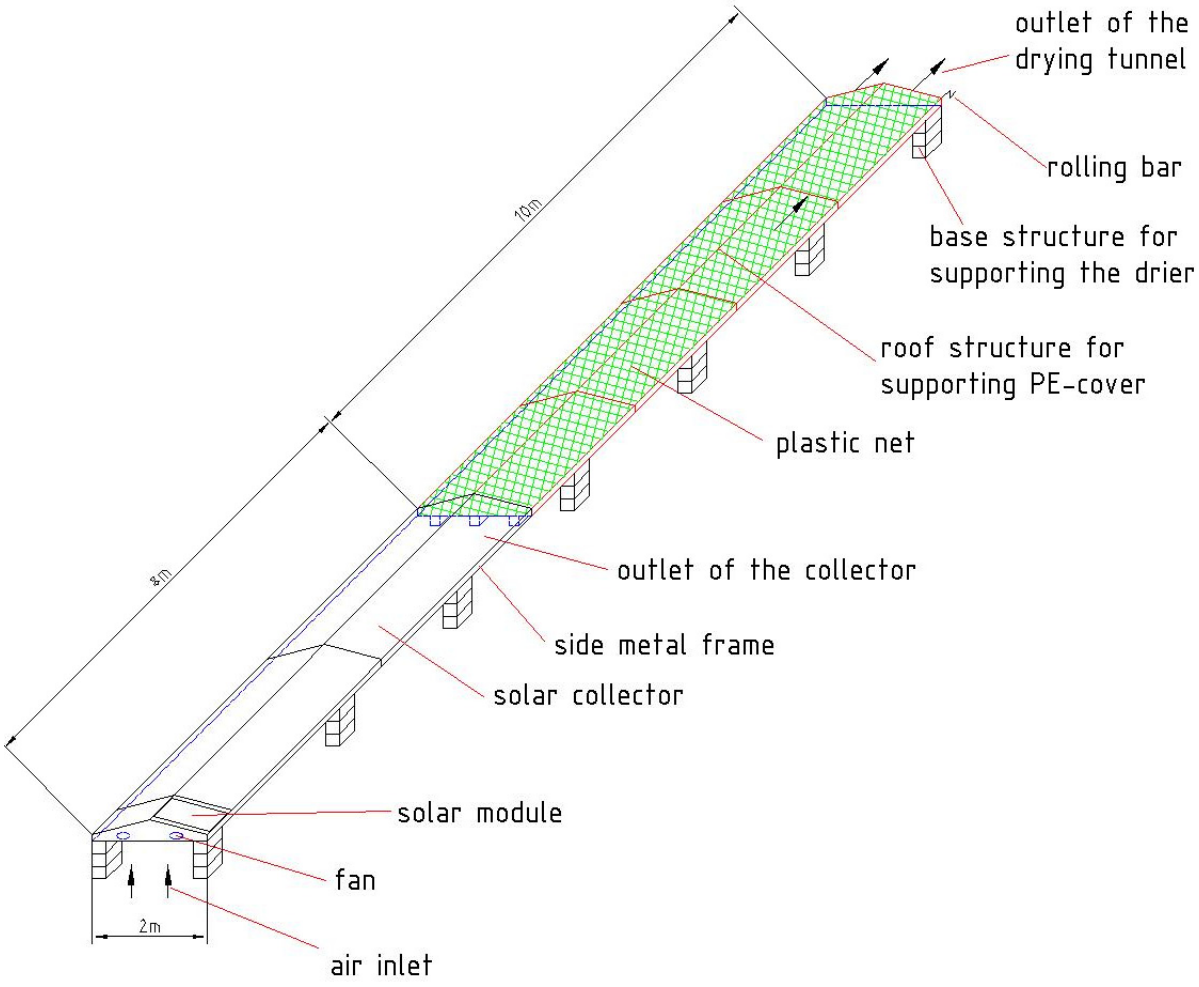

Figure Solar tunnel dryer (Hohenheim design)

Appendix F
Verities of Peppermint

Grown varieties of MENTHA
at the experimental and exposure site
for irrigation and solar techniques in Witzenhausen

name : ***Mentha spec.***
leaf : ca. 2 cm long, finely pubescent, bright green
stem : finely pubescent
origin : Dreschflegel
propagation : seeds

name : ***Mentha piperita L.***
leaf : ca. 3 cm long, finely pubescent , circel shaped, bright green
stem : finely pubescent
origin : Hübenthal
propagation : rhizome

name : ***Mentha spicata L.***
leaf : ca. 4 cm long, smooth surface, lance-shaped , dark green with light violet
stem : finely pubescent
origin : Hübenthal
propagation : rhizome

ISSN 0931-6264